Transport Dynamics of Quark-Gluon Plasma in Perturbative QCD with Magnetic fields/Vorticity

by

SHIYONG LI
B.S. (Central South University) 2012

Thesis submitted in partial fulfillment of the requirements
for the degree of Doctor of Philosophy in Physics
in the Graduate College of the
University of Illinois at Chicago, 2021

Chicago, Illinois

Defense Committee:
Ho-Ung Yee, Chair and Advisor
Wai-Yee Keung
Mikhail Stephanov
James Unwin
Rob Pisarski, Brookhaven National Laboratory

This thesis is dedicated to my parents for their endless love and support.

ACKNOWLEDGMENTS

First and foremost, I would like to express my sincere gratitude to my advisor Prof. Ho-Ung Yee for the continuous support of my Ph.D study and research, for his dedicated help, patience, inspiration, enthusiasm and immense knowledge. My advisor has deeply influenced my understanding of physics and has cultivated my ability to explore the secrets of nature, without whose supervision the dissertation would not be possible.

I appreciate the rest of my thesis committee: Prof. James Unwin, Prof. Misha Stephanov, Prof. Wai-Yee Keung, Prof. Rob Pisarski for their insightful comments and suggestions.

My sincere thanks also go to my collaborators for the works reported in this dissertation, in particularly, Dr. Koichi Hattori, and Dr. Daisuke Satow for Longitudinal electric conductivity, and Prof. Misha Stephanov for the hydrodynamics with spin degrees of freedom.

I would like to express my gratitude to Prof. Dirk Morr, Prof. Tom Imbo whose course I took at UIC and especially to Prof. Wai-Yee Keung for his dedication to teaching.

I would also like to thank other graduate students/postdocs at UIC for discussion. They are Dr. Yin Yi, Dr. Kiminad Mamo, Dr. Masaru Hongo, Bo Ling, Zaochen Ye, Peihong Man, Xin An, Bo-Yan Huang, Maneesha Sushama Pradeep, Bin Shi.

I would like to acknowledge National Nuclear Physics Summer School(2016) at the Massachusetts Institute of Technology; Brookhaven National Laboratory for hospitality, when part of the research reported in this dissertation has been done. The work of S. Li. is supported in part by DOE under Grants No. DESC0018209 and No. DE-FG0201ER41195.

CONTRIBUTION OF AUTHORS

The part of this dissertation are based on my previous publications. Sec.(2.1) is based on the paper with K. Hattori, D. Satow, and H.U. Yee in Ref.[1]. The work presented in Sec.(2.2) is based on work with Ho-Ung Yee in Ref.[2]. Sec.(3.1) is based on work with Ho-Ung Yee in Ref.[3] and review paper in Ref.[4]. Sec.(3.2) is based on work with M. Stephanov and Ho-Ung Yee in Ref.[5]. All reproduction of part of my previous publications in this dissertation is in accordance with the copyright policies of the corresponding publishers.

TABLE OF CONTENTS

TABLE OF CONTENTS (Continued)

CHAPTER **PAGE**

LIST OF TABLES

LIST OF FIGURES

LIST OF ABBREVIATIONS

CVE	Chiral Vortical Effect
CME	Chiral Magnetic Effect
DoF	Degrees of Freedom
EM	Electromagnetism
HIC	Heavy-Ion Collisions
HTL	Hard-Thermal Loop
LHC	Large Hadron collider
LLL	Lowest Landau Level
MHD	Magnetohydrodynamics
pQCD	perturbative Quantum Choromdynamics
QCD	Quantum Choromdynamics
QGP	Quark-Gluon plasma
RHIC	Relativistic Heavy-ion Collider

SUMMARY

In this dissertation, I have studied transport dynamics of Quantum Chromodynamics(QCD) under extreme conditions and Heavy-Ion Collisions(HIC) phenomenology in the presence of Magnetic fields and/or Vorticity.

Electrical conductivity is one of the important parameters characterizing the transport properties of quark-gluon plasma(QGP). In this thesis, I studied the quark mass contribution to the longitudinal electrical conductivity in the strong background magnetic field based on leading order perturbative QCD(pQCD) kinetic theory. An effective kinetic theory of the lowest Landau level quarks is formulated to study charge transport. It is also shown that charge transport of color degrees of freedom is enhanced while the sphaleron transition rate in pQCD is suppressed in the presence of strong magnetic field due to the enhanced Lenz's law for the color field.

Shear viscosity is another important transport coefficient that governs the rate of momentum transfer in the presence of inhomogeneity of fluid velocity profile. In the presence of magnetic field, the moving charged quarks are subject to Lorentz force, which could affect the time evolution of the QGP. In this thesis, I studied the shear viscosity due to the interplay between Lorentz force and QCD collision.

A novel quantum kinetic description of the spin polarization of massive quarks is first formulated in the context of pQCD. This framework shows that the order of time scale of spin polarization is the same as that of charge transport and shear viscosity, which is not captured by usual classical kinetic theory. It also opens the possibility to study relaxation dynamics of spin degrees of freedom in the pQCD regime.

Furthermore, we constructed the novel framework of non-dissipative second-order hydrodynamics for a slowly rotating fluid. We introduced a new power counting scheme that allows us to systematically construct the non-dissipative second-order hydrodynamics. New transport coefficients arise and we showed that they are not independent of each other but constrained by the second law of thermodynamics. We also constructed the generic framework for the ideal spin hydrodynamics, and we discovered that the thermal Hall effect naturally arises from the spin coupling with the gradient of temperature. Most importantly, we have made a profound observation that by doing the pseudo gauge transformation the spin hydrodynamics is equivalent to the non-dissipative second-order hydrodynamics.

CHAPTER 1

INTRODUCTION

1.1 Overview

The Heavy-Ion Collisions(HIC) experiments at Brookhaven National Laboratory(BNL) and CERN provide us the way to explore the physics of nuclear matter under extremely high temperature and/or density. In this deconfined quantum matter, a lot of interesting physics can take place. The direction that I will pursue in my thesis is that I mainly use the weak coupling description based on leading order QCD kinetic theory. I will report the researches that I have done on the interplay between HIC phenomenology and the QCD matter under extreme conditions. It includes two parts, in the first part I mainly focus on studying the transport properties of QGP in the presence of magnetic field; in the second part, I will discuss the vorticity related phenomena, namely the microscopic description of spin polarization and macroscopic theory that incorporates the spin degrees of freedom within hydrodynamics. Highlights of this dissertation are listed below:

- **Transport properties of QGP in the presence of magnetic field:** In Chapter 2, an effective kinetic theory of the lowest Landau level quarks is formulated with the leading order QCD collision term arising from 1-to-2 processes that become possible due to 1+1 dimensional Landau level kinematics. In this framework, the longitudinal electric conductivity is found to behave as $\sigma_{zz} \sim e^2(eB)T(\alpha_s m_q^2 log(T/m_q))^{-1}$ which is largely enhanced along the direction of the magnetic field, and its dependence on the quark mass is closely related to the relaxation of axial charge in the chiral anomaly. By computing the dominant damping rates for quarks and gluons which are responsible for color charge transportation, it is shown that the longitudinal color conductivity is also enhanced by the strong magnetic field, which implies that the sphaleron transition rate in perturbative QCD is suppressed by the strong magnetic field due to the enhanced Lenzs law in color field dynamics. Another important transport coefficient of QGP, shear viscosity, was computed in weak magnetic fields limit in perturbative QCD, for which we observed an interesting interplay between the Lorentz force and QCD collisions.

- **Spin dynamics of QGP:** in Chapter 3, motivated by the measurement of the polarization of Lambda baryon, the quantum kinetic theory for the massive quarks with collision terms from the pQCD was developed. This framework not only provides the concrete collision terms that are missing in the previous construction, but it also shows insight into the relaxation rate of the spin polarization, which is proportional to $(\alpha_s^2 \log(1/\alpha_s)T)$. The relaxation rate for spin polarization is found to be of the same order as that of other transport phenomena such as shear viscosity and charge conductivity. It indicates that even in the classical kinetic regime we must take into account the quantum correlation of spin degrees of freedom and it also complements our previous work on the similar question in the strongly coupled regime described by AdS/CFT correspondence. On the other hand, from the macroscopic point of view, the generalization of hydrodynamics to incorporate the spin DoF received a lot of attention. The generic framework for the ideal spin hydrodynamics is constructed. It is shown that the thermal Hall effect naturally arises from the spin coupling with the gradient of temperature. Along the way, a novel non-dissipative second-order hydrodynamics for a slowly rotating fluid is formulated. A new power counting scheme is introduced which allows one to systematically construct the non-dissipative second-order hydrodynamics. There are certain new transport coefficients allowed and constrained by the second law of thermodynamics. Most importantly, the spin hydrodynamics is proved to be equivalent to the non-dissipative second-order hydrodynamics by performing the pseudo gauge transformation.

The remainder of this chapter is organized as follows. I will first review the evolution of the matter created during heavy-ion collisions(HICs), the induction of magnetic field, and vorticity in Sec.(1.2). Then, in Sec.(1.3), I shall briefly review relativistic hydrodynamics. The outline of this dissertation is sketched in Sec.(1.4).

1.2 Introduction to Relativistic Heavy-Ion Collision

The overarching science goal is that we want to explore and understand the structure and dynamics of the fundamental constituents of matter, thus at the most fundamental level that we know about today, is described by the theory of strong interactions of quarks and gluons, i.e the Quantum Chromodynamics(QCD). However QCD has some peculiar properties such as under normal conditions, we don't see free quarks and gluons since they are confined in color-neutral bounds states such as protons, neutrons, pions, kaons, etc. To get access to the QCD fundamental degrees of freedom, we need very extreme conditions. This can be achieved in many different ways, either we can look at some hadronic bound states such as proton at very very high resolution by doing deep inelastic scattering experiments Another possibility is to heat or compress nuclear matter to high temperature and high density, that is illustrated over here in Figure 1. This is a plot of the QCD phase diagram, which shows the different phases of strong interaction matter as a function of temperature and baryon chemical potential on the vertical and horizontal axis, respectively. It is firmly established from first principle lattice QCD calculations that at temperatures of order around 155 Mev, the hadronic gas undergoes a smooth crossover phase transition to a phase that we call the QGP [6; 7], which exists at extremely high temperature and/or density. This state is thought to consist of asymptotically free strong-interacting quarks and gluons, which are ordinarily confined by color confinement inside atomic nuclei or other hadrons. So how can we create extreme conditions with such high temperatures? There are several possibilities, on one hand, our early universe is cooling down follow the trajectory here at presumably low chemical potential, down the temperature axis, but this does not give us any immediate prospect for observations since the birth of the universe was far behind us. To explore these extreme states of matter in high energy heavy-ion collisions, there are current experiments at high energy frontier being performed at relativistic heavy ion collider(RHIC) at Brookhaven National Laboratory, and also at Large Hadron Collider(LHC) in CERN.

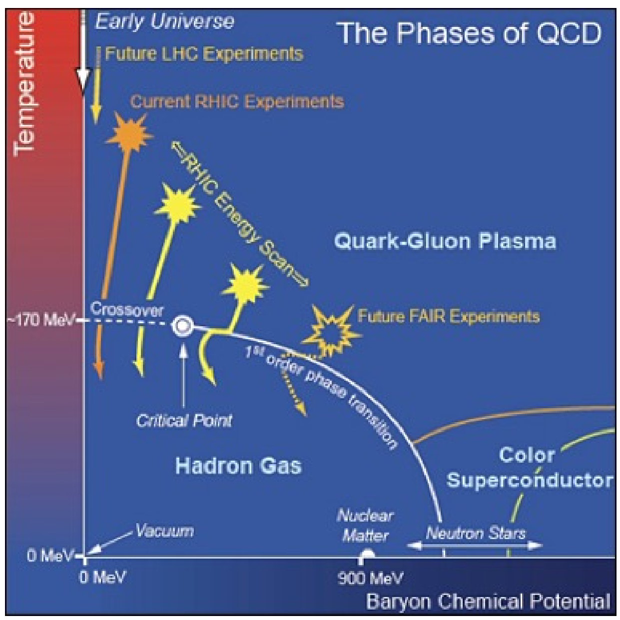

Figure 1: The phase diagram of QCD in the $\mu_B - T$ plane

What happens in the Heavy-Ion collisions(HIC) is that large nuclei, such as gold(Au) or lead(Pb) ions, travel at nearly the speed of light and smash into each other. According to current understanding, just right after the collision, the complex space-time dynamic evolution of nuclear matter is subject to a clearly defined separation of time scales where different physics happen at different times as illustrated in Figure 2. The time it takes for two nuclei to collide at high energy is very short, typically it is much less than 1fm/c. In the collision, the nuclei deposit into a highly excited state of nuclear matter which is far from equilibrium, which is often referred to as 'pre-equilibrium state'. It takes about time order of fm/c to evolve into a state where the system is sufficiently close to equilibrium so that it can be described by (viscous) relativistic hydrodynamics subsequently. So after about an fm/c the matter created at HICs somehow deposit into the center of the collision region then continuously go through a hydrodynamic expansion, during the expansion the matter cools down until about a time scale of about 10fm/c, reach a temperature that is no longer high enough to maintain QGP phase, the quarks and gluons degrees of freedom(DoF) then recombine into hadrons which undergo few scatterings before eventually free stream to detectors. Throughout the lifetime of the HICs, it is mostly dominated by hydrodynamics expansion of the quark and gluon plasma, in general, there is a very successful phenomenology that is based on hydrodynamic models of HICs.

In the off central HICs, strong magnetic fields can be generated. This is due to the fact that the fast moving and colliding nuclei generate electric currents in the opposite directions but produce the same magnetic field perpendicular to the reaction plane (the plane which is defined by the impact parameter and the beam direction) as illustrated in Figure 3. Its magnitude can be roughly estimated using classical Lienard-Wierchard formula, $eB \sim \gamma\alpha_{EM} Z/R_A^2$, where γ is the Lorentz contraction factor, α_{EM} is the fine structure constant, Z is the number of protons

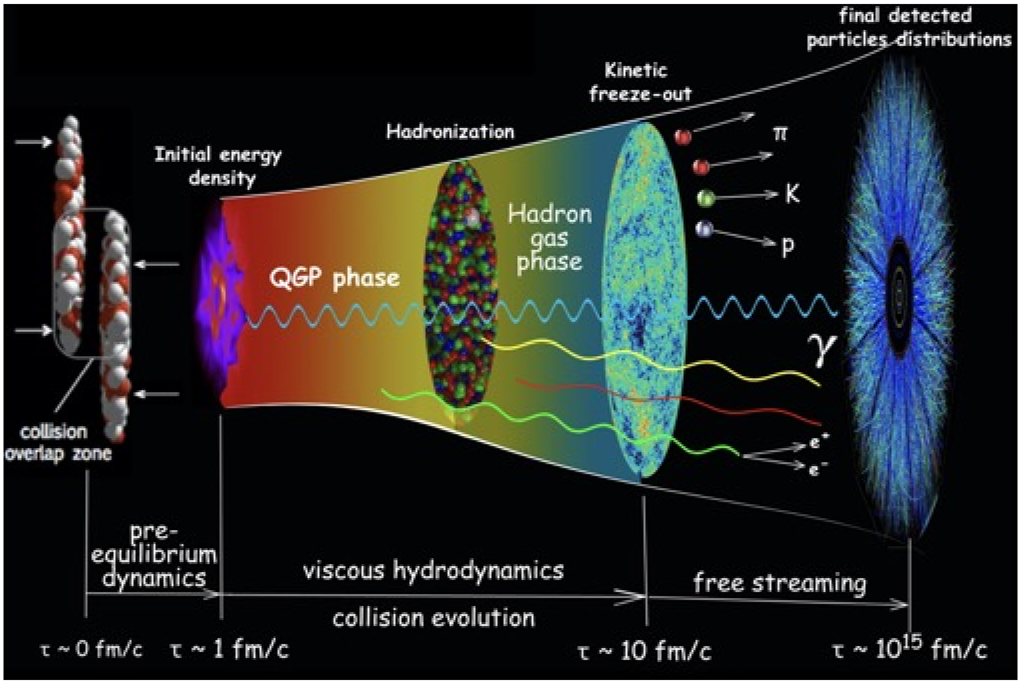

Figure 2: A schematic view of heavy-ion collision experiment. Picture credit: Chun Shen.

inside the nuclei and R_A is the radius of nuclei. Thus, for example, one finds that the magnetic field created in RHIC AU + AU collisions at center mass energy $\sqrt{s} = 200$ GeV can be as large as 10^{18} Gauss, and in LHC Pb + Pb collisions at $\sqrt{s} = 2.76$ GeV, can reach the order of 10^{23} Causs. More detailed numerical calculations can be found in ([8], [9], [10]). The magnetic fields could induce a number of novel quantum phenomena, such as the charge separation in the chiral system: the chiral magnetic effect(CME) ([8], [11]), chiral separation effect [12], chiral magnetic wave ([13],[14]). Its presence can also affect the heavy quark transport ([15], [16]), and the magnetic field induced anisotropic viscosities in hydrodynamic equations ([17], [18], [19]). See the recent review [20] and reference therein.

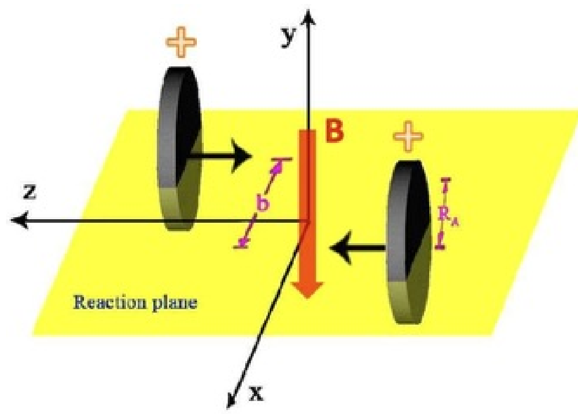

Figure 3: Magnetic field created in heavy-ion collisions.

Vortices are another interesting objects that exist in very broad systems ranging from the small scales such as the swirl quantum vortices in a superfluid to the very large scales such as the rotating galaxies. The strength of a vertex is commonly measured by the vorticity, in the context of non-relativistic hydrodynamics it is defined as $\boldsymbol{\omega} = \frac{1}{2}\boldsymbol{\nabla} \times \boldsymbol{v}$ where $\boldsymbol{v}$ the fluid velocity. In the off-central HIC, an orbital angular momentum can be generated, whose magnitude can be estimated as large as $\boldsymbol{J} \sim \sqrt{s}Ab/2 \sim 10^6\hbar$ for Au + Au collision at $\sqrt{s} = 200GeV$ at an impact parameter $b = 10$ fm, where A is the nucleon number of the ion. A part of the orbital angular momentum that resides in this fluid motion, or vorticity, will then be transferred to spin angular momenta of quasi-particles by interactions [21; 22; 23; 24; 25; 26; 27; 28; 29; 30; 31; 32]. In equilibrium, the resulting spin-dependent distribution function of quasi-particles can be shown to be equal to what one would have as if the energy of a particle of spin $\boldsymbol{S}$ was shifted by $\Delta E = -\boldsymbol{S}\cdot\boldsymbol{\omega}$ in thermal distribution [33; 34][1]. Since $\boldsymbol{S} \sim \mathcal{O}(\hbar)$, the net spin angular momentum is quantum in nature and is parametrically small (by $\hbar$) compared to the macroscopic orbital angular momentum of the fluid. The recent experimental observation of spin polarization of Λ baryons in off-central heavy-ion collisions [36] confirms the existence of this phenomenon that involves a quantum spin of quasi-particles. This opens a new avenue to study the spin-dependent observable. The presence of strong vorticity can induce many interesting effects. One of them is the Chiral Vortical Effect [37]; in a chirality imbalanced system(for example there could be more left handed fermions than the right handed fermions) where a vector current can be generated along the direction of vorticity. To have a better understanding of the spin-orbital coupling, a lot of progress has been made on both formulating an underlying microscopic kinetic theory of spin-1/2 massive particles [3; 38; 39; 40] and a macroscopic hydrodynamics with spin DoF [41; 42]. There is much other interesting physics related to the phase transition under rotation that one can find in the recent review [43].

What are the theoretical tools that can be applied to study this kind of phenomena? Even though one can employ first principle lattice QCD calculations [44; 45] to investigate the static properties of QCD matter, there is no analogous approach to study non-equilibrium QCD.

---

[1] An intuitive derivation of this fact, based on a detailed balance argument with total angular momentum conservation was given in Ref.[35].

Nevertheless, with regard to high energy QCD that we are interested in, there are still two limits where one can perform first principle studies. On the one hand in the weak coupling limit of QCD, one would employ a description in terms of fundamental quarks and gluons DoF based on kinetic theory. The other frontier a lot of progress has been made in understanding non-equilibrium properties of gauge theories is the strong coupling limit, that is large 't Hooft coupling limit which are theories not QCD but related to QCD, where one can have a holographic description for strongly coupled plasma such as the N=4 SYM [46; 47; 48].

The existence of weakly interacting quark matter is expected based on the asymptotic freedom of QCD[49]. In this thesis, I shall focus rather on the high temperature QGP phase, exploiting the fact that at asymptotically high temperature/energy where the effective gauge coupling constant $g(T)$ becomes smaller enough $\alpha_s = g^2/(4\pi) \ll 1$, so that it allows us to perform weak coupling calculations at leading order in the coupling, that is neglecting all relative corrections to the leading order(higher order weak coupling behavior are suppressed by powers of g).

In a hot, weakly coupled QCD plasma, one constructs the effective kinetic theory of QCD[50](and reference therein), in which framework that an appropriate set of Boltzmann equations, at sufficiently long time and distance scales, correctly describes the dynamics of typical ultra-relativistic excitation(i.e., quarks and gluons). The standard Boltzmann equation takes the form as

$$(\partial_t + \boldsymbol{v_p} \cdot \partial_{\boldsymbol{x}} + \boldsymbol{F}_{ext} \cdot \partial_{\boldsymbol{p}}) f(\boldsymbol{x}, \boldsymbol{p}, t) = -\mathcal{C}_{2\leftrightarrow 2}[f(\boldsymbol{x}, \boldsymbol{p}, t)] - C_{1\leftrightarrow 2}[f(\boldsymbol{x}, \boldsymbol{p}, t)], \quad \boldsymbol{v_p} = \partial\epsilon_p/\partial_{\boldsymbol{p}}, \tag{1.1}$$

where $f(\boldsymbol{x},\boldsymbol{p},t)$ represents the phase space density of (quasi-)particles at a time t, $\boldsymbol{v_p}$ is the velocity associated with an excitation of momentum $\boldsymbol{p}$, $\boldsymbol{F}_{ext}$ is the external force acting on the (quasi-)particles. The local collision terms appearing on the right hand side of Eq.(1.1) represent the rate at which particles get scattered out of the momentum state $\boldsymbol{p}$ minus the rate at which they get scattered into this state. The challenging part is coming from understanding the collision process and constructing the correct and effective collision operator $\mathcal{C}[f(\boldsymbol{x},\boldsymbol{p},t)]$. The collision operator $\mathcal{C}_{2\leftrightarrow 2}[f(\boldsymbol{x},\boldsymbol{p},t)]$ describes the 2-to-2 scattering process such as the quark-antiquark annihilation, the Compton scattering, etc. In addition to the usual 2-to-2 scattering, hard (quasi-)particles in the plasma can undergo so-called bremsstrahlung processes in such a way that they split into two different, nearly collinear hard particles, which is described by $C_{1\leftrightarrow 2}[f(\boldsymbol{x},\boldsymbol{p},t)]$ [1]. In this thesis, I will present our effective kinetic framework and apply it to study the transport of a hot, weakly coupled QCD plasma in the presence of the magnetic field. Our analysis is limited to the leading-log approximation where collinear bremsstrahlung are neglected for typical particles.

---

[1]Such bremsstrahlung processes cannot occur in a vacuum(because of the energy-momentum conservation), but they become kinematically possible when combined with a soft exchange involving some other excitation in the plasma, and it plays a very important role in the equilibration process of the highest momentum modes[51].

1.3 Relativistic Hydrodynamics

The transport properties of nuclear matter under extremely high temperature and/or density play important roles in our understanding of dynamic time evolution of the Quark-Gluon Plasma (QGP) created in relativistic heavy-ion collision (RHIC) experiments and/or dense quark-matters that could possibly be formed at the center of neutron stars. The relevant space-time scales in real-time descriptions of these systems (or the inverse scales of momentum and energy of inhomogeneity) are reasonably assumed or argued to be much larger than the scale of the microscopic QCD interactions that may be called an effective mean-free path. In such case, the powerful universal framework of hydrodynamics, which needs only a small number of inputs such as equation of states and a few transport coefficients together with the conservation laws of energy-momentum and charges, can be used to describe the interesting real-time evolution of the system (see Refs.[52; 53] for recent reviews). Especially, currently many of the realistic numerical simulations of the QGP in HIC and the nuclear matter of (merging) neutron stars are based on the hydrodynamics framework (See the overview [54] and reference therein).

The relativistic hydrodynamics equations were formulated many years ago [55], which describe the dynamics of an interacting theory at a large distance and time scales. The hydrodynamic variables are the local velocity $u^\mu(x)$(where $u^2 = -1$), the local temperature $T(x)$ and chemical potential $\mu(x)$. The hydrodynamic equations are the conservation laws for energy-momentum $\partial_\mu T^{\mu\nu} = 0$, and charge $\partial_\mu j^\mu = 0$, supplemented by their constitutive relations which are organized in terms of the order of derivative expansions involved with hydrodynamics variables. The hydrodynamic equations play very important roles in nuclear physics, astrophysics, and cosmology.

The constitutive relations for hydrodynamics are:

$$T^{\mu\nu} = (\epsilon + p)u^\mu u^\nu + p\eta^{\mu\nu} + \tau^{\mu\nu}, \tag{1.2}$$

$$j^\mu = nu^\mu + \nu^\mu, \tag{1.3}$$

where ϵ the energy density and p the pressure. $\tau^{\mu\nu}$ and ν^μ are terms of first order corrections which incorporate, in particular, dissipative effects. Following Landau and Lifshitz, one can always choose the Landau frame, where $u_\mu t^{\mu\nu} = u_\mu \nu^\mu = 0$. The dissipative terms are given by

$$\tau^{\mu\nu} = -\eta\Delta^{\mu\nu}\Delta^{\nu\beta}(\partial_\alpha u_\beta + \partial_\beta u_\alpha) - (\zeta - \frac{2}{3}\eta)\Delta^{\mu\nu}\partial \cdot u, \tag{1.4}$$

$$\nu^\mu = -\sigma T\Delta^{\mu\nu}\partial_\nu(\frac{\mu}{T}) + \sigma E^\mu, \tag{1.5}$$

where projection operator $\Delta^{\mu\nu} = g^{\mu\nu} + u^\mu u^\nu$, σ the conductivity, η the shear viscosity, ζ the bulk viscosity, electric field $E^\mu = F^{\mu\nu}u_\nu$ in local rest frame, and electric magnetic field strength $F^{\mu\nu}$.

Electrical conductivity is a fundamental property of a material that quantifies how strongly it conducts electric current. Shear viscosity is another important transport coefficient in these hydrodynamics descriptions, which governs the rate of momentum transfer in a presence of inhomogeneity of fluid velocity. The bulk viscosity, however, describes the change of local pressure when the fluid element is subject to a uniform expansion or contraction. In the case of QGP in relativistic heavy-ion collisions, a detailed comparison between the hydrodynamic predictions and the experimental data on the momentum anisotropy of emitted particles (which is also called elliptic flow) in the azimuthal angle perpendicular to the beam direction [56; 57] indicates that the shear viscosity to entropy density ratio of QGP is close to probably the smallest value that has ever been realized in Nature [58]; $\eta/s \sim 1/4\pi$, that could only be possible when the QCD is strongly coupled in these systems, that is, the coupling constant of QCD is not small.

Although the values of transport coefficients in perturbative regime are of little significance to the actual experiments, the computations of transport coefficients in high-temperature perturbative regime [59; 60; 61; 62] have given us useful insights into the underlying physics of transport coefficients, and could also provide useful bench-mark information on the value of the transport coefficients in one extreme end, compared to those in the other end of infinitely strong coupling that may be computed in the AdS/CFT correspondence [58]. On a more practical side, the perturbative regime is where one can perform a systematic and reliable theoretical computation typically allowing even analytic results, at least up to certain lowest orders. We shall look at and study these transport coefficients in the presence of the magnetic field, namely, the interesting interplay between QCD interactions and magnetic field in Chap. 2.

1.4 Outline and notations

The remainder of this dissertation is organized as follows.

Chapter 2 will focus on the transport properties of QGP in the presence of the magnetic field. I will introduce an effective 1+1 kinetic theory for the lowest landau level quarks. As an application, I will present the computation details of the conventional longitudinal electric conductivity in the strong magnetic field. The color charge conductivity in the presence of a magnetic field is also estimated in Sec.(2.1.5). All these two are based on the paper with K. Hattori, D. Satow, and Ho-Ung Yee in Ref.[1]. Another computation of shear viscosity in the weak magnetic field is presented in the last Sec.(2.2) of this Chapter, which is based on the work with Ho-Ung Yee in Ref.[2].

Chapter 3 is devoted to studying the spin dynamics of QGP. A formulation of spin polarization of massive spin-1/2 quarks is presented in Sec.(3.1) which is based on the work with Ho-Ung Yee in Ref.[3] and my single review paper [4]. Another generic framework of non-dissipative second-order hydrodynamics is proposed in Sec.(3.2). Then, in Sec.(3.2.2), A novel spin hydrodynamics framework is developed to incorporate the spin DOF in the hydrodynamics. Sec.(3.2.2) and Sec.(3.2.3) are based on the work with M. Stephanov and Ho-Ung Yee in Ref.[5].

In the last Chapter 4, I will summarize the main results of the dissertation and offer an outlook.

Throughout this dissertation, we shall adopt natural units in which $\hbar$, c, $k_B = 1$. We choose the most plus convention for the metric tensor, i.e., $g^{\mu\nu} = \mathrm{d}iag(-1, 1, 1, 1)$.

CHAPTER 2

TRANSPORT COEFFICIENTS OF QUARK-GLUON PLASMA IN THE PRESENCE OF MAGNETIC FIELD

2.1 Electrical conductivity of Quark-Gluon Plasma in the presence of Strong Magnetic field

(Previously published as: K. Hattori, S. Li, D. Satow, and H.-U. Yee, Longitudinal Conductivity in Strong Magnetic Field in Perturbative QCD: Complete Leading Order, Phys. Rev. D95, 076008 (2017))

2.1.1 Motivation and Summary

In this section, I will present the details of the computation on the longitudinal electric conductivity of a deconfined QGP in the presence of a strong background magnetic field in a complete leading order of pQCD. Recently, the interplay between the magnetic field and QGP matter has attracted a lot of attention. The motivation comes from that a strong, albeit short-lived, magnetic field of strength $eB \sim (200\,MeV)^2$ can be created on top of a deconfined quark-gluon plasma fireball ([8], [63]) in RHIC(see Ref. [20] for recent reviews), and also from the possible quark matter phase in the neutron star core with temperature much smaller than the magnetic field $T^2 \ll eB$ (see Ref. [64] for a review). The QCD phase diagram and the phase transitions in such strong magnetic fields have been studied extensively in literature(see Refs. [65; 66; 67; 68; 69] and references therein).

Throughout this subject, we focus on a neutral QGP system that is more relevant to the HIC. We assume the following hierarchy of scales: $\alpha_s eB \ll T^2 \ll eB$, as introduced in Ref.[15]. The second inequality is what we mean by the strong magnetic field, which allows us to focus only on the lowest Landau level(LLL) states of quarks or antiquarks, and to neglect the higher Landau level thermal occupation since whose density of states are exponentially suppressed by $e^{-\frac{\sqrt{eB}}{T}}$, hence they do not participate in the transport phenomena in our leading order computation. On the other hand, the first inequality is justified in the following way: the dominant charge carriers that contribute to the transport coefficients in leading order are from hard (quasi-)particles with typical momenta $\sim T$, whose dispersion relation deviates from the free one by $\alpha_s eB/p^2 \sim \alpha_s eB/T^2$, since the leading thermal self-energy goes as $\Sigma \sim \alpha_s eB$ because of the above assumed second inequality $T^2 \ll eB$ (the dominant contribution to the 1-loop self-energy comes from the LLL states due to their larger density of states than the gluons). As a consequence, the first inequality allows us to neglect these corrections for hard particles in leading order. Therefore, the above hierarchy of scales leads to a consistent Hard-thermal loop(HTL) counting scheme with thermally excited "hard" LLL states as the dominant source of HTL self-energies (the density of states for LLL is $\sim (eB)T$ while that for gluons is only T^3 hence subleading).

Furthermore, we introduce a finite quark mass to obtain a finite longitudinal conductivity in the presence of the magnetic field. In the massless limit, the axial anomaly equation indicates that there is a continuous production of axial charge along the direction of the electric and magnetic field as

$$\partial_t n_A = \frac{e^2 N_c N_F}{2\pi^2} \boldsymbol{E} \cdot \boldsymbol{B}\,, \tag{2.1}$$

where n_A is the axial charge in the chiral imbalanced system, N_c is the number of colors for quarks and/or antiquarks and N_F is the number of massless flavors that contribute to the anomaly. From the known relation that the axial charge is proportional to axial chemical potential by $n_a = \mu_A/\chi$ (χ is the charge susceptibility), and the Chiral Magnetic Effect(CME) [11], one finds that the axial charge grows linearly in time without any cutoff,

$$\boldsymbol{J} = \frac{e^2 N_c N_F}{2\pi^2} \mu_A \boldsymbol{B} = \frac{e^2 N_c N_F}{2\pi^2 \chi} n_A \boldsymbol{B} = \frac{e^4 (N_c N_F)^2 B^2}{4\pi^4 \chi} tE\,, \tag{2.2}$$

As time goes on, this conductivity goes to infinity. To obtain a finite conductivity, we must consider the relaxation dynamics of the axial charge. Including the relaxation term of $-\frac{1}{\tau_R} n_A$ on the right-hand side of Eq.(2.1), one finds a stationary solution $n_A = \frac{e^2 N_c N_F}{2\pi^2} \boldsymbol{E} \cdot \boldsymbol{B} \tau_R$, which leads to a finite contribution to the longitudinal conductivity from CME[70],

$$\sigma_{zz} = \frac{e^4 (N_c N_F)^2 B^2}{4\pi^4 \chi} \tau_R\,. \tag{2.3}$$

There are mainly two contributions to the relaxation dynamics of the axial charge: either from a finite quark mass [71] or sphaleron transitions. On one hand, the inverse relaxation time from sphaleron dynamics is proportional to the sphaleron transition rate Γ_s, whose expression is determined by a fluctuation-dissipation relation [72]

$$\tau_{R,s}^{-1} = \frac{(2N_F)^2\Gamma_s}{2\chi T}\,, \tag{2.4}$$

where the sphaleron transition rate Γ_s in the absence of magnetic field is known to be of order $\Gamma_s \sim \alpha_s^5 \log(1/\alpha_s) T^4$ [73; 74; 75]. An evaluation of Γ_s in the presence of strong magnetic field is given in the Sec.(2.1.5), but whose result is further suppressed due to an enhanced Lenz's law from the increased color conductivity along the magnetic field direction (while transverse color conductivity remains as $\sigma_c \sim T$ (neglecting any logarithms in power counting)). Nevertheless, such a weak coupling behavior is different from the strong coupling one from AdS/CFT correspondence [76]. On the other hand, the finite quark mass contribution to the inverse relaxation time behaves as

$$\tau_{R,m}^{-1} \sim \alpha_s m_q^2/T\,, \tag{2.5}$$

either with or without the strong magnetic field. In the case with a strong magnetic field in LLL approximation for quarks, the 1+1 dimensional dispersion relation makes it possible for an on-shell gluon to create a quark/antiquark pair and vice versa [77; 78]. This 1-to-2 (and/or 2-to-1) process rate is only of α_s, and is the dominant contribution over the usual 2-to-2 processes under the assumption $\alpha_s eB \ll m_q^2$ that will be explained in the following. Our explicit computations of the collision terms from 2-to-2 processes in Appendix.(B) of our work[1] show that these are indeed sub-leading compared to the 1-to-2 process in the main text when $\alpha_s eB \ll m_q^2$.) . The resulting chirality flipping rate is again expected to be $\alpha_s m_q^2/T$. In fact, this expectation is further confirmed by an explicit computation [1] (see Sec.(2.1.4)). In the case without a magnetic field, it can be shown that the dominant chirality flipping rate comes from the small angle scatterings with soft transverse space like magnetic degrees of freedom [80], that is, the same one for the leading damping rate of hard particles. It gives rise to a single power of α_s rather than α_s^2. The m_q^2 dependence comes from that chirality flipping amplitude should be proportional to the mass.

Since the smallest relaxation time determines the final conductivity, the finite quark mass will be the dominant contribution over the sphaleron dynamics if $\alpha_s m_q^2 \gg \alpha_s^5 T^2$, such a condition can be satisfied in the small coupling constant limit. We will assume this to be true so that we can neglect non-perturbative sphaleron dynamics and focus only on perturbative (quasi-)particle dynamics of the LLL state quarks interacting with 3+1 dimensional thermal gluons. With $\tau_R \sim T/(\alpha_s m_q^2)$ in Eq.(2.3), and given that the charge susceptibility of LLL state in strong magnetic field limit is

$$\chi = N_c \frac{1}{2\pi}\left(\frac{eB}{2\pi}\right) , \tag{2.6}$$

[1] In the meantime, K. Hattori and D. Satow also evaluate the conductivity in a complementary paper [79], by using the diagrammatic method instead of the kinetic approach.

where the first $1/(2\pi)$ is the 1+1 dimensional charge susceptibility, and $(eB/2\pi)$ is understood to be the transverse density of LLL state. The longitudinal electric conductivity in small quark mass limit $m_q \to 0$ is expected as

$$\sigma_{zz} \sim e^2 N_c (eB) T \frac{1}{\alpha_s m_q^2}\,, \quad m_q \to 0\,. \tag{2.7}$$

Our explicit computation Eq.(2.40) indeed confirms this expectation, up to a logarithmic correction of $1/\log(T/m_q)$.

The full result of σ_{zz} for an arbitrary value of m_q/T in complete leading order in α_s is given in Sec.(2.1.4), within the assumed hierarchy $\alpha_s eB \ll (T^2, m_q^2) \ll eB$. The final result takes a form

$$\sigma_{zz} = e^2 \frac{dimR}{C_2(R)} \left(\frac{eB}{2\pi}\right) \frac{1}{\alpha_s T} \sigma_L(m_q/T)\,, \tag{2.8}$$

with a dimensionless function $\sigma_L(m_q/T)$ given by Eq.(2.42).

It is worth remarking that in the opposite limit of $m_q^2 \ll \alpha_s eB$, which is a quite interesting problem for the future, the situation is complicated due to some non-chirality flipping 2-to-2 processes become of the same order as the above 1-to-2 processes. Nevertheless, at the leading-log approximation, the 2-to-2 process is negligible compared to the 1-to-2 process even when $m_q^2 \ll \alpha_s eB$. This case is studied in the complementary paper [79] at the leading-log accuracy. (see Appendix.(2.A.1) too). The chirality flipping processes is still the main contribution to the final conductivity (otherwise, the conductivity diverges): essentially, these chirality flipping processes are the "bottle-neck" for the relaxation of axial charges that would grow with anomaly, and should be included in the kinetic theory.

The real complication arises when $m_q \ll \alpha_s T$: in the small momentum region $p_z \sim m_q$, the chirality is maximally violated and chirality can effectively be flipped by going through this IR region. In 1+1 dimensions, the phase space for this IR region gives only one power of m_q: $\int^{m_q} p_z \sim m_q$, which means that the effective chirality flipping rate from this IR region is suppressed only by a single power m_q, $1/\tau \sim \alpha_s^2 m_q$, thwarting the above $\alpha_s m_q^2/T$ chirality flipping rates from hard momentum region when $m_q \ll \alpha_s T$. What this all means is that in 1+1 dimensions with $m_q \ll \alpha_s T$, the major "bottle-neck" for axial charge relaxation happens in the IR region near the origin $p_z \sim m_q$, and these IR dynamics determines the global shape of the distribution function and the final conductivity. Topologically, the two large p_z regions, $p_z > 0$ and $p_z < 0$, are connected by the IR region of $p_z = 0$, and without knowing the boundary condition at $p_z = 0$, one cannot determine the global solution uniquely. Since the self-energy is of order $\alpha_s eB$, the dispersion relation for these IR modes of $p \sim m_q$ gets thermal correction of $\alpha_s eB/m_q^2 \gg 1$, and we no longer should use kinetic theory with free dispersion relation for these IR modes. This problem shall be deferred to future study.

2.1.2 Effective kinetic theory in the LLL approximation

In this section, I will set up the kinetic theory framework that describes weakly interacting quasi-particles. For simplicity, only one-flavor case is considered here, and the generalization to the multiflavor case is straightforward. In the presence of a strong magnetic field $eB \gg T^2$, its effect on the motion of quarks and/or antiquarks should be treated non-perturbatively. This can be achieved by quantizing the quark field in the presence of the magnetic field, which is summarized in the Appendix.(2.A.1). Now the quark wave functions are the Landau levels whose density of states in the transverse plane perpendicular to the magnetic field is known to be of $eB/(2\pi)$. Working in the Landau gauge $A^2 = Bx^1$, there are two momentum quantum numbers for each Landau level states the momentum p_2 going along spatial x^2 direction, which labels the transverse position of each Landau levels and encodes the transverse density of states $eB/(2\pi)$, whereas p_z is the conventional momentum for the motion of each state along the longitudinal direction. Correspondingly, the dispersion relation of quasi-particles is

$$E_{p_z,n} = \sqrt{p_z^2 + 2|eB|n + m_q^2}\,, \tag{2.9}$$

where $n = \{0, 1, 2, \cdots\}$ is the Landau levels and m_q is the bare quark mass.

A weakly coupling quasi-particle picture should be a good description for the system under an external perturbation. For the case we are considering with the strong magnetic field, the fermionic quasi-particles are Landau level quarks and/or antiquarks that move only along the 1+1 dimensions with the above dispersion relation, while their transverse positions do not change in the free limit. Therefore, we have an effective theory describing the collection of 1+1 dimensional fermionic quasi-particles that are distributed in the transverse plane with the transverse density $\frac{eB}{2\pi}$ for each n. At a finite temperature in an equilibrium state, each Landau level state is occupied by the usual equilibrium thermal distribution functions. In the regime, $eB \gg T^2$, only the LLL state with $n = 0$ are populated due to the large energy gap of $\Delta \sim \sqrt{eB} \gg T$ for higher Landau levels, and thus they do not participate in the charge transport. From here and the rest of this section, only LLL are considered.

What about the gluons? Well, the gluons at leading order are still 3+1 dimensional quasi-particles. Their dominant self-energy correction arising from QCD interaction with thermally populated LLL quarks is of order $\Sigma \sim \alpha_s eB$. In our assumed hierarchy $\alpha_s eB \ll T^2$, this correction is sub-leading compared to the bare momentum $p \sim T$ of hard particles. thus, these hard gluons have the bare dispersion relation at leading order.

As shown in the Appendix.(2.A.1), the Landau level wave function with momentum quantum number p_2 is localized around $x_1 = p_2/eB$ with a width of order $1/\sqrt{|eB|}$. One can construct a wave packet with a central value of p_2^{center} with a width Δp_2 that is localized in x_2^{center} (note that there is no velocity associated with p_2^{center} since $\partial E/\partial p_2 = 0$). Then this wave packet has a spatial width of $\Delta x_2 \sim 1/\Delta p_2$. Since $\Delta p_2 = \Delta x_1 |eB|$, we have the transverse uncertainty of $\Delta x_1 \Delta x_2 \sim 1/|eB|$, which is the well-known transverse size of the Landau levels. An accurate counting of available states in the Appendix.(2.A.1) shows that the transverse density of such states is $eB/(2\pi)$. In this way, the label p_2 is effectively transformed into a transverse space position variable $\boldsymbol{X}_T$ (up to an ambiguity of $1/\sqrt{|eB|}$),

$$p_2 \to (p_2^{center}\,,\, x_2^{center}) \to (x_1^{center}\,,\, x_2^{center}) = \boldsymbol{X}_T\,. \tag{2.10}$$

Such a decomposition is very similar to the decomposition of space and momentum up to ambiguity of $\hbar$: the transverse space is roughly a phase space with $\Delta \boldsymbol{X}_T^2 \sim 1/|eB|$. Thus p_2 is a good quantum label for the Landau levels.

Scatterings with other quarks/antiquarks or gluons cause the momentum as well as transverse position change for each Landau level quasi-particles. As one can see that in addition to conventional 2-to-2 scatterings that have been widely considered in literature, there are additional leading 1-to-2 scatterings due to the presence of magnetic field. Explicit computations in Sec.(2.1.3) and Appendix.(2.A.1) show that the changes in p_2 due to QCD scatterings is bounded by $\Delta p_2 \lesssim \sqrt{eB}$ due to a form factor $R_{00}(q_\perp) = e^{-\frac{\boldsymbol{q}_\perp^2}{4eB}}$, which indicates that these interactions are local in the transverse space within a distance of $\Delta p_2/eB \sim 1/\sqrt{eB}$. Therefore if the variation scale of external parameters (such as electric field or temperature gradient) is much larger than $1/\sqrt{eB}$, one can rewrite momentum p_2 as

$$p_2 = p_2^{global} + \tilde{p}_2\,, \tag{2.11}$$

where p_2^{global} encodes a large scale (compared to $1/\sqrt{eB}$) transverse position $\boldsymbol{X}_T$, while $\tilde{p}_2 \lesssim \sqrt{eB}$ takes into account a local collection of Landau levels around $\boldsymbol{X}_T$. The above rewriting is possible because the theory is invariant under a constant shift of p_2.

Based on above argument, one introduces the quark and/or antiquark distribution functions

$$f_\pm(z, p_z, \boldsymbol{X}_T, p_2, n)\,, \tag{2.12}$$

as an occupation number per unit $dzdp_z/(2\pi)$ for the state labeled by (p_2, n) around the global position $\boldsymbol{X}_T$. The $+$ refers to quark and $-$ for antiquark, respectively, while gluons take usual (color diagonal) distribution function $f_g(\boldsymbol{x}, \boldsymbol{k})$. The dynamics of these distributions obey the well known Boltzmann equation,

$$\frac{\partial f_\pm}{\partial t} + \dot{z}\frac{\partial f_\pm}{\partial z} + \dot{\boldsymbol{p}}_z\frac{\partial f_\pm}{\partial \boldsymbol{p}_z} = C[f_\pm, f_g]\,, \tag{2.13}$$

where $\dot{\boldsymbol{p}}_z = \pm e\boldsymbol{E}$ is the external force, $\boldsymbol{E}$ is the applied electrical field along the longitudinal direction, $\boldsymbol{E} = E\hat{z}$. It is worth remarking that the dynamical change of the transverse position of Landau level states $(\boldsymbol{X}_T, p_2)$ is only from QCD interactions, and it is part of the collision term on the right-hand side. The reason for this is that the transverse motions of quark/antiquark are quantum processes, classically it means the absence of transverse motion of Landau level states in the free limit. By the same argument, the above framework is useful for calculating the transverse conductivities.

One can find the specific Feynman rules for the collision terms due to the QCD interaction in Appendix.(2.A.1).

In terms of the effective distribution functions $f_\pm$, one easily writes down the electric current from a state of $(\boldsymbol{X}_T, p_2, n)$ as

$$\boldsymbol{J}_z = e\,\mathrm{d}imR\int\frac{dp_z}{(2\pi)}\,\boldsymbol{v}_p\left(f_+(p_z, \boldsymbol{X}_T, p_2, n) - f_-(p_z, \boldsymbol{X}_T, p_2, n)\right), \tag{2.14}$$

where $\boldsymbol{v}_p = \frac{\boldsymbol{p}_z}{E_p}$ is the longitudinal velocity and dim R is the dimension of color representation.

The kinetic theory is applicable only when the mean free path is larger than the Compton wavelength of dominant quasi-particles governing the transport. Such a criterion can be justified with a sufficiently small $\alpha_s \ll 1$ and a reasonable ratio of $m_q^2/T^2 \lesssim O(1)$. Since for most of the transport coefficients, the dominant charge carriers typically have momenta of order temperature $|\boldsymbol{p}_z| \sim T$ (hence the wave-length of $1/T$), while the mean free path arising from scatterings with other ambient particles are found to be about $l_{\mathrm{m}fp} \sim T/(\alpha_s m_q^2)$ in Sec.(2.1.3) (for "kinetic relaxation" of quarks or $l_{\mathrm{m}fp} \sim 1/(\alpha_s T)$ in Sec.(2.1.5)(for "color" relaxation).

It is now kinematically possible to have on-shell 1-to-2 processes of a single gluon decaying into a quark/antiquark pair and vice verse[77; 78]. Due to the 1+1 dimensional dispersion relation for quark/antiquarks and the usual 3+1 dimensional dispersion relation for gluons, the transverse part of gluon momentum plays the role of the mass term. These are the only on-shell 1-to-2 processes, and their rate turns out to be proportional to only a single power of α_s instead of α_s^2, even for the "kinetic relaxation rate" that are relevant for electric conductivity. An explicit computation in Sec.(2.1.3) shows that it is $\sim \alpha_s m_q^2/T$, featuring a universal factor of m_q^2 for both chirality flipping and non-flipping rates. As one can find in the Appendix.(2.A.2), the kinetic relaxation relevant for conductivity arising from the conventional 2-to-2 processes is at most of $\alpha_s^2(eB/T)\log(m_q^2/\alpha_s eB)$[1]. With our assumed hierarchy of scales $\alpha_s eB \ll (T^2, m_q^2) \ll$

[1]However, one can find that in Sec.(2.1.5) that the damping rate relevant for "color conductivity" from 2-to-2 processes is of order $\alpha_s T$, which is similar to the conventional case. As the damping rate from 1-to-2 processes is the same $\alpha_s m_q^2/T$, the 2-to-2 scatterings are the leading processes than 1-to-2 scattering for color conductivity when $m_q \lesssim T$.

eB, these novel 1-to-2 processes are leading compared to 2-to-2 processes in the presence of a strong magnetic field.

2.1.3 Collision term in Leading Order

In this section, I shall work out the details of the leading order collision term from the pair 1-to-2 creation/annihilation processes as discussed above. For simplicity, to compute the longitudinal conductivity, let's consider that the applied external electric field $\boldsymbol{E}$ is parallel to the magnetic field and is homogeneous in the two-dimensional transverse space. Thus, the resulting distribution functions for 1+1 dimensional Landau levels will be homogeneous too in the transverse space, i.e., there will be no dependence on the label of the LLL states, p_2 in Landau gauge: $f_\pm(p_z, p_2) \equiv f_\pm(p_z)$.

Using the Feynman rules summarized in the Appendix.(2.A.1), it is straightforward to obtain the collision term for the quark distribution $f_+(p_z)$ as

$$\begin{aligned} C[f_+(p_z)] &= \frac{1}{2E_p}\int \frac{d^2\boldsymbol{p}'}{(2\pi)^2 2E_{p'}}\int \frac{d^3\boldsymbol{k}}{(2\pi)^3 2E_k}\,|\mathcal{M}|^2\,(2\pi)^3\delta^{(2)}\left(\boldsymbol{p}+\boldsymbol{p}'-\boldsymbol{k}\right)\delta(E_p+E_{p'}-E_k) \\ &\times \Big(\left(1-f_+(p_z)\right)\left(1-f_-(p'_z)\right)f_g(\boldsymbol{k}) - f_+(p_z)f_-(p'_z)\left(1+f_g(\boldsymbol{k})\right)\Big)\ , \end{aligned} \tag{2.15}$$

where $E_p = \sqrt{\boldsymbol{p}_z^2 + m_q^2}$, $E_k = |\boldsymbol{k}|$, $d^2\boldsymbol{p} \equiv dp_z dp_2$, and shorthand notation $\delta^{(2)}(\boldsymbol{p}) \equiv \delta(p_z)\delta(p_2)$, which includes only spatial two dimensions (p_z, p_2) (recall that p_2 is the label for the LLL states), while the energy δ-function is written down explicitly. Note that the gluon momentum $\boldsymbol{k}$ is fully three dimensional. The above collision term is the sum over the pair creation and annihilation processes with the imposed detailed balance condition, such that one can combine them with a common matrix element $\mathcal{M}$. The collision term for the antiquark distribution is similar.

Following the conventional approach, one rewrites the distribution function around the equilibrium in linear order as

$$\begin{aligned} f_{\pm}(p_z) &= f_F^{eq}(E_p) + \beta f_F^{eq}(E_p)\left(1 - f_F^{eq}(E_p)\right)\chi_{\pm}(p_z)\,, \\ f_g(k) &= f_B^{eq}(E_k) + \beta f_B^{eq}(E_k)\left(1 + f_B^{eq}(E_k)\right)\chi_g(k)\,, \end{aligned} \tag{2.16}$$

with $f_{F/B}^{eq}(\epsilon) = 1/(e^{\beta\epsilon} \pm 1)$, $\beta = 1/T$, and $\chi_{g/\pm}$ are unknown scalar function that will be determined later. Using the energy δ-function and the detailed balance condition

$$\left(1 - f_+^{eq}(p_z)\right)\left(1 - f_-^{eq}(p_z')\right) f_g^{eq}(k) = f_+^{eq}(p_z) f_-^{eq}(p_z')\left(1 + f_g^{eq}(k)\right)\,, \tag{2.17}$$

one can show that

$$\begin{aligned} &\left(1 - f_+(p_z)\right)\left(1 - f_-(p_z')\right) f_g(k) - f_+(p_z) f_-(p_z')\left(1 + f_g(k)\right) \\ =\;& \beta f_F^{eq}(E_p) f_F^{eq}(E_{p'})\left(1 + f_B^{eq}(E_k)\right)\left(\chi_g(k) - \chi_-(p_z') - \chi_+(p_z)\right)\,. \end{aligned} \tag{2.18}$$

In the current specific consideration, it is clear that $\chi_-(p_z) = -\chi_+(p_z)$, since the effect of the applied electric field on the antiquarks is precisely opposite to that of quarks. Similarly, Charge-conjugation (C-) invariance indicates that gluon distribution should not be affected:

$\chi_g(k) = 0$ [1]. Furthermore, $\boldsymbol{E}$ is a 1 dimensional vector in $\hat{z}$ space, and $\chi_\pm(p_z)$ is a scalar function, which dictates that the response should take a form

$$\chi_+(p_z) = (\boldsymbol{E} \cdot \boldsymbol{p}_z) F(|\boldsymbol{p}_z|) = -\chi_+(-p_z)\,, \tag{2.19}$$

that is, $\chi_+(p_z)$ is an odd function on p_z. All these facts can be explicitly derived from the structure of the collision term and the source term with the applied electric field in the Boltzmann equation. They are similar to the 3+1 dimensional case in Refs.[61; 62].

The matrix element from the Feynman rules in the Appendix.(2.A.1) is given by

$$\mathcal{M} = i g_s \epsilon_\mu(k) \left[\bar{v}(p') \gamma_\parallel^\mu t_R^a u(p)\right] R_{00}(\boldsymbol{k}_\perp) e^{i\Sigma}\,, \tag{2.20}$$

where $\epsilon(k)$ is the polarization of the external gluon, t_R is the color generator in the quark representation R. The phase factor $e^{i\Sigma}$ is called the Schwinger phase [69] whose expression is irrelevant here, since it will disappear eventually in square of the matrix element. The subscript $\parallel$ denotes 1+1 dimension with the one spatial direction being parallel to $\boldsymbol{B}$, and it is important to note that $\gamma_\parallel^\mu$ is 1+1 dimensional γ-matrix which is effectively 2×2 matrix by the

[1]The magnetic field is C-odd quantity which breaks C-invariance. However, its effects on 1+1 dimensional LLL dynamics depend only on $|eB|$ except the Schwinger phase. Because the Schwinger phase is irrelevant for the leading order collision term, one can effectively use C-invariance.

projection operator. Correspondingly, the spinors $u(p)$ and $v(p')$ are 1+1 dimensional spinors with relativistic normalization

$$u(p)\bar{u}(p) = \gamma_{\parallel}^{\mu} p_{\mu} + m_q \,, \quad v(p')\bar{v}(p') = \gamma_{\parallel}^{\mu} p'_{\mu} - m_q \,. \tag{2.21}$$

Finally the form factor originating from the finite transverse size $l_B \sim 1/\sqrt{|eB|}$ of the LLL wave function is

$$R_{00}(\boldsymbol{k}_{\perp}) = e^{-\frac{\boldsymbol{k}_{\perp}^2}{4|eB|}} \,. \tag{2.22}$$

One has to sum over all incoming antiquark color states and the out-going gluon states, and average over the color states of the incoming quark in $|\mathcal{M}|^2$. The color algebra gives a Casimir factor $C_2(R)$ as usual, and the gluon polarization sum is

$$\sum_{\epsilon} \epsilon_{\mu}(\epsilon_{\nu})^{*} = \delta_{ij} - \frac{\boldsymbol{k}_i \boldsymbol{k}_j}{|\boldsymbol{k}|^2} \,. \tag{2.23}$$

The explicit square of matrix element $|\mathcal{M}|^2$ is

$$\begin{aligned} |\mathcal{M}|^2 &= g_s^2 C_2(R) e^{-\frac{\boldsymbol{k}_{\perp}^2}{2|eB|}} \left(\delta_{ij} - \frac{\boldsymbol{k}_i \boldsymbol{k}_j}{|\boldsymbol{k}|^2} \right) \mathrm{T}r \left[(\gamma_{\parallel}^{\mu} p'_{\mu} - m_q) \gamma_{\parallel}^{i} (\gamma_{\parallel}^{\mu} p_{\mu} + m_q) \gamma_{\parallel}^{j} \right] \\ &= 2 g_s^2 C_2(R) e^{-\frac{\boldsymbol{k}_{\perp}^2}{2|eB|}} \frac{\boldsymbol{k}_{\perp}^2}{|\boldsymbol{k}|^2} \left(E_p E_{p'} + p_z p'_z + m_q^2 \right) \,. \end{aligned} \tag{2.24}$$

The form factor $e^{-\frac{\boldsymbol{k}_\perp^2}{2|eB|}}$ features the finite transverse size of the LLL states, and $\boldsymbol{k}_\perp \ll \sqrt{|eB|} \sim 1/l_B$ modes can not resolve the LLL states.

Without loss of any generality, one can choose $p_2 = 0$ in Eq.(2.15), and perform p_2' and k_z integration to arrive at

$$\begin{aligned} C[f_+(p_z)] &= 2g_s^2 C_2(R)\frac{1}{2E_p}\int \frac{dp_z'}{2E_{p'}}\int \frac{d^2\boldsymbol{k}_\perp}{(2\pi)^2 2E_k} e^{-\frac{\boldsymbol{k}_\perp^2}{2|eB|}} \frac{\boldsymbol{k}_\perp^2}{|\boldsymbol{k}|^2}\left(E_pE_{p'} + p_zp_z' + m_q^2\right) \\ &\times \delta(E_k - E_p - E_{p'})\beta f_F^{eq}(E_p) f_F^{eq}(E_{p'})\left(1 + f_B^{eq}(E_k)\right)\left(\chi_+(p_z') - \chi_+(p_z)\right) \end{aligned} \quad (2.25)$$

and it is understood that $k_z = p_z + p_z'$. The energy δ-function can be worked out as

$$\begin{aligned} \delta(E_k - E_p - E_{p'}) &= \delta\left(\sqrt{(p_z + p_z')^2 + \boldsymbol{k}_\perp^2} - E_p - E_{p'}\right) \\ &= (2E_k)\,\delta\left(\boldsymbol{k}_\perp^2 - (p_\parallel + p_\parallel')^2\right) \end{aligned} \quad (2.26)$$

and performing $\boldsymbol{k}_\perp$ integration, one finally obtains the leading order collision integral

$$C[f_+(p_z)] = \alpha_s C_2(R) m_q^2 \int dp_z' \frac{\beta}{E_pE_{p'}} f_F^{eq}(E_p) f_F^{eq}(E_{p'})\left(1 + f_B^{eq}(E_p + E_{p'})\right)\left(\chi_+(p_z') - \chi_+(p_z)\right)\,, \quad (2.27)$$

where one can safely neglect the form factor $e^{-\frac{\boldsymbol{k}_\perp^2}{2|eB|}}$ in assumed hierarchy $T^2 \ll eB$, because $\boldsymbol{k}_\perp^2 = (p + p')^2 \sim T^2$ due to the Boltzmann factor in the collision term which ensures that the dominant leading contribution to the collision integral and the conductivity comes from the hard momentum modes $(p_z, p_z') \sim T$.

It is worth mentioning that the above simple collision integrand is a result of the two competing effects: "fermion-chirality selction rule" and "gluon-polarization selection rule" . The “chirality selection rule” is coming from the spinor trace in Eq.(2.24) and due to the factor

$$E_p E_{p'} + p_z p'_z + m_q^2 \to |p_z||p'_z| + p_z p'_z \,, \tag{2.28}$$

where the right-hand side is the expression in the massless limit ($m_q \to 0$). This is related to the chirality selection, because when the spin of the LLL fermions are aligned along the magnetic field, the signs of the longitudinal momentum is slaved to that of the chirality. To be specific, the chirality of the LLL massless fermion is identical to the sign of $sgn(eB)p_z$: if one quantizes a right-handed spinor field ψ_R, both quarks and antiquarks carry only the $sgn(eB)p_z > 0$ modes. Likewise, the quarks and antiquarks from a left-handed field ψ_L carry only the $sgn(eB)p_z < 0$ modes. An important fact is that gauge interactions via γ-matrix do not mix ψ_R and ψ_L fields, which means that the $sgn(eB)p_z > 0$ modes and $sgn(eB)p_z < 0$ modes decouple in the massless limit. Therefore, the chirality selection imposes the longitudinal momenta p_z and p'_z must have the same sign as in Eq.(2.28).

The other "gluon polarization selection rule" comes from the gluon polarization factor

$$\frac{\boldsymbol{k}_\perp^2}{|\boldsymbol{k}|^2} = \frac{(p_\parallel + p'_\parallel)^2}{(E_p + E_{p'})^2} = 2\frac{(E_p E_{p'} - p_z p'_z + m_q^2)}{(E_p + E_{p'})^2} \to 2\frac{(|p||p'| - p_z p'_z)}{(|p| + |p'|)^2} \,, \tag{2.29}$$

where the last expression is the result in the massless limit ($m_q \to 0$). The role of this factor can be understood as follows. If the momentum of the external gluon line is parallel to the $\hat{z}$

direction, that is $\boldsymbol{k}_\perp = 0$, then its polarization will be along the transverse space. However, the motion of the LLL quarks and antiquarks are (1+1)-dimensional and their current is strictly longitudinal, therefore, the gluon emission vertex should vanish in the $\boldsymbol{k}_\perp = 0$ limit. In the massless limit, this factor imposes that the p_z and p'_z to should take the opposite sign.

The "fermion-chirality selection" and "gluon-polarization selection" rules impose the competing conditions on the signs of p_z and p'_z. However, these two rules are not compatible in such a way that the collision term vanishes in the massless limit. Indeed, with a finite mass, the product of these two factors, and thus the collision term, is proportional to the mass square and is independent of the relative sign of p_z and p'_z. This is an exact form of the mass dependence, and shows the universal suppression of the collision integral $C[f_+(p_z)] \sim m_q^2$ in the small mass limit.

2.1.4 The longitudinal conductivity in the leading order

With the above constructed leading order collision term in the effective Boltzmann equation in the previous section, one can easily compute the longitudinal electric conductivity. The Boltzmann equation for the quark distribution subject to an applied external electric field $\boldsymbol{E} = E\hat{z}$ is

$$\frac{\partial f_+(p_z)}{\partial t} + e\boldsymbol{E}\frac{\partial f_+(p_z)}{\partial \boldsymbol{p}_z} = C[f_+(p_z)]\,. \tag{2.30}$$

One is interested in find a stationary solution in the linear order in $\boldsymbol{E}$ for the equilibrium conductivity. From $f_+(p_z) = f_F^{eq}(E_p) + \beta f_F^{eq}(E_p)\left(1 - f_F^{eq}(E_p)\right)\chi_+(p_z)$, and $\frac{\partial E_p}{\partial p_z} \equiv \boldsymbol{v}_p = \frac{\boldsymbol{p}_z}{E_p}$, one finally obtains the integral equation for $\chi_+(p_z)$,

$$\begin{aligned} & -eE\frac{p_z}{E_p} f_F^{eq}(E_p)\left(1 - f_F^{eq}(E_p)\right) \\ = \ & \alpha_s C_2(R) m_q^2 \int dp'_z \frac{1}{E_p E_{p'}} f_F^{eq}(E_p) f_F^{eq}(E_{p'})\left(1 + f_B^{eq}(E_p + E_{p'})\right)\left(\chi_+(p'_z) - \chi_+(p_z)\right) \end{aligned} \quad (2.31)$$

This one dimensional integral equation can be solved as follows. Recall that $\chi_+(p'_z)$ is an odd function of p'_z, but the other components of the integrand are an even function of p'_z, then the integral with $\chi_+(p'_z)$ simply vanishes. Therefore, $\chi_+(p_z)$ is easily solved as

$$\chi_+(p_z) = \frac{eE}{2C_2(R)\alpha_s m_q^2} \frac{p_z\left(1 - f_F^{eq}(E_p)\right)}{\int_0^\infty dp'_z \frac{1}{E_{p'}} f_F^{eq}(E_{p'})(1 + f_B^{eq}(E_p + E_{p'}))} \,. \quad (2.32)$$

Note that what appears in front of $\chi_+(p_z)$ in Eq.(2.31) is nothing but the quark damping rate

$$\gamma_q = \frac{\alpha_s C_2(R) m_q^2}{E_p\left(1 - f_F^{eq}(E_p)\right)} \int dp'_z \frac{1}{E_{p'}} f_F^{eq}(E_{p'})\left(1 + f_B^{eq}(E_p + E_{p'})\right) \,, \quad (2.33)$$

which gives a relaxation dynamics in the Boltzmann equation

$$\partial_t \chi_+(p_z) \sim -\gamma_q \, \chi_+(p_z) \,. \quad (2.34)$$

Then, the solution Eq.(2.32) is nothing but

$$\chi_+(p_z) = eE\frac{p_z}{E_p}\frac{1}{\gamma_q}\,, \tag{2.35}$$

that is, the relaxation time approximation with the momentum dependent relaxation time $\tau_R = 1/\gamma_q$ is in fact an exact solution of the full Boltzmann equation in our special case.

After finding the solution $\chi_+(p_z)$, the longitudinal current j_z is given by

$$\boldsymbol{j}_z = e\left(\frac{eB}{2\pi}\right) 2\,\mathrm{d}imR\int\frac{dp_z}{(2\pi)}\,\boldsymbol{v}_p\,\beta f_F^{eq}(E_p)\left(1-f_F^{eq}(E_p)\right)\chi_+(p_z)\,,\quad \boldsymbol{v}_p = \frac{\boldsymbol{p}_z}{E_p}\,. \tag{2.36}$$

The factor $(eB/2\pi)$ is the transverse density of LLL states, and the next factor 2 comes from that antiquarks contribute equally as that of quarks. The final expression for longitudinal conductivity is then

$$\sigma_{zz} = e^2\left(\frac{eB}{2\pi}\right)\frac{\mathrm{d}imR}{C_2(R)\alpha_s m_q^2}\int_{-\infty}^{+\infty}\frac{dp_z}{(2\pi)}\frac{p_z^2}{TE_p}\frac{f_F^{eq}(E_p)(1-f_F^{eq}(E_p))^2}{\int_0^\infty dp'_z\frac{1}{E_{p'}}f_F^{eq}(E_{p'})(1+f_B^{eq}(E_p+E_{p'}))}\,. \tag{2.37}$$

For a general value of m_q/T, one needs a simple numerical integration to get the result, but for both the small and large m_q limit, it can be handled analytically, respectively. In small mass limit, note that the p'_z integral in the denominator has a logarithmic IR enhancement in $p'_z \sim 0$ regime due to $1/E_{p'} = 1/\sqrt{p'^2_z + m_q^2}$ factor, which produces in leading log of m_q/T as

$$\int_0^\infty dp'_z\frac{1}{E_{p'}}f_F^{eq}(E_{p'})(1+f_B^{eq}(E_p+E_{p'})) \sim \frac{1}{2}(1+f_B^{eq}(E_p))\log(T/m_q)\quad (\text{leading log in } m_q/T) \tag{2.38}$$

Using the integral

$$\int_{-\infty}^{\infty} \frac{dp_z}{(2\pi)} \frac{p_z^2}{TE_p} \frac{f_F^{eq}(E_p)(1-f_F^{eq}(E_p))^2}{(1+f_B^{eq}(E_p))} = \frac{T}{2\pi}\,, \quad m_q \to 0\,, \tag{2.39}$$

one has the small m_q limit as

$$\sigma_{zz} \to \frac{e^2}{\pi} \frac{\mathrm{d}imR}{C_2(R)} \left(\frac{eB}{2\pi}\right) \frac{T}{\alpha_s m_q^2 \log(T/m_q)}\,, \quad m_q \to 0\,. \tag{2.40}$$

This result can be easily generalized to the multi-flavor case. Writing the longitudinal conductivity in terms of dimensionless variables $\bar{p} = p_z/T$ and $\bar{m} = m_q/T$, and taking the sum of the flavor dependences arising from the electric charge (e_f) and mass ($\bar{m}_f$) of the fermion, one obtains

$$\sigma_{zz} = \sum_f e_f^2 \frac{\mathrm{d}imR}{C_2(R)} \left(\frac{e_f B}{2\pi}\right) \frac{1}{\alpha_s T} \sigma_L(\bar{m}_f)\,, \tag{2.41}$$

where

$$\sigma_L(\bar{m}) = \frac{2}{\bar{m}^2} \int_0^{\infty} \frac{d\bar{p}}{(2\pi)} \frac{\bar{p}^2}{\epsilon_{\bar{p}}} \frac{n_F(\epsilon_{\bar{p}})\,(1-n_F(\epsilon_{\bar{p}}))^2}{\int_0^\infty \frac{d\bar{p}'}{\epsilon_{\bar{p}'}} n_F(\epsilon_{\bar{p}'})(1+n_B(\epsilon_{\bar{p}}+\epsilon_{\bar{p}'}))}\,, \tag{2.42}$$

and $\epsilon_{\bar{p}} = \sqrt{\bar{p}^2 + \bar{m}^2}$ and $n_{F/B}(\epsilon) = 1/(e^\epsilon \pm 1)$. In the small $\bar{m} \to 0$ limit, one has

$$\sigma_L(\bar{m}) \to \frac{1}{\pi \bar{m}^2 \log(1/\bar{m})}\,, \tag{2.43}$$

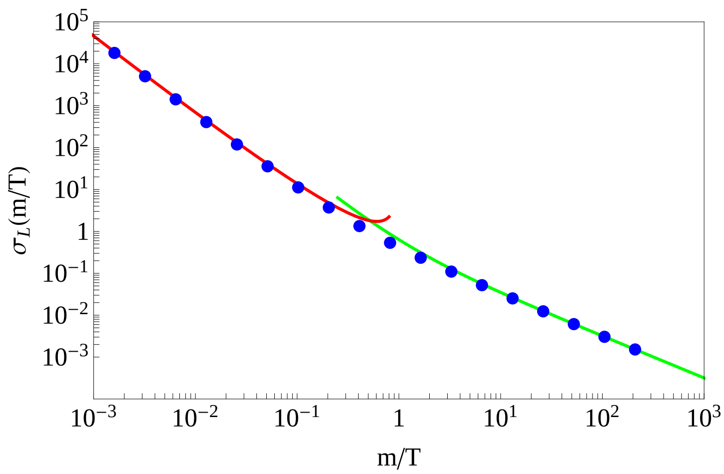

Figure 4: A plot of $\sigma_L(m_q/T)$ from numerical evaluations (blue dots), compared to the leading-log expression of m_q/T in Eq.(2.43) (red curve) and heavy quark limit Eq.(2.44) (green curve).

while, in the opposite limit ($\bar{m} \to \infty$),

$$\sigma_L(\bar{m}) \to \frac{1}{\pi \bar{m}} \,. \tag{2.44}$$

The full numerical evaluation of $\sigma_L(m_q/T)$ is showed in Figure 4, in comparison with the asymptotic expressions in the two limits. It shows that the analytic leading-log result Eq.(2.43) can be trusted when $m_q/T \lesssim 0.1$, and the heavy-quark limit Eq.(2.44) is reliable for $m_q/T \gtrsim 5$.

2.1.5 "Color conductivity" in the presence of Strong Magnetic field

The purpose of this subsection is devoted to evaluating the "color conductivity"[81] in the presence of a magnetic field. The "color conductivity" plays an important role in computing the sphaleron transition rate in the leading order of pQCD [73; 74]. In the effective Bodeker theory

[73], the color conductivity governing ultra-soft color magnetic field dynamics is responsible for non-perturbative sphaleron transitions. At such low frequency-momentum scales, the color field dynamics reduces to "magneto-hydrodynamics" where the magnetic fields diffuse at a rate given by the well-known diffusion-type dispersion formula

$$\omega \sim -i\frac{k^2}{\sigma_c}\,, \tag{2.45}$$

where σ_c is the color conductivity. Lenz's law indicates that the diffusion of a magnetic field is resisted by the Faraday current. In Eq.(2.45), the diffusion rate is inversely proportional to the color conductivity σ_c, due to the Faraday current is proportional to the conductivity σ_c. The Bodeker theory is a non-Abelian magneto-hydrodynamics with this color conductivity, with additional thermal noise from the fluctuation-dissipation relation that ensures equilibrium thermal distributions.

The key difference between non-abelian "color conductivity" and the usual abelian conductivity computed in the previous sections is that even scatterings with small momentum exchange (or small q_z scatterings in the case of LLL quarks) can contribute to the effective mean-free path of color transportation, since colors can be changed even without significant change of the momentum [81]. This means that the mean-free path of color transportation is determined by the (largest) damping rate, which is roughly a total scattering rate of a given hard quasi-particle, up to a color charge factor which is not important and we shall not precise about. One shall focus only on the parametric dependence of color conductivity on the coupling, magnetic field, temperature, and quark mass. Denoting the dominant damping rate by γ, the color conductivity is parametrically given by

$$\sigma_c \sim \alpha_s \, \frac{(\mathrm{d}ensity\ of\ states)/T}{\gamma}\,, \tag{2.46}$$

where α_s in front is a trivial coupling factor in the definition[1]. The rest of this subsection is devoted to computing the damping rate for both LLL quarks and the gluons.

The LLL quarks and/or antiquarks can only transport the color charges along the direction of the magnetic field, and the only charge carriers in the transverse direction are gluons. On the other hand, the LLL fermions have a larger density of states $(eB)T$ than that for the thermal gluons T^3(because of our assumption that $eB \gg T^2$), and one will find that the quark damping rate is parametrically smaller than the gluon damping rate by a factor of T^2/eB. Therefore, one concludes that the longitudinal color conductivity is larger than the transverse color conductivity by a factor of $(eB/T^2)^2 \gg 1$. A more detailed discussion about this implication in the sphaleron transition rate is at the end of this subsection.

One can easily read the damping rate of a quasi-particle of momentum p from the Boltzmann equation for $\chi(p)$ by keeping only $\chi(p)$ term in the collision term, dropping all other χ's with different momenta than p. Then the Boltzmann equation gives relaxation for $\chi(p)$ as

$$\partial_t \chi(p) = -\gamma_p \chi(p)\,, \tag{2.47}$$

---

[1] More precisely, the numerator is the phase space integral of $-\partial f^{eq}(p)/\partial p = \beta f^{eq}(p)(1 \pm f^{eq}(p))$.

with the damping rate γ_p (see Eq.(2.34) as an example). In this way, one finds how a particular single mode of momentum p relaxes to the equilibrium with the damping rate.

There are mainly three major contributions to the LLL quark damping rate: 1) 1-to-2 process, 2) 2-to-2 quark-quark/antiquark t-channel scatterings, and 3) 2-to-2 quark-gluon t-channel scatterings. Since t-channel scatterings are expected to be at least larger than s-channel by potential IR enhancement, these computations are enough to find the parametric dependence of the leading order damping rate of hard quarks.

The collision terms of all these processes are worked out in the other sections: 1) is in Sec.(2.1.3) and above point 2) and point 3) are in the Appendix 2.A.2, so one can easily use the results computed from these subsections. For instance, the damping rate from the 1-to-2 process is already given in Eq.(2.34), which one can easily reproduce it here,

$$\gamma_q^{1-2} = \frac{\alpha_s C_2(R) m_q^2}{E_p\left(1-f_F^{eq}(E_p)\right)} \int dp'_z \frac{1}{E_{p'}} f_F^{eq}(E_{p'})\left(1+f_B^{eq}(E_p+E_{p'})\right) \sim \alpha_s m_q^2/T\,,$$

where the last expression is the parametric estimate for a hard momentum $E_p \sim T$.

In the rest part of this subsection, let me skip all the tedious computations of the remaining damping rates(the detailed computation can be found in Ref.[1]) but give a quick summary of dominant quark and gluon damping rate:

1) When $m_q^2/T^2 \gg T^2/eB$,

$$\gamma_q \sim \alpha_s(m_q^2/T)\log\left(T^4 eB/\alpha_s m_q^6\right)\,, \quad \gamma_g \sim \alpha_s m_q^2/T\left(\frac{eB}{T^2}\right)\,.$$

2) When $m_q^2/T^2 \ll T^2/eB$,

$$\gamma_q \sim \alpha_s T \left(\frac{T^2}{eB}\right) , \quad \gamma_g \sim \alpha_s T \, .$$

As claimed before, the quark damping rate is parametrically smaller than the gluon damping rate by $T^2/eB \ll 1$. The resulting color conductivity from Eq.(2.46) is

1) When $m_q^2/T^2 \gg T^2/eB$,

$$\sigma_c^L \sim \frac{(eB)T}{m_q^2 \log\left(T^4 eB/\alpha_s m_q^6\right)} , \quad \sigma_c^T \sim \frac{T^5}{m_q^2 eB} \, .$$

2) When $m_q^2/T^2 \ll T^2/eB$,

$$\sigma_c^L \sim \frac{(eB)^2}{T^3} , \quad \sigma_c^T \sim T \, .$$

In terms of sphaleron transitions, the typical length scale is given by the magnetic scale $l_{sph}^{-1} = k \sim \alpha_s T$ while the time scale is governed by the magnetic diffusion time (Lenz's law) Eq.(2.45), $t_{sph}^{-1} \sim k^2/\sigma_c \sim \alpha_s^2 T^2/\sigma_c$, so the sphaleron transition rate scales as $\Gamma_s \sim (l_{sph}^{-1})^3 t_{sph}^{-1} \sim \alpha_s^5 T^5/\sigma_c$ [74]. The increased σ_c along the magnetic field (while the transverse color conductivity remains similar) would therefore reduce the transition rate. However, the σ_c to be used in this estimate should be the one defined at the spatial scale $k \sim \alpha_s T$, and if the mean free path (equivalently, the inverse damping rate γ^{-1}) that gives the above results for color conductivity is larger than this spatial scale, one needs to use $k^{-1} \sim (\alpha_s T)^{-1}$ instead as the effective mean free path to determine the σ_c used in the estimate for sphaleron transitions [74]. Considering this fact, one finds that the effective longitudinal σ_c^L to be used for sphaleron transitions becomes universally

$$\sigma_c^L(k \sim \alpha_s T) \sim \frac{eB}{T} \gg T\,, \tag{2.48}$$

while the transverse color conductivity is

$$\begin{aligned}
\sigma_c^T(k \sim \alpha_s T) &\sim \frac{T^5}{m_q^2 eB} \lesssim T \quad (\text{when } m_q^2/T^2 \gtrsim T^2/eB)\,, \\
\sigma_c^T(k \sim \alpha_s T) &\sim T \qquad\qquad\quad (\text{when } m_q^2/T^2 \ll T^2/eB)\,.
\end{aligned} \tag{2.49}$$

The σ_c^L is larger than the usual value $T/\log(1/\alpha_s)$, while σ_c^T remains similar to, means that the sphaleron transition rate will be smaller in the presence of strong magnetic field due to the enhanced Lenz's law in color field dynamics, as claimed in Sec.(2.1.1).

2.2 Shear viscosity of Quark-Gluon Plasma in the presence of weak magnetic field

(Previously published as: S. Li and H.-U. Yee, Shear viscosity of the quark-gluon plasma in a weak magnetic field in perturbative QCD: Leading log, Phys. Rev. D97, 056024 (2018))

2.2.1 Motivation and Summary

The shear viscosity of QCD plasma in the presence of a magnetic field in a high enough temperature(where pQCD can be applied) is computed in this section. This study is motivated by the off-central heavy-ion collisions, where a huge magnetic field, albeit transient, is present and may affect the time evolution of the created QGP fireball [8]. The typical strength of the magnetic field at very early time is $eB \sim (200 - 400\ MeV)^2$ [63; 10; 9; 82], however it quickly reduces to one-tenth of its initial strength after about 1 fm/c, beyond which it remains more or less constant over a few fm/c due to the Lenz effect [83; 84]. Compared to the expected temperature of the QGP of about $250 - 400$ MeV, the scale of the magnetic field is comparable to the temperature initially but becomes smaller in most of the stages after 1 fm/c. This motivates us to assume that the strength of the magnetic field is parametrically smaller than the temperature (that is, $eB \ll T^2$) in powers of coupling constant $g \ll 1$ in the leading pQCD computation. One should be aware that our assumption with a particular g-dependence of magnetic field described in next Sec.(2.2.2) is not entirely motivated by the experiments, but also by the practical reason that we can perform a reliable and interesting (at least to our eyes) pQCD computation with this assumption. A systematic pQCD computation of shear viscosity either in the weak magnetic field limit that we study in this work or in the strong magnetic field limit (that is, $eB \gg T^2$) is required. Computation of bulk viscosity in strong magnetic field limit is given in Ref.[85]. See also Ref.[86] for the shear viscosity in the magnetic field in the AdS/CFT correspondence for strong coupling regime.

A simplified set-up where the magnetic field is homogeneous and static is assumed. This also means that one can neglect back reactions from the plasma to the electromagnetic fields, that is, one does not consider the dynamics of electrodynamics, hence the magnetic field is treated as an external environment (for example, there is no induced electric field). This approximation can be formally justified in the limit where the electric coupling that governs the back reaction goes to zero $e \to 0$ while keeping eB fixed. Note that the Lenz effect mentioned above is due to the backreaction from the plasma to the magnetic field. Therefore, this interesting limit itself is purely from the point of view of theoretical nature and is not driven by any experimental conditions. As one will find out in the next subsection that in this case, the components of fluid velocity transverse to the magnetic field direction *freeze* to zero, that is, they decay with a finite relaxation rate even in a zero spatial gradient limit, so that they are no longer long-lived hydrodynamics variables in the emerging new hydrodynamics at a sufficient low momentum regime. The transport coefficients in this new effective hydrodynamics at low energy are identified, and it is shown that there are only one shear viscosity and two bulk viscosities surviving in this regime. Only the shear viscosity is considered and computed in this section.

If one considers a more realistic case of dynamical electromagnetism(EM) coupled to the plasma, it is well known that there emerges new hydrodynamics at scales below $k < \sigma$ (σ is the conductivity), noted as magnetohydrodynamics (MHD) (see Refs.[87; 88; 89; 90] for recent developments of relativistic MHD). The hydrodynamics variables of MHD are the magnetic field in the local rest frame, $B^\mu \equiv \epsilon^{\mu\nu\alpha\beta}u_\nu F_{\alpha\beta}$, and the fluid velocity u^μ, while the electric field in the local rest frame $E^\mu = u_\nu F^{\mu\nu}$ and the local charge density $n = u_\mu j^\mu$ decay to zero with a finite relaxation time $\tau \sim 1/\sigma$ and are thus excluded in the hydrodynamics variables of MHD by the same reason as above. Note that in the lab frame, $E^\mu \propto \vec{E} + \vec{v} \times \vec{B}$. In more physical terms, what is happening is that for any $\vec{v}$ and $\vec{B}$, the plasma back-reacts to Lorentz force via induced currents to ensure that $\vec{E}$ relaxes to the $l$ocal equilibrium value $\vec{E}_{eq} = -\vec{v} \times \vec{B}$ within a time scale $1/\sigma$ (it is the local equilibrium value since E^μ is the electric field in the local rest frame of fluid which should vanish in order to achieve equilibrium condition). In the presence of a background magnetic field $\vec{B}_0$ in this set-up, this essentially fixes the electric field fluctuations in terms of transverse velocity fluctuations to the magnetic field at the linearized level: $\delta\vec{E} = -\delta\vec{v} \times \vec{B}_0$. The ensuing MHD equations of motion give rise to a propagating wave of these fluctuations along the background magnetic field, called Alfven wave with velocity $v_A^2 = B_0^2/(\epsilon + p + B_0^2)$ (ϵ and p are energy density and pressure). It is also worth pointing out that there are currently many efforts to simulate the heavy-ion collisions with dynamical electromagnetism coupled to the plasma fireball Refs.[91; 92], aiming at reliable theoretical predictions of various transport phenomena associated with magnetic and electric fields, such as the Chiral Magnetic Effect [11; 93], the charge-dependent elliptic flows [14; 94] and the slope of v_1 in rapidity due to Lorentz force [95].

In our simplified limit of non-dynamical electromagnetism ($e \to 0$), we don't have such an MHD regime, noting that σ is proportional to e^2 in our convention, so the time scale for the

MHD is arbitrarily long and is never realized. Instead, we can make the following connection between the above discussion and our limit of non-dynamical electromagnetism: in our limit of non-dynamical electromagnetism, let's work in the lab frame where $\vec{E} = 0$ always, while $\vec{B} = \vec{B}_0$ is a fixed external field. Making $E^\mu \sim \vec{v} \times \vec{B}_0 = 0$ for local equilibrium is only possible with the transverse components of velocity to the magnetic field vanishing. This is the ultimate reason why the transverse velocity is excluded in the low energy description in our limit (note that the transverse velocity is *not* excluded in the MHD. Only the combination $\vec{E} + \vec{v} \times \vec{B}_0$ is excluded in the MHD and $\vec{v}$ can be an independent MHD variable). However, the relaxation mechanism (and therefore the relaxation time) is different from that in the MHD via dynamical Maxwell's equation: in our case, it will be shown in Eq.(2.52) that it comes solely from the induced current and the associated Lorentz force (without any dynamical Maxwell equations) with the relaxation time $\tau \sim \frac{(\epsilon+p)}{\sigma B_0^2}$, which is finite in our limit recalling that σ contains e^2 and eB_0 is finite in our $e \to 0$ limit. The new low energy hydrodynamics in our limit appears in the scales $k < 1/\tau$.

In summary, in the case of dynamical EM (either with or without a background magnetic field), there appears a new low energy effective hydrodynamics, called the MHD in the scales $k < 1/\sigma$. The hydrodynamical variables of the MHD are significantly reduced compared to the original “microscopic hydrodynamics” that is valid when $k > 1/\sigma$. In our case of non-dynamical electrodynamics ($e \to 0$) with a finite background magnetic field $eB_0 \neq 0$, there appears new low energy hydrodynamics at the scales $k < \frac{\sigma B_0^2}{\epsilon+p}$. The hydrodynamics variables in this low energy hydrodynamics are also reduced compared to the microscopic hydrodynamics, and one such reduction leads to the absence of the transverse velocity to the background magnetic field (if there is no other external electromagnetic field applied). As explained in the paragraph around Eq.(2.59) in the next section, another reduction is the absence of transverse charge current and hence the transverse conductivity in a neutral plasma[1].

It is worth emphasizing that our consideration of hydrodynamics in a background magnetic field is not at all new, and there are several previous studies on the subject with notable progress [87; 18; 88; 89], and it is pertinent to summarize how our low energy effective hydrodynamics and the corresponding shear viscosity is related to those studies. One important criterion in this comparison is whether electrodynamics is assumed to be dynamical or non-dynamical. For example, Ref.[86] works with non-dynamical electrodynamics, the Refs.[87; 18] consider the dynamical case, and the Ref.[88] considered both non-dynamical and dynamical cases. In the non-dynamical case, our result for the relaxation time $\tau \sim \frac{(\epsilon+p)}{\sigma B_0^2}$ in fact agrees the one in Ref.[88], for example Eq.(3.14) in a neutral case. The difference is not about the result, but instead about what energy regime we are focusing on, and what effective description we have for different regimes. Since the dispersion Eq.(3.14) in Ref.[88] is not truly hydrodynamic as it doesn't vanish in $k \to 0$ limit, this mode corresponding to transverse velocity is excluded in a sufficiently low momentum regime. In the dynamical case, on the other hand, since the full components of fluid velocity remain as the hydrodynamics variables in the MHD, and a back-

---

[1] If the plasma is charged with a charge density n, then there exists a Hall current $\vec{j} = n\vec{v}_{eq} = n\frac{\vec{E}_\perp \times \vec{B}_0}{B_0^2}$ in response to an external small electric field $\vec{E}_\perp$. See for example, Ref.[96] for a recent study. In this work, a relativistic neutral plasma is considered and the Hall effect is absent.

ground magnetic field breaks rotational invariance, there naturally appear five different shear viscosities corresponding to five different shear gradient modes with respect to the magnetic field direction, nicely classified in Refs.[87; 18; 88]. As explained in above, the MHD regime is pushed to zero momentum (that is, $k < \sigma \to 0$) in the limit of non-dynamical electromagnetism ($e \to 0$), and there is no overlap between the MHD regime and the regime of our low energy effective hydrodynamics in the non-dynamical limit: $k < \frac{\sigma B_0^2}{(\epsilon+p)}$, so there is no logical correspondence that can be made between these five shear viscosities and our shear viscosity. Computation of these five shear viscosities in the MHD regime, therefore, remains an open question.

However, in either case, if the momentum scale is higher than the relaxation scale of σ or $\frac{\sigma B_0^2}{(\epsilon+p)}$, so that we go to the regime of "microscopic" hydrodynamics, the full component of velocity is included in the hydrodynamics variables, and the five different shear viscosities make sense in this "UV" regime. The results in Refs.[86; 88] for the non-dynamical case should be viewed in this way. Then, our shear viscosity can be considered as the low energy limit of (one of) those five "UV" shear viscosities, while the other four viscosities lose their meaning in the new low energy hydrodynamics (in fact, two of the five viscosities in Ref.[18], η_3 and η_4, are odd under charge-conjugation and they vanish identically in the neutral plasma $n = 0$ that we are considering, irrespective of the regimes. If we relax the neutrality condition, we also show in the Appendix.(2.B.1) that we have one more shear viscosity coming from η_4 of Ref.[18] surviving in our low energy regime. The same is true for the Hall conductivity, see the footnote on the previous page).

In summary, the five shear and two bulk viscosities in the Refs.[86; 88] in the case of non-dynamical electromagnetism are for the "microscopic hydrodynamics" in high momentum regime and the framework needs to be replaced by our new hydrodynamics at sufficiently low momentum scales. In the Appendix of Ref.[2], we explicitly showed that the five shear and two bulk viscosities classified in Ref.[18] reduce to our one shear and two bulk viscosities in a *neutral* plasma when we remove the transverse components of fluid velocity in the low energy limit [1].

2.2.2 Low energy effective hydrodynamics in magnetic field

In this subsection, I present the framework showing that there emerges a new effective low energy hydrodynamics at sufficiently low scales from a *neutral* plasma in the presence of a non-dynamical external magnetic field. It is shown that the hydrodynamic variables are reduced in this low energy hydrodynamics. Specifically, as one will find that the transverse components of velocity perpendicular to the magnetic field disappear in this regime, and there is only *one* meaningful notion of shear viscosity in these effective hydrodynamics emerging at sufficiently low energy regime.

As in the conventional approach, hydrodynamics describes the modes that live arbitrarily long when their spatial gradient is arbitrarily small. This can only be possible if these modes correspond to the parameters characterizing possible equilibrium states so that they stay constant when they are homogeneous. All other modes have finite relaxation times even in the

[1] Note that the classification in Ref.[18] rely only on the tensor structures thus symmetries can be applied to any regime, either in the MHD regime or in the "UV" regime

homogeneous limit, and are excluded in the hydrodynamic description at a sufficiently low energy regime: they are quasi-normal modes. To construct hydrodynamics in a non-dynamical magnetic field, one should first identify all equilibrium parameters of the plasma in the presence of an external magnetic field. To be specific, let's assume the magnetic field is along z-direction in a fixed lab frame, $e\boldsymbol{B} = eB\hat{\boldsymbol{z}}$. Detailed balance with energy conservation gives us the temperature T as one of such parameters. Without a magnetic field, the momentum conservation would give us a vector parameter, the fluid velocity $\boldsymbol{v}$, as another parameter for equilibrium. However, in the presence of an external magnetic field, the transverse momentum perpendicular to $\hat{z}$ direction is not conserved due to Lorentz force, and only the longitudinal momentum along the magnetic field direction is conserved. One, therefore, expects that the longitudinal fluid velocity, $v_\parallel = v_z$, remains as an equilibrium parameter, but $\boldsymbol{v}_\perp$ is no longer an equilibrium parameter and should be excluded in the emerging low-energy hydrodynamics with an external magnetic field. One can easily show that $\boldsymbol{v}_\perp$ indeed becomes a quasi-normal mode in the following.

Let's assume the existence of conventional hydrodynamics valid in the regime where the magnetic field can be treated as a first-order in gradient expansion, namely, one can call this "microscopic hydrodynamics". The 4-velocity $u^\mu = (\gamma, \gamma\boldsymbol{v})$ is a hydrodynamic variable in this microscopic hydrodynamics. The current in this regime is given by

$$j^\mu = \sigma E^\mu\,, \quad E^\mu \equiv F^{\mu\nu}u_\nu\,, \tag{2.50}$$

where σ is the conductivity. In non-relativistic limit $\gamma \approx 1$ with a finite $\boldsymbol{v}_\perp$, the spatial component of the current becomes,

$$\boldsymbol{j} = \sigma \boldsymbol{v}_\perp \times \boldsymbol{B}\,, \tag{2.51}$$

whose origin is nothing but the Lorentz force in the lab frame, or equivalently the Ohmic current in the rest frame of the fluid. From the transverse component of the energy-momentum conservation, $\partial_\mu T^{\mu\nu} = F^{\nu\alpha} j_\alpha$ (which originates from Lorentz force again), and the constitutive relation $T^{0\perp} = (\epsilon + p)\boldsymbol{v}_\perp$, one has

$$\partial_t \boldsymbol{v}_\perp = \frac{1}{(\epsilon+p)} \boldsymbol{j} \times \boldsymbol{B} = -\frac{\sigma B^2}{(\epsilon+p)} \boldsymbol{v}_\perp \equiv -\frac{1}{\tau_R} \boldsymbol{v}_\perp\,, \tag{2.52}$$

which means that $\boldsymbol{v}_\perp$ is a quasi-normal mode with a relaxation time τ_R. In the emerging low-energy hydrodynamics, $\boldsymbol{v}_\perp$ no longer can be treated as a hydrodynamic variable in the energy regime smaller than $1/\tau_R$.

The low energy hydrodynamic variables are T and v_z (or equivalently 1+1 dimensional velocity vector $u_\parallel^\mu$ where μ runs only along (t, z) and it is normalized as $u_\mu u^\mu = -1$), which vary slowly in space-time: $T(x)$, $u_\parallel^\mu(x)$. Note that the variation can happen along the transverse direction as well as in the longitudinal direction. In the Appendix of Ref.[2], it is shown that the energy-momentum tensor up to first order in gradient generally takes a form,

$$T^{\mu\nu} = (\epsilon + p_\parallel) u_\parallel^\mu u_\parallel^\nu + p_\parallel g_\parallel^{\mu\nu} + p_\perp g_\perp^{\mu\nu} - \eta(\partial_\perp^\mu u_\parallel^\nu + \partial_\perp^\nu u_\parallel^\mu) - (\zeta(u_\parallel^\mu u_\parallel^\nu + g_\parallel^{\mu\nu}) + \zeta' g_\perp^{\mu\nu})(\partial_{\parallel\alpha} u_\parallel^\alpha)\,, \tag{2.53}$$

with one shear viscosity η and two bulk viscosities (ζ, ζ'). In the following, I shall present the details of the computation of η. Choosing metric convention to be $g^{\mu\nu} = (-1, +1, +1, +1)$, where the first two indices correspond to 1+1 dimension of (t, z) and the last two the transverse dimensions $x_\perp = (x, y)$. Let's define $g_\parallel^{\mu\nu} = (-1, 1, 0, 0)$, $g_\perp^{\mu\nu} = (0, 0, 1, 1)$, $\partial_\parallel^\mu = (-\partial_t, \partial_z, 0, 0)$, $\partial_\perp^\mu = (0, 0, \partial_x, \partial_y)$, and $u_\parallel^\mu = \gamma(1, v_z, 0, 0)$ where $\gamma = (1 - v_z^2)^{-\frac{1}{2}}$. The combination $(u_\parallel^\mu u_\parallel^\nu + g_\parallel^{\mu\nu}) \equiv \Delta_\parallel^{\mu\nu}$ is the rest-frame space projection operator orthogonal to $u_\parallel^\mu$ in 1+1 dimensions, and $g_\perp^{\mu\nu} = \Delta_\perp^{\mu\nu}$ is the space projection to the transverse (x, y) dimensions (see Appendix of Ref.[2] for a detailed discussion). Let's take only the first three ideal parts, then one simply has in components in the rest frame of the fluid (where $u_\parallel^\mu = (1, 0, 0, 0)$)

$$T^{\mu\nu}_{ideal} = (\epsilon, p_\parallel, p_\perp, p_\perp)\,, \tag{2.54}$$

which is the most general form of the ideal energy-momentum in a rest frame with a magnetic field [1]. The ideal part of Eq.(2.53) is obtained by boosting this along the z direction by $u_\parallel^\mu$. In non-relativistic limit, the shear viscosity appears as

$$T^{\perp z} = -\eta \partial_\perp v_z\,, \tag{2.55}$$

and the following computation is based on this.

---

[1]Recall that the magnetic field is invariant under the boost direction, so it is the same in an arbitrary fluid rest frame

Although this is not the main subject in this study, it is worth mentioning and following the same logic to find that there is no notion of transverse electric conductivity in the emerging low energy hydrodynamics with an external magnetic field. Let's apply a small transverse electric field $\boldsymbol{E}_\perp$ so that $|\boldsymbol{E}_\perp| \ll |\boldsymbol{B}|$. The microscopic hydrodynamics gives the current from $j^\mu = \sigma E^\mu$ as

$$\boldsymbol{j} = \sigma(\boldsymbol{E}_\perp + \boldsymbol{v}_\perp \times \boldsymbol{B})\,, \tag{2.56}$$

and the energy-momentum conservation gives the equation

$$\partial_t \boldsymbol{v}_\perp = \frac{1}{(\epsilon+p)}\boldsymbol{j}\times\boldsymbol{B} = \frac{\sigma}{\epsilon+p}\left(\boldsymbol{E}_\perp\times\boldsymbol{B} - B^2\boldsymbol{v}_\perp\right) = -\frac{1}{\tau_R}(\boldsymbol{v}_{eq} - \boldsymbol{v}_\perp)\,, \tag{2.57}$$

where the equilibrium transverse velocity $\boldsymbol{v}_{eq}$ is

$$\boldsymbol{v}_{eq} = \frac{\boldsymbol{E}_\perp \times \boldsymbol{B}}{B^2}\,. \tag{2.58}$$

The above equation tells us that the transverse velocity relaxes to $\boldsymbol{v}_{eq}$ with the same relaxation time τ_R, that is, any deviation from $\boldsymbol{v}_{eq}$ is a quasi-normal mode in the low energy hydrodynamics. With $\boldsymbol{v}_{eq}$, the current vanishes

$$\boldsymbol{j} = \sigma(\boldsymbol{E}_\perp + \boldsymbol{v}_{eq} \times \boldsymbol{B}) = 0\,. \tag{2.59}$$

This result can be understood in the following way: the frame moving with velocity $\boldsymbol{v}_{eq}$ is precisely the frame where the electric field vanishes and there exists only a non-zero magnetic field. In such a frame, the transverse velocity should relax to zero with the relaxation time τ_R according to the previous discussion. In the original lab frame, this is equivalent to the relaxation of the velocity to $\boldsymbol{v}_{eq}$. Since there is no electric field in the equilibrium rest frame, the current vanishes in this frame and hence in the original frame as well (recall that our plasma is neutral).

However, the situation is different when $|\boldsymbol{E}_\perp| > |\boldsymbol{B}|$ and there is no such frame where electric field vanishes. Instead, one has a frame moving with velocity $\boldsymbol{v}_\perp = \frac{\boldsymbol{E}_\perp \times \boldsymbol{B}}{E_\perp^2}$ where the magnetic field vanishes, and the electric field becomes

$$\boldsymbol{E}'_\perp = \boldsymbol{E}_\perp \left(1 - \frac{B^2}{E_\perp^2}\right) . \tag{2.60}$$

One then has a current

$$\boldsymbol{j} = \sigma \boldsymbol{E}'_\perp = \sigma \boldsymbol{E}_\perp \left(1 - \frac{B^2}{E_\perp^2}\right) \Theta(E_\perp - B) . \tag{2.61}$$

2.2.3 QCD Boltzmann equation in leading log

In this section, I provide the technical details of the computation of shear viscosity in weak/soft magnetic field in pQCD. More explicitly, let's assume that the magnetic field is weak or soft in the sense that its scale is comparable to the effective 2-to-2 QCD collision rate in the leading log, or more precisely,

$$eB \sim g^4 \log(1/g) T^2 \ll T^2 \,. \tag{2.62}$$

In this case, one will see later that the shear viscosity in leading log takes a form

$$\eta = \bar{\eta}(\bar{B}) \frac{T^3}{g^4 \log(1/g)} \,, \quad \bar{B} \equiv \frac{eB}{g^4 \log(1/g) T^2} \,, \tag{2.63}$$

with a dimensionless function $\bar{\eta}(\bar{B})$. A full numerical result for this function in the massless $N_F = 2$ QCD is shown in Sec.(2.2.4). In the limit $eB \to 0$, it reduces to the previously known shear viscosity without magnetic field in leading log order [61].

In this regime, the magnetic field appears only in the advective term in the effective Boltzmann kinetic theory, and its effects on the QCD collision term is of higher-order and sub-leading compared to the usual leading order collision term $\mathcal{C}$ which is already of order $\mathcal{C} \sim g^4 \log(1/g) T$. This is because the dominant energy-momentum carriers responsible for the shear viscosity are hard particles of momentum $p \sim T$, and possible corrections from the magnetic field to the dispersion relation of hard particles are suppressed by $\sqrt{eB}/T \sim g^2$. It is for the same reason that the leading order collision term is obtained by using free dispersion relations of external hard particles without thermal corrections. Moreover, the screening mass (or the Debye mass) is of order $m_D \sim gT$ that regulates IR divergences of t-channel collision terms between these hard particles should also be the one without the magnetic field corrections. This is because the screening mass is provided by "hard thermal 1-loop", that is, the screening is provided by hard particles themselves. Any correction to the dispersion relation of these hard particles is of order $\sqrt{eB}/T \sim g^2$, and therefore the correction to m_D from magnetic field is naturally of order $m_D \times \sqrt{eB}/T \sim m_D g^2$. Since the net collision term is already of $\mathcal{C} \sim g^4 \log(1/g)T$, the correction to $\mathcal{C}$ from the correction to the screening mass is of a higher order than this, which is not relevant in our computation.

Any remaining effect of eB can only appear in the possible on-shell singularity in quark propagators with a long-lived intermediate fermion interacting with the background eB field, that may have an IR enhancement. But, this is precisely what the advective term of the Boltzmann equation captures. The effect of background eB on the long-lived charged quasi-particles is described by the Lorentz force in the advective term,

$$\frac{\partial f}{\partial t} + \hat{\boldsymbol{p}} \cdot \frac{\partial f}{\partial \boldsymbol{x}} + \dot{\boldsymbol{p}} \cdot \frac{\partial f}{\partial \boldsymbol{p}} = \mathcal{C}[f] \,, \quad \dot{\boldsymbol{p}} = \pm q_F \hat{\boldsymbol{p}} \times (e\boldsymbol{B}) \,, \tag{2.64}$$

where $q_F = (\frac{2}{3}, -\frac{1}{3})$ for (u, d)-quarks, and also $\pm$ refers to quark and anti-quark, respectively.

Another way of thinking about it is in terms of time scales. The space-time duration of each collision, l_{coll}, satisfies $T^{-1} \ll l_{coll} \ll (gT)^{-1}$, due to the fact that the log-enhancement in the t-channel 2-to-2 processes arises from the momentum exchanges lying between gT and T. This time scale is much shorter than the time scale of cyclotron orbits induced by a magnetic field which is $l_{cyclo} \sim p/(eB) \sim (g^4 \log(1/g)T)^{-1}$, so that each collision look localized during any significant cyclotron motion, and are not affected by the magnetic field. This is why $\mathcal{C}$ in the

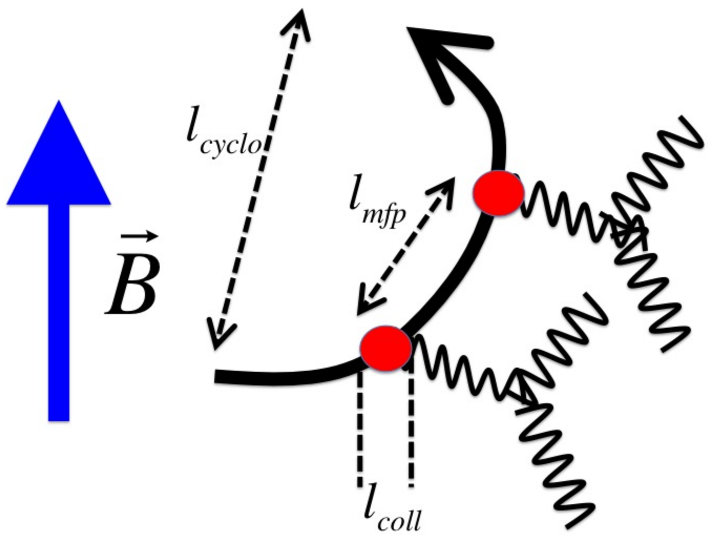

Figure 5: The meaning of the three length scales, l_{coll}, l_{mfp} and l_{cyclo}.

Boltzmann equation remains the same. However, the inverse rate of large-angle collisions, or equivalently the mean-free distance *between* each collisions is $l_{mfp} \sim \mathcal{C}^{-1} \sim (g^4 \log(1/g)T)^{-1}$, which is comparable to l_{cyclo}. This means that the cyclotron motions and the QCD collisions are equally important in the transport dynamics of hard particles. Therefore, one has to solve the above Boltzmann equation keeping both the Lorentz force term and the collision term $\mathcal{C}$, to capture the interplay between cyclotron motions and the QCD collisions. The dimensionless variable $\bar{B}$ in Eq.(2.63) corresponds to the relative strength of the effect of cyclotron motions compared to the QCD collisions: $\bar{B} \sim l_{mfp}/l_{cyclo}$.

To compute the shear viscosity, one considers the kinetic theory of quarks/anti-quarks and gluons, whose distribution functions $(f^q, f^{\bar{q}}, f^g)$ satisfy the following Boltzmann equation with leading log collision term,

$$\begin{aligned}
\partial_t f^q + \hat{\boldsymbol{p}}\cdot\partial_{\boldsymbol{x}} f^q + q_F e(\hat{\boldsymbol{p}}\times\boldsymbol{B})\cdot\partial_{\boldsymbol{p}} f^q &= \mathcal{C}^q\,,\\
\partial_t f^{\bar{q}} + \hat{\boldsymbol{p}}\cdot\partial_{\boldsymbol{x}} f^{\bar{q}} - q_F e(\hat{\boldsymbol{p}}\times\boldsymbol{B})\cdot\partial_{\boldsymbol{p}} f^{\bar{q}} &= \mathcal{C}^{\bar{q}}\,,\\
\partial_t f^g + \hat{\boldsymbol{p}}\cdot\partial_{\boldsymbol{x}} f^g &= \mathcal{C}^g\,.
\end{aligned} \tag{2.65}$$

The equilibrium distribution with an arbitrary longitudinal velocity $u^\mu_\parallel = \gamma(1, v_z, \boldsymbol{0}_\perp)$, $\gamma \equiv (1-v_z^2)^{-\frac{1}{2}}$ satisfies the detailed balance (that is, $\mathcal{C}=0$), and is a solution of the Boltzmann equation since $(\hat{\boldsymbol{p}}\times\boldsymbol{B})\cdot\partial_{\boldsymbol{p}} f_{eq} = 0$,

$$f^{q,\bar{q},g}_{eq}(\boldsymbol{p}, u^\mu_\parallel) = 1/(e^{-\frac{1}{T}p_\mu u^\mu_\parallel} \pm 1)\,,\quad p^\mu = (|\boldsymbol{p}|, \boldsymbol{p})\,. \tag{2.66}$$

When there is a non-zero gradient of $u^\mu_\parallel$ or v_z along the transverse space, $\partial_\perp v_z \neq 0$, the collision term which is local in space-time still vanishes with the above distribution, but the spatial gradient term in the advective term on the left no longer vanishes. Considering the local rest frame of a point $x = 0$ in space-time where the velocity is expanded in first order gradient as $v_z = (\partial_\perp v_z)x_\perp + \mathcal{O}(x_\perp^2)$, one has

$$\hat{\boldsymbol{p}}\cdot\partial_{\boldsymbol{x}} f_{eq}(\boldsymbol{p}, u^\mu_\parallel(x))\Big|_{x=0} = (\hat{\boldsymbol{p}}_\perp\cdot\partial_\perp v_z)\beta p_z n_{F/B}(\boldsymbol{p})(1\mp n_{F/B}(\boldsymbol{p}))\,,\quad \beta = 1/T\,, \tag{2.67}$$

where $n_{F/B}$ is the Fermi-Dirac/Bose-Einstein distribution function $n_{F/B}(\boldsymbol{p}) = 1/(e^{\beta|\boldsymbol{p}|} \pm 1)$. This gradient term acts as a source for the disturbance of the distribution function away from the local equilibrium given by $f_{eq}(\boldsymbol{p}, u_{\parallel}^{\mu}(x))$. The solution of the Boltzmann equation in linear order in $(\partial_\perp v_z)$ at the point $x = 0$ is then

$$f = f_{eq}(\boldsymbol{p}, u_{\parallel}^{\mu}(x)) + \delta f(\boldsymbol{p}) \,, \tag{2.68}$$

where δf satisfies the linearized Boltzmann equation

$$\begin{aligned}
(\hat{\boldsymbol{p}}_\perp \cdot \partial_\perp v_z)\beta p_z n_F(\boldsymbol{p})(1 - n_F(\boldsymbol{p})) + q_F e(\hat{\boldsymbol{p}}_\perp \times \boldsymbol{B}) \cdot \partial_{\boldsymbol{p}} \delta f^q &= \mathcal{C}^q[\delta f^q, \delta f^{\bar{q}}, \delta f^g] \,, \\
(\hat{\boldsymbol{p}}_\perp \cdot \partial_\perp v_z)\beta p_z n_F(\boldsymbol{p})(1 - n_F(\boldsymbol{p})) - q_F e(\hat{\boldsymbol{p}}_\perp \times \boldsymbol{B}) \cdot \partial_{\boldsymbol{p}} \delta f^{\bar{q}} &= \mathcal{C}^{\bar{q}}[\delta f^q, \delta f^{\bar{q}}, \delta f^g] \,, \\
(\hat{\boldsymbol{p}}_\perp \cdot \partial_\perp v_z)\beta p_z n_B(\boldsymbol{p})(1 + n_B(\boldsymbol{p})) &= \mathcal{C}^g[\delta f^q, \delta f^{\bar{q}}, \delta f^g] \,,
\end{aligned} \tag{2.69}$$

where one assumes that a stationary state $\partial_t = 0$ is achieved in the time scale much longer than the expected relaxation time $1/\tau_R \sim g^4 \log(1/g) T$ that defines the boundary of the low energy hydrodynamics.

Once δf is found from the above equations, the energy momentum tensor of our interest is computed as

$$T^{\perp z} = \int \frac{d^3\boldsymbol{p}}{(2\pi)^3} \frac{\boldsymbol{p}_\perp p_z}{E_{\boldsymbol{p}}} \left(\nu_q \sum_F (\delta f^q + \delta f^{\bar{q}}) + \nu_g \delta f^g \right) \,, \tag{2.70}$$

where $\nu_q = 2N_c = 2d_q$ and $\nu_g = 2(N_c^2 - 1) = 2d_A$ are the number of states of quarks/anti-quarks or gluons with a given momentum $\boldsymbol{p}$. (d_q and d_A are the dimensions of color representation). Comparing the result with Eq.(2.55), one obtains the shear viscosity η.

The leading log QCD collision term has been well known in literature starting from Refs.[59; 60] culminating in the full determination in Ref.[61]. It was nicely re-derived and summarized in Ref.[97] and let's follow the notations of Ref.[97]. There are two types of contributions to the leading log collision term: I) t-channel soft gluon exchanges and II) t-channel soft fermion exchanges. The type I processes do not change the particle species and give rise to diffusions in momentum space, whereas the type II processes convert fermions into gluons and vice versa. Writing δf as

$$\delta f^a = n_{F/B}(1 \mp n_{F/B})\chi^a\,, \quad a = q, \bar{q}, g\,, \tag{2.71}$$

the linearized collision term is obtained by

$$\mathcal{C}^a[\delta f(\boldsymbol{p})] = -\frac{(2\pi)^3}{\nu_a}\frac{\delta \mathcal{I}[\chi]}{\delta \chi^a(\boldsymbol{p})}\,, \tag{2.72}$$

where $\mathcal{I} = \mathcal{I}^I + \mathcal{I}^{II}$ with

$$
\begin{aligned}
\mathcal{I}^I &= \frac{Tm_D^2 g^2 \log(1/g)}{16\pi} \sum_a C_a \nu_a \int_{\boldsymbol{p}} n_a(\boldsymbol{p})(1 \mp n_a(\boldsymbol{p})) \left(\frac{\partial \chi^a(\boldsymbol{p})}{\partial \boldsymbol{p}^i}\right)^2 \\
&- \frac{g^4 \log(1/g)}{16\pi d_A} \left(\sum_a C_a \nu_a \int_{\boldsymbol{p}} n_a(\boldsymbol{p})(1 \mp n_a(\boldsymbol{p})) \left(\hat{\boldsymbol{p}} \cdot \frac{\partial \chi^a(\boldsymbol{p})}{\partial \boldsymbol{p}}\right)\right)^2 \\
&- \frac{g^4 \log(1/g)}{16\pi d_A} \left(\sum_a C_a \nu_a \int_{\boldsymbol{p}} n_a(\boldsymbol{p})(1 \mp n_a(\boldsymbol{p})) \frac{\partial \chi^a(\boldsymbol{p})}{\partial \boldsymbol{p}^i}\right)^2 , \qquad (2.73) \\
\mathcal{I}^{II} &= \gamma \sum_{a=q,\bar{q}} \nu_a \int_{\boldsymbol{p}} \frac{1}{|\boldsymbol{p}|} n_F(\boldsymbol{p})(1 + n_B(\boldsymbol{p})) \left(\chi^a(\boldsymbol{p}) - \chi^g(\boldsymbol{p})\right)^2 \\
&+ \frac{16\gamma}{T^2} \sum_{a=q} \nu_a \int_{\boldsymbol{p}} \frac{1}{|\boldsymbol{p}|} n_F(\boldsymbol{p})(1 + n_B(\boldsymbol{p})) \left(\chi^a(\boldsymbol{p}) - \chi^g(\boldsymbol{p})\right) \int_{\boldsymbol{k}} \frac{1}{|\boldsymbol{k}|} n_F(\boldsymbol{k})(1 + n_B(\boldsymbol{k})) \left(\chi^{\bar{a}}(\boldsymbol{k}) - \chi^g(\boldsymbol{k})\right) \\
&- \frac{8\gamma}{T^2} \sum_{a=q,\bar{q}} \nu_a \left(\int_{\boldsymbol{p}} \frac{1}{|\boldsymbol{p}|} n_F(\boldsymbol{p})(1 + n_B(\boldsymbol{p})) \left(\chi^a(\boldsymbol{p}) - \chi^g(\boldsymbol{p})\right)\right)^2 , \qquad (2.74)
\end{aligned}
$$

where C_a is the quadratic Casimir of the species a and $\int_{\boldsymbol{p}} \equiv \int \frac{d^3\boldsymbol{p}}{(2\pi)^3}$ and

$$
m_D^2 = \frac{g^2 T^2}{3}\left(N_c + \frac{N_F}{2}\right) , \quad \gamma = \frac{C_F^2 T^2 g^4 \log(1/g)}{64\pi} . \qquad (2.75)
$$

Since the collision term is rotationally invariant, an inspection of the linearized Boltzmann Eq.(2.69) dictates the following form of the solution,

$$
\begin{aligned}
\chi^q(\boldsymbol{p}) &= (\boldsymbol{p}_\perp \cdot \partial_\perp v_z)\, p_z\, \chi_+(|\boldsymbol{p}|) + (\boldsymbol{p}_\perp \times \partial_\perp v_z)\, p_z\, \chi_-(|\boldsymbol{p}|) , \\
\chi^{\bar{q}}(\boldsymbol{p}) &= (\boldsymbol{p}_\perp \cdot \partial_\perp v_z)\, p_z\, \chi_+(|\boldsymbol{p}|) - (\boldsymbol{p}_\perp \times \partial_\perp v_z)\, p_z\, \chi_-(|\boldsymbol{p}|) , \\
\chi^g(\boldsymbol{p}) &= (\boldsymbol{p}_\perp \cdot \partial_\perp v_z)\, p_z\, \chi_G(|\boldsymbol{p}|) , \qquad (2.76)
\end{aligned}
$$

where

$$(\boldsymbol{p}_\perp \cdot \partial_\perp v_z) \equiv \boldsymbol{p}_\perp^i \cdot \partial_{\boldsymbol{x}_\perp^i} v_z\,, \quad (\boldsymbol{p}_\perp \times \partial_\perp v_z) \equiv \epsilon^{ij} \boldsymbol{p}_\perp^i \partial_{\boldsymbol{x}_\perp^j} v_z\,, \quad i,j = x,y\,, \tag{2.77}$$

and the functions $\chi_\pm, \chi_G$ depend only on $p \equiv |\boldsymbol{p}|$. This is the most general form consistent with the isometry of the collision term and the residual $SO(2)_\perp$ rotational symmetry in the advective term in the presence of a background magnetic field. Note that the second term in the first two equations involving χ_- comes from the Lorentz force term in Eq.(2.69) due to the magnetic field, and takes opposite sign between quark and anti-quark. When $B = 0$, χ_- vanishes.

Inserting this form of the solution into Eq.(2.69) and working out the collision term Eq.(2.72) explicitly, one obtains a coupled set of second order differential equations for $\chi_\pm(p)$ and $\chi_G(p)$. It is easy to see that only the first lines in Eq.(2.73) and Eq.(2.74) contribute to the final collision term, while the other terms vanish for our solutions in Eq.(2.76). After some amount of algebra, we get the differential equations ($' \equiv \frac{\partial}{\partial p}$ and $n_{F/B} \equiv n_{F/B}(p)$),

$$\begin{aligned}
&\frac{1}{8\pi} T m_D^2 g^2 \log(1/g) C_F \left([n_F(1-n_F)]' \left(2\chi_+(p) + p\chi_+'(p)\right) + n_F(1-n_F)\left(6\chi_+'(p) + p\chi_+''(p)\right)\right) \\
= \;& \beta n_F(1-n_F) + q_F eB n_F(1-n_F)\chi_-(p) + 2\gamma n_F(1+n_B)\left(\chi_+(p) - \chi_G(p)\right) , \qquad (2.78) \\
&\frac{1}{8\pi} T m_D^2 g^2 \log(1/g) C_F \left([n_F(1-n_F)]' \left(2\chi_-(p) + p\chi_-'(p)\right) + n_F(1-n_F)\left(6\chi_-'(p) + p\chi_-''(p)\right)\right) \\
= \;& -q_F eB n_F(1-n_F)\chi_+(p) + 2\gamma n_F(1+n_B)\chi_-(p) , \qquad (2.79) \\
&\frac{1}{8\pi} T m_D^2 g^2 \log(1/g) C_A \left([n_B(1+n_B)]' \left(2\chi_G(p) + p\chi_G'(p)\right) + n_B(1+n_B)\left(6\chi_G'(p) + p\chi_G''(p)\right)\right) \\
= \;& \beta n_B(1+n_B) + 2\gamma \frac{2N_c}{(N_c^2-1)} n_F(1+n_B) \sum_F \left(\chi_G(p) - \chi_+(p)\right) . \qquad (2.80)
\end{aligned}$$

Once the solution is found, inserting Eq.(2.76) into Eq.(2.70) and performing angular integration using

$$\int \frac{d^3\boldsymbol{p}}{(2\pi)^3} \frac{\boldsymbol{p}_\perp^i \boldsymbol{p}_\perp^j p_z^2}{E_{\boldsymbol{p}}} = \frac{\delta^{ij}}{2} \int \frac{d^3\boldsymbol{p}}{(2\pi)^3} \frac{\boldsymbol{p}_\perp^2 p_z^2}{E_{\boldsymbol{p}}} = \frac{\delta^{ij}}{2(2\pi)^2} \int_{-1}^{+1} dx\, x^2(1-x^2) \int_0^\infty dp\, p^5 = \frac{\delta^{ij}}{30\pi^2} \int_0^\infty dp\, p^5 , \qquad (2.81)$$

one obtains the shear viscosity

$$\eta = -\frac{1}{30\pi^2} \int_0^\infty dp\, p^5 \left(2(N_c^2-1) n_B(1+n_B)\chi_G(p) + \sum_F 4N_c n_F(1-n_F)\chi_+(p) \right) . \qquad (2.82)$$

2.2.4 Results and discussion for shear viscosity in magnetic field

To proceed, it is more convenient to formulate the equations in the previous section in terms of dimensionless variable $\bar{p} \equiv p/T$. In our numerical analysis in this study, one takes a simplifying approximation of considering two identical flavors with a same charge $\bar{q}_F$, and replace $\sum_F \to N_F = 2$. One expects that this will not affect the major features of our result presented below. A full consideration of the case of different charges can be easily generalized and is neglected here. Note that the sign of the charge should not matter for shear viscosity, since the effects from magnetic field appear in combination of $q_F^2(eB)^2$ due to charge-conjugation symmetry. Defining the dimensionless magnetic field strength as

$$\bar{B} \equiv \frac{|\bar{q}_F eB|}{g^4 \log(1/g) T^2}\,, \tag{2.83}$$

with the similar definitions for dimensionless quantities

$$\bar{m}_D^2 \equiv m_D^2/T^2\,, \quad \bar{\gamma} \equiv \gamma/(T^2 g^4 \log(1/g))\,, \tag{2.84}$$

and the dimensionless functions

$$\bar{\chi}_\pm \equiv T^3 g^4 \log(1/g) \chi_\pm\,, \quad \bar{\chi}_G \equiv T^3 g^4 \log(1/g) \chi_G\,, \tag{2.85}$$

One rewrites the following dimensionless differential equations as (note that $' \equiv \frac{\partial}{\partial \bar{p}}$)

$$\begin{aligned}
&\frac{1}{8\pi}\bar{m}_D^2 C_F \left([n_F(1-n_F)]'\left(2\bar{\chi}_+ + \bar{p}\bar{\chi}_+'\right) + n_F(1-n_F)\left(6\bar{\chi}_+' + \bar{p}\bar{\chi}_+''\right)\right) \\
= \; & n_F(1-n_F) + \bar{B}n_F(1-n_F)\bar{\chi}_- + 2\bar{\gamma}n_F(1+n_B)\left(\bar{\chi}_+ - \bar{\chi}_G\right) , \qquad (2.86) \\
&\frac{1}{8\pi}\bar{m}_D^2 C_F \left([n_F(1-n_F)]'\left(2\bar{\chi}_- + \bar{p}\bar{\chi}_-'\right) + n_F(1-n_F)\left(6\bar{\chi}_-' + \bar{p}\bar{\chi}_-''\right)\right) \\
= \; & -\bar{B}n_F(1-n_F)\bar{\chi}_+ + 2\bar{\gamma}n_F(1+n_B)\bar{\chi}_- , \qquad (2.87) \\
&\frac{1}{8\pi}\bar{m}_D^2 C_A \left([n_B(1+n_B)]'\left(2\bar{\chi}_G + \bar{p}\bar{\chi}_G'\right) + n_B(1+n_B)\left(6\bar{\chi}_G' + \bar{p}\bar{\chi}_G''\right)\right) \\
= \; & n_B(1+n_B) + 2\bar{\gamma}\frac{2N_cN_F}{(N_c^2-1)}n_F(1+n_B)\left(\bar{\chi}_G - \bar{\chi}_+\right) , \qquad (2.88)
\end{aligned}$$

in terms of which the shear viscosity is written as

$$\eta = \bar{\eta}(\bar{B})\frac{T^3}{g^4\log(1/g)} , \qquad (2.89)$$

with the dimensionless function

$$\bar{\eta}(\bar{B}) = -\frac{1}{30\pi^2}\int_0^\infty d\bar{p}\,\bar{p}^5\left(2(N_c^2-1)n_B(1+n_B)\bar{\chi}_G(\bar{p}) + 4N_cN_Fn_F(1-n_F)\bar{\chi}_+(\bar{p})\right) . \quad (2.90)$$

In principle one can numerically solve the above inhomogeneous second order differential equations imposing regular boundary conditions at $\bar{p} = 0$ and $\bar{p} = \infty$ that uniquely determine the solution for given $\bar{B}$. However one finds that it is not practically easy to do this using the shooting method since we have three functions and we need to scan three dimensional parameter space of initial conditions. For the case of $B = 0$, we have $\chi_- = 0$ and we can barely manage to find the solution scanning the reduced two dimensional space of initial conditions. We get in this way $\bar{\eta} = 86.46$ for $B = 0$ and $N_F = 2$. For $N_F = 0$ where both χ_+ and χ_- vanish, we get $\bar{\eta} = 27.12$. These results agree very well with the previous results by Arnold-Moore-Yaffe [61], and give us confidence that our differential equations in the above do not contain trivial mistakes.

On the other hand, it is possible to solve the above equations in the limiting case of $\bar{B} \to \infty$. It can be shown without difficulty that in this limit,

$$\bar{\chi}_+ \sim \mathcal{O}(1/\bar{B}^2)\,, \quad \bar{\chi}_- \sim \mathcal{O}(1/\bar{B})\,, \quad \bar{\chi}_G \sim \mathcal{O}(1)\,, \tag{2.91}$$

so that it is enough to solve the last Eq.(2.88) for $\bar{\chi}_G$ neglecting $\bar{\chi}_+$ to get the limiting value of $\bar{\eta}(\infty)$. This can easily be done by the shooting method, and we obtain

$$\bar{\eta}(\bar{B}) = 18.87 + \mathcal{O}(1/\bar{B}^2)\,, \quad \bar{B} \to \infty\,. \tag{2.92}$$

Instead of directly solving the differential equations by the shooting method, we follow Ref.[61] to find approximate solutions within a finite dimensional functional space formed by a well-chosen set of basis functions. We first show that our original problem of solving the differential equations and computing the integral Eq.(2.90) for the shear viscosity is equivalent to a variational problem of a quadratic action. Defining the "Lagrangians" $\mathcal{I}_+$, $\mathcal{I}_-$, $\mathcal{I}_G$ and $\mathcal{I}_{\mathrm{m}ix}$ by

$$
\begin{aligned}
\mathcal{I}_+ &= -\frac{4N_cN_F}{30\pi^2}\left(\frac{1}{8\pi}\bar{m}_D^2C_Fn_F(1-n_F)\left(\bar{p}^2([\bar{p}^2\bar{\chi}_+]')^2+6\bar{p}^4\bar{\chi}_+^2\right)+2\bar{\gamma}\bar{p}^5n_F(1+n_B)\bar{\chi}_+^2\right) ,\\
\mathcal{I}_- &= +\frac{4N_cN_F}{30\pi^2}\left(\frac{1}{8\pi}\bar{m}_D^2C_Fn_F(1-n_F)\left(\bar{p}^2([\bar{p}^2\bar{\chi}_-]')^2+6\bar{p}^4\bar{\chi}_-^2\right)+2\bar{\gamma}\bar{p}^5n_F(1+n_B)\bar{\chi}_-^2\right) ,\\
\mathcal{I}_G &= -\frac{2(N_c^2-1)}{30\pi^2}\left(\frac{1}{8\pi}\bar{m}_D^2C_An_B(1+n_B)\left(\bar{p}^2([\bar{p}^2\bar{\chi}_G]')^2+6\bar{p}^4\bar{\chi}_G^2\right)+2\bar{\gamma}\frac{2N_cN_F}{(N_c^2-1)}\bar{p}^5n_F(1+n_B)\bar{\chi}_G^2\right) ,\\
\mathcal{I}_{\mathrm{m}ix} &= -\frac{1}{15\pi^2}4N_cN_F\left(-2\bar{\gamma}\bar{p}^5n_F(1+n_B)\bar{\chi}_+\bar{\chi}_G+\bar{B}\bar{p}^5n_F(1-n_F)\bar{\chi}_+\bar{\chi}_-\right) ,
\end{aligned}
\tag{2.93}
$$

and the source by

$$
\mathcal{S} = -\frac{1}{15\pi^2}\left(4N_cN_F\bar{p}^5n_F(1-n_F)\bar{\chi}_+ + 2(N_c^2-1)\bar{p}^5n_B(1+n_B)\bar{\chi}_G\right) . \tag{2.94}
$$

Let's consider the action functional

$$
\bar{\eta}[\bar{\chi}_+,\bar{\chi}_-,\bar{\chi}_G] \equiv \int_0^\infty d\bar{p}\ \left(\mathcal{I}_+ + \mathcal{I}_- + \mathcal{I}_G + \mathcal{I}_{\mathrm{m}ix} + \mathcal{S}\right) , \tag{2.95}
$$

which is at most quadratic in $\bar{\chi}$'s. It is then straightforward to show that the equations of motions from the above action coincide with the differential equations in Eq.(2.86), Eq.(2.87), and Eq.(2.88), so that the solution of the differential equations corresponds to the extrema of

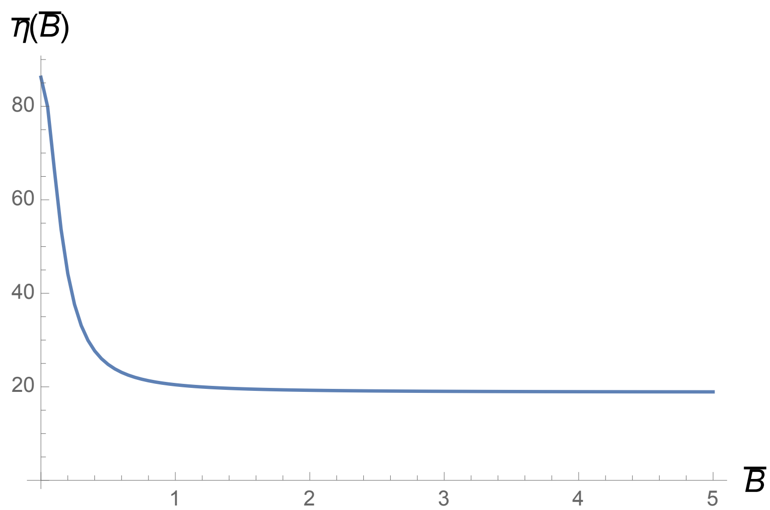

Figure 6: The numerical result for $\bar{\eta}(\bar{B})$ with $N_F = 2$.

the action functional. Moreover the value of the action evaluated at the extrema is equal to the dimensionless function $\bar{\eta}(\bar{B})$ in Eq.(2.90), that is

$$\bar{\eta}(\bar{B}) = \bar{\eta}[\bar{\chi}_+, \bar{\chi}_-, \bar{\chi}_G]\Big|_{solution} . \tag{2.96}$$

We perform this variational analysis in a finite dimensional functional space spanned by a set of basis functions $\phi^{(m)}(\bar{p})$ $(m = 1, \ldots, N)$: writing $\bar{\chi}_\pm$ and $\bar{\chi}_G$ as

$$\bar{\chi}_\pm(\bar{p}) = \sum_m a_\pm^{(m)} \phi^{(m)}(\bar{p}) , \quad \bar{\chi}_G(\bar{p}) = \sum_m b^{(m)} \phi^{(m)}(\bar{p}) , \tag{2.97}$$

with variational coefficients $(a_\pm^{(m)}, b^{(m)}) \equiv A$, we evaluate the action to find

$$\bar{\eta}[A] = -\frac{1}{2}A^T\mathcal{I}A + A^T\mathcal{S}\,, \tag{2.98}$$

with a $(3N)\times(3N)$ symmetric matrix $\mathcal{I}$ and a $(3N)$-dimensional column vector $\mathcal{S}$. Solving for the extremum by $A = \mathcal{I}^{-1}\mathcal{S}$ and evaluating the action at the extremum, we get the approximate result for the shear viscosity

$$\bar{\eta}(\bar{B}) = \frac{1}{2}\mathcal{S}^T\mathcal{I}^{-1}\mathcal{S}\,. \tag{2.99}$$

Following Ref.[61] let's choose the basis functions

$$\phi^{(m)}(\bar{p}) = \frac{\bar{p}^{m-1}}{(1+\bar{p})^{N-1}}\,, \quad m = 1,\ldots,N\,, \tag{2.100}$$

with N up to 10 which was claimed to produce a good precision in the case of $B = 0$. In our case with $B \neq 0$, we expect the numerical results to be less accurate, since the action functional $\bar{\eta}[\bar{\chi}_+, \bar{\chi}_-, \bar{\chi}_G]$ with $B \neq 0$ is not bounded above and the extremum doesn't correspond to a global maximum of $\bar{\eta}$: note that $\mathcal{I}_-$ in Eq.(2.93) is positive definite, while $\mathcal{I}_+$ and $\mathcal{I}_G$ is negative definite. Our numerical result is estimated to be trustable within $\pm 1\%$ level. Figure 6 shows our numerical result of $\bar{\eta}(\bar{B})$ for $N_F = 2$. Starting from $\bar{\eta}(0) \approx 86.46$, it rapidly decreases up to $\bar{B} = 1$, beyond which $\bar{\eta}(\bar{B})$ decreases slowly to the limiting value $\bar{\eta}(\infty) = 18.87$.

We shall emphasize that our result is limited to the case where the strength of magnetic field is weak compared to the temperature, with a parametric dependence $eB = \bar{B}g^4\log(1/g)T^2$ where $\bar{B}$ is a dimensionless number. In our computation, we also assume that the electromagnetism is non-dynamical and external, which means that the MHD regime is never realized. With these assumptions, our leading log value of shear viscosity takes the following scaling form $\eta = \bar{\eta}(\bar{B})T^3/(g^4\log(1/g))$, where $\bar{\eta}(\bar{B})$ depends only on the ratio $\bar{B} = eB/(g^4\log(1/g)T^2)$. Our result could give a useful insight on the effects of magnetic field on the shear viscosity of quark-gluon plasma in late stages of the heavy-ion collisions where the magnetic field becomes weak compared to temperature scale. However, a more realistic study of the transport coefficients in the MHD regime with five shear and bulk viscosities classified in Refs.[18; 88] still remains demanding.

It is worth remarking that a peculiar feature in our result shown in Figure 6 is a steep fall of the value of $\bar{\eta}(\bar{B})$ within a narrow region of $\bar{B}$ near zero. This can be understood as follows. Firstly, the limiting *finite* value at $\bar{B} \to \infty$ comes solely from the contribution of gluons which are neutral and have no cyclotron orbits, whereas the quarks and anti-quarks do not contribute to the transport in this limit because their cyclotron orbits become very small compared to the collisional mean free path. This can be explicitly seen in Eq.(2.91). Note that the transport of gluons still feel the presence of quarks and anti-quarks via the collisions with the background quarks and anti-quarks (that is reflected in the value of the Debye mass m_D^2 in the collision terms depending on the number of flavors), and this is why the shear viscosity in this limit is not equal to the one in $N_F = 0$ case. Indeed, in a pure gluon case of $N_F = 0$, it is checked that if one simply replaces the Debye mass in the $N_F = 0$ case with the one in $N_F = 2$ case, one obtains precisely our limiting value of 18.87 for the shear viscosity.

One shall ask a question why the quark and anti-quark contributions drop quickly? Let's first recall from our discussion around Figure 5 that their contributions would drop significantly when the size of the cyclotron orbit l_{cyclo} becomes comparable to the collisional mean free path l_{mfp}. Denoting the characteristic size of the collision term as $\mathcal{C} \sim C\, g^4 \log(1/g)T$ with a dimensionless number C, we have $l_{mfp} \sim \mathcal{C}^{-1} \sim C^{-1}/(g^4 \log(1/g)T)$. On the other hand, the cyclotron orbit size is $l_{cyclo} \sim p/(eB) \sim \bar{B}^{-1}/(g^4 \log(1/g)T)$ with our dimensionless parameter $\bar{B}$. This means that their ratio is

$$l_{mfp}/l_{cyclo} \sim \bar{B}/C\,, \tag{2.101}$$

and therefore we expect that $\bar{\eta}(\bar{B})$ will drop significantly around $\bar{B} \sim C$. Now the shear viscosity at $\bar{B} = 0$ is simply proportional to $l_{mfp} \sim \mathcal{C}^{-1} \sim C^{-1}/(g^4 \log(1/g)T)$ (times kinematic factors): in other words, the numerical value of $\bar{\eta}(0)$ should be roughly given by C^{-1}. It is just a feature of explicit QCD collision terms that C is a numerically small number: for example, it should be about $1/80$ to give the value $\bar{\eta}(0) = 86.46$ for $N_F = 2$. This would mean that an order 1 value of $\bar{B}$ is already in the regime where $l_{mfp}/l_{cyclo} \gg 1$ and the quark contribution should be negligible. In summary, the numerical smallness of the QCD collision term in unit of $g^4 \log(1/g)T$ is responsible for both a large value of $\bar{\eta}(0)$ *and* the narrowness of the $\bar{B}$

dependence. This inverse correlation between $\bar{\eta}(0)$ and the width in $\bar{B}$ is universal, and can also be found, for example, in the Drude picture of transport in magnetic field.

2.3 Summary and outlook

In this chapter, we have formulated an effective kinetic description of the charge transport of QGP in the presence of a strong and/or weak/soft magnetic field. We apply this framework to study the transport coefficients, such as the electric conductivity in the strong $\boldsymbol{B}$ and shear viscosity in the weak $\boldsymbol{B}$. We find that the longitudinal electric conductivity is enhanced in the small mass limit with strong $\boldsymbol{B}$ and our main result for electric conductivity is showed in Figure 4. For the weak $\boldsymbol{B}$ field, one has to sum over all the Landau Level quarks/anti-quarks contribution to the electric conductivity, see Ref.[96]. However, the electric conductivity of QGP in the intermediate $\boldsymbol{B}$ still needs to be worked out. We also find that there emerges effective low energy hydrodynamics in the weak $\boldsymbol{B}$. As an application, we compute the shear viscosity and find that shear viscosity is largely suppressed due to the interplay between the magnetic field and QCD interactions. For this one, our main result is plotted in Figure 6. As a future direction, it seems possible to go one step further and compute the shear viscosity in a soft magnetic field in complete leading order, using the variational approach as in Ref.[62]. It will also be interesting to compute the bulk viscosities in magnetic field appearing in the constitutive relation Eq.(2.53). See Ref.[85] for recent development.

2.A.1 FEYNMAN RULES IN THE LLL APPROXIMATION

This appendix gives brief summary of the quantization of quark field in the presence of a strong magnetic field and the effective Feynman rules that are used in computing the collision terms in the Boltzmann equation. Choosing to work in the Landau gauge $A^2 = Bx^1$ (with $\boldsymbol{B} = B\hat{x}^3 \equiv B\hat{z}$) which seemingly breaks the translational invariance in x^1 direction, while keeping that in x^2 direction. This allows us to introduce two momentum quantum numbers, p_z and p_2, along $\hat{z}$ and $\hat{x}^2$. It is important to keep in mind that 1) there is no concept of p_1 in the quark wave functions (while the gluon wave functions have it), and 2) p_2 serves as a label for the degenerate Landau levels in the transverse $(x^1, x^2) \equiv \boldsymbol{x}_\perp$ space.

To take care of the transverse density of states of the Landau levels in a clear manner, one first considers a finite box of each sides (L_1, L_2, L_3), and then takes an infinite volume limit at the end. The two dimensional momenta (p_z, p_2) take discrete values, which can be collectively denoted as $\boldsymbol{p}_n$. Solving the Dirac equation with the background magnetic field, one obtains positive/negative energy solutions as usual,

$$e^{-iE_{n,l}x^0+i\boldsymbol{p}_n\cdot\boldsymbol{x}}u^l_\parallel(p_z)\mathcal{H}_l\left(x^1-\frac{p_2}{eB}\right)\,,\quad e^{+iE_{n,l}x^0-i\boldsymbol{p}_n\cdot\boldsymbol{x}}v^l_\parallel(p_z)\mathcal{H}_l\left(x^1+\frac{p_2}{eB}\right)\,, \tag{2.102}$$

where the energy is

$$E_{n,l} = \sqrt{p_z^2+(2l+1\mp 1)|eB|+m_q^2} \equiv \sqrt{p_z^2+m_l^2}\,, \tag{2.103}$$

depending on the spinor projection $i\gamma^1\gamma^2 = \pm 1$, and $\mathcal{H}_l(x^1)$ are the normalized l-th eigenstate of simple harmonic oscillator with frequency $\omega = |eB|$, such that

$$\mathcal{H}_0(x^1) = \left(\frac{|eB|}{\pi}\right)^{\frac{1}{4}} \exp\left(-\frac{(x^1)^2}{2|eB|}\right) , \tag{2.104}$$

and $u^l_{\|}(p_z)$ and $v^l_{\|}(p_z)$ are 1+1 dimensional spinors (due to the projection $i\gamma^1\gamma^2 = \pm 1$) for quarks and antiquarks with the mass m_l in relativistic normalization $u^\dagger u = v^\dagger v = 2E_{n,l}$. It is important to notice that the quark state with p_2 is localized in $x^1 \sim p_2/eB$ with a width $\Delta x^1 \sim 1/\sqrt{|eB|}$, while the antiquark state is localized in $x^1 \sim -p_2/eB$.

Let's first reproduce the well-known transverse density of states of Landau levels in this gauge: $|eB|/(2\pi)$. The p_2 takes discrete value, and is quantized as $p_2 = 2\pi k/L_2$, with integers k, and the quark state with a given Landau level l with this momentum is localized in $x^1 \sim p_2/eB = 2\pi k/(L_2 eB)$. Since x^1 should lie in the interval $[0, L_1]$, we have $0 < k < L_1L_2(|eB|/2\pi)$, that is, the total number of such states is $L_1L_2(|eB|/2\pi)$ per the transverse area L_1L_2.

The special case with $l = 0$ and $i\gamma^1\gamma^2 = +1$ gives the lowest possible 1+1 dimensional mass $m_0^2 = m_q^2$, which is separated by multiples of $|eB|$ from other higher level states. These states are the Lowest Landau Levels (LLL). In the language of 1+1 dimension, their spinors $u^0_{\|}(p_z)$, $v^0_{\|}(p_z)$ form a single Dirac fermion field in 1+1 dimension. For higher Landau levels with $m_l^2 = 2l|eB| + m_q^2$ $(l \geq 1)$, we have two possibilities to get the same mass: one with $i\gamma^1\gamma^2 = +1$

and the level l, and the other with $i\gamma^1\gamma^2 = -1$ and the level $l-1$. These two possibilities result in two Dirac fermion fields with the common mass m_l in the language of 1+1 dimensions.

Following the standard quantization scheme, one writes the quark field operator as

$$\psi(\boldsymbol{x}) = \frac{1}{\sqrt{L_2L_3}} \sum_{\boldsymbol{p}_n,l} \frac{1}{\sqrt{2E_{n,l}}} \left(e^{i\boldsymbol{p}_n\cdot\boldsymbol{x}} \mathcal{H}_l\left(x^1 - \frac{p_2}{eB}\right) u_\parallel^l(p_z) a_{\boldsymbol{p}_n,l} + e^{-i\boldsymbol{p}_n\cdot\boldsymbol{x}} \mathcal{H}_l\left(x^1 + \frac{p_2}{eB}\right) v_\parallel^l(p_z) b^\dagger_{\boldsymbol{p}_n,l} \right) \tag{2.105}$$

where the sum over $i\gamma^1\gamma^2 = \pm 1$ is assumed, and

$$\{a_{\boldsymbol{p}_n,l}, a^\dagger_{\boldsymbol{p}_{n'},l'}\} = \{b_{\boldsymbol{p}_n,l}, b^\dagger_{\boldsymbol{p}_{n'},l'}\} = \delta_{n,n'}\delta_{l,l'}\,. \tag{2.106}$$

Using the completeness relation

$$\sum_l \mathcal{H}_l(x)\mathcal{H}_l(y) = \delta(x-y)\,, \tag{2.107}$$

it is easy to show the canonical commutation relation is satisfied

$$\{\psi_\alpha(\boldsymbol{x}), \psi^\dagger_\beta(\boldsymbol{y})\} = \delta^{(3)}(\boldsymbol{x}-\boldsymbol{y})\delta_{\alpha\beta}\,. \tag{2.108}$$

Since the higher Landau level states have the energy at least of order $\sqrt{|eB|}$, their thermal occupation numbers are exponentially small $e^{-\sqrt{|eB|}/T}$ in our assumed hierarchy $T^2 \ll eB$, hence they don't contribute to the transport coefficients such as electric conductivity of our interest. This justifies the LLL approximation that we use in this work, that is keeping only $l=0$ and $i\gamma^1\gamma^2 = +1$ component in the above expansion of quark field operator. From here and the following, we shall call the LLL spinors $(u^0_\parallel(p_z), v^0_\parallel(p_z))$ simply by $(u(p_z), v(p_z))$, and similarly $E_{n,0} \equiv E_n$ and $a_{\boldsymbol{p}_n,0} \equiv a_{\boldsymbol{p}_n}$, so that

$$\psi(\boldsymbol{x}) \sim \frac{1}{\sqrt{L_2 L_3}} \sum_{\boldsymbol{p}_n} \frac{1}{\sqrt{2E_n}} \left(e^{i\boldsymbol{p}_n \cdot \boldsymbol{x}} \mathcal{H}_0 \left(x^1 - \frac{p_2}{eB} \right) u(p_z) a_{\boldsymbol{p}_n} + e^{-i\boldsymbol{p}_n \cdot \boldsymbol{x}} \mathcal{H}_0 \left(x^1 + \frac{p_2}{eB} \right) v(p_z) b^\dagger_{\boldsymbol{p}_n} \right) \tag{2.109}$$

One consequence of the LLL approximation is that the quark current $j^\mu = \bar{\psi}\gamma^\mu\psi$ has zero component in the transverse $\boldsymbol{x}_\perp$ direction, due to the projection $i\gamma^1\gamma^2 = +1$ which anti-commutes with $\gamma^\perp$. Physically this is because Landau level states move only along 1+1 dimensions. The transverse current or transverse motion necessarily involves mixing with higher Landau levels.

What we are interested in is the QCD interaction with the gluon fields living in 3+1 dimensions. One can do a time-ordered perturbation theory, but the matrix element for a given Feynman diagram ends up to a (1+1 dimensional) relativistic expression after summing over all time-ordered processes. Feynman rules in the LLL approximation can be derived in the following few example time-ordered perturbation theory computations.

The interaction Hamiltonian is

$$H_I = g_s \int d^3\boldsymbol{x}\ A^a_\mu(\boldsymbol{x}) \bar{\psi}(\boldsymbol{x}) \gamma^\mu_\parallel t^a \psi(\boldsymbol{x}) \,, \tag{2.110}$$

where a is the color index, and recall that in the LLL approximation μ runs only along 1+1 dimensions indicated by $\gamma_{\parallel}^{\mu}$. Since ψ field is already projected by $i\gamma^1\gamma^2 = +1$, the $\gamma_{\parallel}^{\mu}$ matrices are effectively 2×2 γ matrices in 1+1 dimensions. The gluon field is quantized as usual:

$$A_\mu(\boldsymbol{x}) = \frac{1}{\sqrt{V}}\sum_{\boldsymbol{q}_m,\epsilon}\frac{1}{\sqrt{2|\boldsymbol{q}_m|}}e^{i\boldsymbol{q}_m\cdot\boldsymbol{x}}\epsilon_\mu\, a^g_{\boldsymbol{q}_m} + \text{h.c.}\,, \tag{2.111}$$

where $V = L_1L_2L_3$ and $\boldsymbol{q}_m$ is the discrete 3-momentum, and $[a_{\boldsymbol{q}_m}, a^\dagger_{\boldsymbol{q}_{m'}}] = \delta_{m,m'}$. The H_I has non-zero matrix elements for four types of processes: absorption/emission of a gluon by/from quark or antiquark, and pair creation/annihilation of quark-antiquark pair from/to a gluon. For example, denoting a normalized one quark state as $|\boldsymbol{p}_{n'}\rangle$, and one quark+one gluon state as $|\boldsymbol{p}_n, \boldsymbol{k}_m\rangle$, one has

$$\langle\boldsymbol{p}_{n'}|H_I|\boldsymbol{p}_n,\boldsymbol{k}_m\rangle = \frac{g_s}{\sqrt{V}}\frac{1}{\sqrt{2E_n}}\frac{1}{\sqrt{2E_{n'}}}\frac{1}{\sqrt{2|\boldsymbol{k}_m|}}\epsilon_\mu\left(\bar{u}(p'_z)\gamma_{\parallel}^{\mu}u(p_z)\right)R_{00}(\boldsymbol{k}_{m\perp})e^{i\Sigma}\delta^{(2)}_{\boldsymbol{p}_n+\boldsymbol{k}_m-\boldsymbol{p}_{n'}} \tag{2.112}$$

where $\delta^{(2)}$ is only about $\boldsymbol{p}_n = (p_z, p_2)$ (so that k^1_m is not constrained at all), and the form factor $R_{00}(\boldsymbol{k}_{m\perp})$ and the Schwinger phase $e^{i\Sigma}$ arise from the overlap integral

$$\int dx^1\, e^{i\boldsymbol{k}^1_m x^1}\mathcal{H}_0\left(x^1 - p_2/eB\right)\mathcal{H}_0\left(x^1 - p'_2/eB\right) = R_{00}(\boldsymbol{k}_{m\perp})e^{i\Sigma}\,, \tag{2.113}$$

with

$$R_{00}(\boldsymbol{k}_\perp) = e^{-\frac{\boldsymbol{k}^2_\perp}{4|eB|}}\,,\quad \Sigma = -\frac{k^1_m}{2eB}\left(p_2 + p'_2\right)\,. \tag{2.114}$$

Note that we have used the fact that $k_m^2 = p_2' - p_2$ in the expression of $R_{00}(\boldsymbol{k}_{m\perp})$. The other matrix elements of H_I are similar with the form factor and the Schwinger phase. From these and by applying the Fermi's Golden rule, one constructs the collision term in the Boltzmann equation as a transition probability rate per unit time from a given initial state to a final state. In this way, the normalization issue is taken care of clearly in a finite volume we are considering before we take an infinite volume limit. In the following, we show a few examples how to extract the Feynman rules.

As a first example, let's consider the collision term for the quark distribution of momentum $\boldsymbol{p}_n$ from 2-to-2 quark scattering: $\boldsymbol{p}_n + \boldsymbol{p}_{n''} \to \boldsymbol{p}_{n'} + \boldsymbol{p}_{n'''}$. There are two time ordered diagrams in the second order perturbation theory where the transition rate is given by

$$T_{i\to f} = \sum_m \frac{\langle f|H_I|m\rangle\langle m|H_I|i\rangle}{E_m - E_i}(2\pi)\delta(E_f - E_i)\,, \tag{2.115}$$

Summing the two time ordered processes, for which $|m\rangle = |\boldsymbol{p}_{n'}, \boldsymbol{p}_{n''}, \boldsymbol{q}_m\rangle$ or $|m\rangle = |\boldsymbol{p}_n, \boldsymbol{p}_{n'''}, \boldsymbol{q}_m\rangle$ ($\boldsymbol{q}_m$ is the exchanged gluon momentum), we get after a short algebra

$$\begin{aligned} \sum_{n',n'',n'''} T_{i\to f} &= \frac{1}{(L_2L_3)^2} \sum_{n',n'',n'''} \frac{1}{2E_n}\frac{1}{2E_{n'}}\frac{1}{2E_{n''}}\frac{1}{2E_{n'''}}\delta^{(2)}_{\boldsymbol{p}_n+\boldsymbol{p}_{n''}-\boldsymbol{p}_{n'}-\boldsymbol{p}_{n'''}} \\ &\times \; |\mathcal{M}|^2\,(2\pi)\delta\left(E_n + E_{n''} - E_{n'} - E_{n'''}\right)\,, \end{aligned} \tag{2.116}$$

where the matrix element is given by

$$\mathcal{M} = g_s^2 \frac{1}{L_1} \sum_{\boldsymbol{q}_m^1} \frac{\eta_{\mu\nu}}{(q_m^0)^2 - \boldsymbol{q}_m^2} \left(R_{00}(\boldsymbol{q}_{m\perp})\right)^2 e^{-i\frac{q_m^1}{2eB}(p_2+p_2'-p_2''-p_2''')} [\bar{u}(p_z')\gamma^\mu u(p_z)][\bar{u}(p_z''')\gamma^\nu u(p_z'')] \tag{2.117}$$

with $q_m^0 = E_{n'} - E_n$ and $\boldsymbol{q}_m^{(2)} = \boldsymbol{p}_n - \boldsymbol{p}_{n'}$. The structure of $\mathcal{M}$ is a product of 1+1 dimensional relativistic matrix element for quarks and the form factors/Schwinger phase. The gluon propagator is 3+1 dimensional. Recall that there is no constraint for $\boldsymbol{q}_m^1$ and we have a summation over it in $\mathcal{M}$. We omit color factors in the above and the following, but can easily be reinstated. The above transition probability rate with distribution functions of incoming and outgoing states attached is what should appear in the collision term in the Boltzmann equation. Taking to an infinite volume limit, one gets a collision term

$$\begin{aligned} C[f_+(\boldsymbol{p})] &= -\frac{1}{2E_p} \int_{\boldsymbol{p}'} \int_{\boldsymbol{p}''} \int_{\boldsymbol{p}'''} |\mathcal{M}|^2 (2\pi)^2 \delta^{(2)} \left(\boldsymbol{p} + \boldsymbol{p}'' - \boldsymbol{p}' - \boldsymbol{p}'''\right) \\ &\times (2\pi)\delta\left(E_p + E_{p''} - E_{p'} - E_{p'''}\right) f_+(\boldsymbol{p}) f_+(\boldsymbol{p}'')(1 - f_+(\boldsymbol{p}'))(1 - f_+(\boldsymbol{p}''')) \, , \end{aligned} \tag{2.118}$$

with

$$\mathcal{M} = g_s^2 \int \frac{d\boldsymbol{q}^1}{(2\pi)} \frac{\eta_{\mu\nu}}{q^2} \left(R_{00}(\boldsymbol{q}_\perp)\right)^2 e^{-i\frac{q^1}{2eB}(p_2+p_2'-p_2''-p_2''')} [\bar{u}(p_z')\gamma^\mu u(p_z)][\bar{u}(p_z''')\gamma^\nu u(p_z'')] \, , \tag{2.119}$$

and

$$\int_{\boldsymbol{p}} \equiv \int \frac{dp_z dp_2}{(2\pi)^2 2E_p} \, . \tag{2.120}$$

One can work out to see that the Schwinger phase in 2.119 is crucial to get a finite result with correct Landau level density of state.

As another example, let's consider 2-to-2 scattering of a quark with thermal gluons: $\boldsymbol{p}+\boldsymbol{k}'' \to \boldsymbol{p}' + \boldsymbol{k}'''$. Working out similar details as above and taking an infinite volume limit, one arrives at

$$\begin{aligned} C[f_+(\boldsymbol{p})] &= -\frac{1}{2E_p}\int_{\boldsymbol{p}'}\int_{\boldsymbol{k}''}\int_{\boldsymbol{k}'''} |\mathcal{M}|^2 (2\pi)^2 \delta^{(2)}\left(\boldsymbol{p}+\boldsymbol{k}''-\boldsymbol{p}'-\boldsymbol{k}'''\right) \\ &\times (2\pi)\delta\left(E_p + E_{k''} - E_{p'} - E_{k'''}\right) f_+(\boldsymbol{p}) f_g(\boldsymbol{k}'')(1-f_+(\boldsymbol{p}'))(1+f_g(\boldsymbol{k}''')) \,, \end{aligned} \tag{2.121}$$

where

$$\mathcal{M} = g_s^2 f^{abc} R_{00}(\boldsymbol{q}_\perp) e^{-i\frac{\boldsymbol{q}^1}{2eB}(p_2+p_2')} \frac{\eta_{\mu\nu}}{q^2}[\bar{u}(p_z')\gamma^\mu u(p_z)] \times (g\mathit{luon\ current}) \,, \tag{2.122}$$

is the usual relativistic expression except the form factor/Schwinger phase, and

$$\int_{\boldsymbol{k}} \equiv \int \frac{d^3\boldsymbol{k}}{(2\pi)^3 2E_k} \,. \tag{2.123}$$

As a final example, let's consider 2-to-2 scattering of a gluon with thermal LLL quarks: $\boldsymbol{k}+\boldsymbol{p}'' \to \boldsymbol{k}'+\boldsymbol{p}'''$ (the same process as the second example, but the collision term for the gluon tagged, rather than the quark). Taking an infinite volume limit, we end up to

$$\begin{aligned} C[f_g(\boldsymbol{k})] &= -\frac{1}{2E_k}\frac{1}{L_1}\int_{\boldsymbol{k}'}\int_{\boldsymbol{p}''}\int_{\boldsymbol{p}'''}|\mathcal{M}|^2(2\pi)^2\delta^{(2)}\left(\boldsymbol{k}+\boldsymbol{p}''-\boldsymbol{k}'-\boldsymbol{p}'''\right) \\ &\times (2\pi)\delta\left(E_k+E_{p''}-E_{k'}-E_{p'''}\right)f_g(\boldsymbol{k})f_+(\boldsymbol{p}'')(1+f_g(\boldsymbol{k}'))(1-f_+(\boldsymbol{p}'''))\,, \end{aligned} \tag{2.124}$$

Note the residual $1/L_1$ factor which is correct as we explain in the following. In this case, when one sums over the final quark states with p'' and p''', one easily see that $p_2''+p_2'''$ is unconstrained, and one has a trivial summation over them. The physics is simple to understand: recalling that $x^1=\frac{p_2}{eB}$, the $(p'''+p''')/2\sim eBx_c^1$ represents a center of mass x^1 position of the incoming and out-going quark states, which is free to take any value between $(0,L_1)$. Indeed, in taking an infinite volume limit, one encounters the combination

$$\frac{1}{L_1}\frac{1}{2\pi}\int d(p_2''+p_2''')/2 \to \frac{1}{L_1}(eB/2\pi)\int_0^{L_1} dx_c^1 = (eB/2\pi)\,, \tag{2.125}$$

that is, the unconstrained integral of $(p_2''+p_2''')/2$ always comes with a residual L_1 factor in the denominator, and results in the transverse density of states of LLL, $(eB/2\pi)$. This is generic for any complete fermion line whose phase space is integrated: there is one p_2 integral associated to it that is not constrained at all (which represents the overall x^1 position of the fermions), and it always comes with a residual $1/L_1$ factor to produce $(eB/2\pi)$ at the end. Note that this rule does not apply for the tagged fermion line in the collision term as in the second example, since the tagged fermion momentum is not integrated over.

From these examples, one derives the following Feynman rules in the LLL approximation:

1) For external quark/antiquark lines, the phase space integration is

$$\int_{\boldsymbol{p}} \equiv \int \frac{dp_z dp_2}{(2\pi)^2 2E_p} \,. \tag{2.126}$$

while for external gluons, it is

$$\int_{\boldsymbol{k}} \equiv \int \frac{d^3\boldsymbol{k}}{(2\pi)^3 2E_k} \,. \tag{2.127}$$

2) For quark-quark-gluon vertex, impose the momentum conservation only along two dimensions (p_z, p_2), and attach the form factor and Schwinger phase. The k_1 component of gluon is not constrained.

3) If there is an internal $\boldsymbol{q}^1$ gluon momentum which is not fixed by external gluons, we integrate $\int d\boldsymbol{q}^1/(2\pi)$ in the total matrix element $\mathcal{M}$.

4) The rest of the matrix element simply follows the usual relativistic Feynman rules for 1+1 dimensional relativistic fermions and 3+1 dimensional relativistic gauge theory.

5) In the collision integral, the momentum δ-function is only two dimensional, and the energy δ-function is as usual. There is an overall normalization of $1/(2E_p)$ in front of the collision term.

6) There exists one unconstrained p_2 integral for any complete quark (antiquark) line whose phase space is integrated. We have a simple thumb rule that each of these unconstrained p_2 integral produces the transverse density of states of LLL, $(eB/2\pi)$;

$$\int \frac{dp_2}{(2\pi)} \rightarrow \left(\frac{eB}{2\pi}\right).$$

In fact, only with this thumb rule applied, the final result has the correct energy dimension for the collision term.

CHAPTER 3

SPIN DYNAMICS OF QUARK-GLUON PLASMA

3.1 Spin polarization of Massive quarks

(Previously published as: S. Li and H.-U. Yee, Quantum Kinetic Theory of Spin Polarization of Massive Quarks in Perturbative QCD: Leading Log, Phys. Rev. D100, 056022 (2019))

3.1.1 Motivation and summary

In the early stage of heavy-ion collision, the QCD plasma is presumably in its de-confined phase, where quarks and gluons are the basic degrees of freedom. The magnitudes of vorticity and magnetic field that polarize the quasi-particle spin are strongest at such an early stage. Some of the spin polarization of quarks and gluons in this phase can be transferred to that of hadrons after hadronization, which may affect the experimentally observed spin polarization of hadrons. Whether this effect survives hadronic phase dynamics depends on the relaxation dynamics of spin polarization in the hadronic phase, as well as many other realistic conditions of heavy-ion collisions [98; 99]. As a first step, a reliable tracking of time-evolution of spin polarization of quarks and gluons within the de-confined phase itself would be a prerequisite in any quantitative theory prediction of spin polarization of observed hadrons. The aim of the present work is to address this problem, at least partly, in the leading log order of pQCD. This also complements our previous work on the similar question in strongly coupled regime described by AdS/CFT correspondence [100].

In a time-dependent background such as heavy-ion collisions, the spin polarization of quasi-particles would naturally be driven off equilibrium. The time evolution of spin polarization would roughly be a competition between QCD dynamics that tries to relax the spin to equilibrium and the time-variation of backgrounds, such as vorticity and magnetic field, that drives the spin polarization of the system off the equilibrium. If the time-variation of background is much slower than the characteristic relaxation time due to QCD interactions (which turns out to be $\tau_R \sim (\alpha_s^2 \log(1/\alpha_s)T)^{-1}$), the system would follow closely the instantaneous equilibrium at each time. In the opposite case, the system would deviate significantly from equilibrium, and the spin polarization should be determined by solving the dynamical equation for time-evolution of spin polarization.

This section is devoted to formulating such a dynamical equation of spin polarization of quasi-particles in QGP phase in leading log order of pQCD, focusing only on the spin polarization of massive quark, that may be applicable to strange quark or more massive quark species. Specifically, we assume that the mass is of hard-scale, $m \gg m_D \sim gT$ (g is the QCD coupling constant). We will see that this justifies a few simplifications we will detail below. Therefore, our results would not be applicable for light (u,d) quarks and gluons, the study of which will be our next work to do in the near future.

Schematically, the evolution of spin density matrix $\hat{\rho}$ of massive quark would take a form in linear order as (basically a "Lindblad equation")

$$\frac{\partial \hat{\rho}}{\partial t} = -\Gamma \cdot \hat{\rho} - \frac{i}{\hbar}[H_{eff}, \hat{\rho}]\,, \tag{3.1}$$

with a linear relaxation operator Γ, and the effective one-particle Hamiltonian $H_{\rm eff}$ in a 2-dimensional spin space, that may include vorticity, $\boldsymbol{\omega}$, and magnetic field, $\boldsymbol{B}$, in somewhat phenomenological way as

$$H_{\rm eff} = -\frac{\hbar}{2}\boldsymbol{\sigma}\cdot(\boldsymbol{\omega}+Q\boldsymbol{B})\,, \tag{3.2}$$

where Q is the electromagnetic charge of quark. In general, the Γ should also depend on vorticity and magnetic field in such a way that the equilibrium spin density matrix is given by $\hat{\rho}_{eq} = e^{-H_{\rm eff}/T} \approx \mathbf{1} - H_{\rm eff}/T$, at least in linear order in $\boldsymbol{\omega}$ and $\boldsymbol{B}$. The magnetic field, for example, should modify the wave function and energy spectrum of quark states in the computation of Γ that we describe in the following sections. One would expect to rewrite the Γ in small $\boldsymbol{\omega}$ and $\boldsymbol{B}$ as $\Gamma = \Gamma_0 + \Gamma_1 + \cdots$ where Γ_1 is linear in $\boldsymbol{\omega}$ or $\boldsymbol{B}$, and so on so forth. Γ_0 describes how a spin density matrix, initially polarized, relaxes to the unpolarized one (the identity operator in spin space), when vorticity and magnetic field cease to exist. Although Γ_0 is not sufficient to describe the spin polarization in a time-varying vorticity and magnetic field, it can still be used to compute spin-related correlation functions in a linear response theory. In this section, we present our result for the leading relaxation operator Γ_0, that corresponds to the case of in the absence of $\boldsymbol{\omega}$ and $\boldsymbol{B}$, and the computation of Γ_1 is deferred to future.

In general, the density matrix $\hat{\rho}$ is defined in the phase space $(\boldsymbol{x},\boldsymbol{p})$ in addition to spin space. A convenient way to think about it is in the language of Schwinger-Keldysh contour. The position and momentum operators in forward and backward time contours (labeled as 1

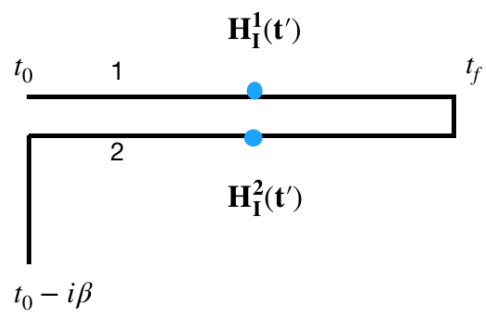

Figure 7: The Schwinger-Keldysh contour appropriate for computing real-time retarded response functions at finite temperature, label 1 and 2 mean the path integral in the time-forward and time-backward contour, respectively.

and 2 respectively) satisfy the commutation relations $[\boldsymbol{x}_1^i, \boldsymbol{p}_1^j] = i\hbar\delta^{ij}$ and $[\boldsymbol{x}_2^i, \boldsymbol{p}_2^j] = -i\hbar\delta^{ij}$. In terms of "ra" variables where $r = \frac{1}{2}(1+2)$ and $a = 1-2$, the only non-vanishing commutators are $[\boldsymbol{x}^i_{r/a}, \boldsymbol{p}^j_{a/r}] = i\hbar\delta^{ij}$, especially $\boldsymbol{x}_r$ and $\boldsymbol{p}_r$ commute with each other. This allows us to introduce a wave function $\hat{\rho}(\boldsymbol{x}_r, \boldsymbol{p}_r)$ which is our density matrix in phase space. Since x_r and p_a are conjugate variables, the wave function (or density matrix) in momentum space $\hat{\rho}(\boldsymbol{p}_r, \boldsymbol{p}_a) = \hat{\rho}(\boldsymbol{p}_1, \boldsymbol{p}_2)$ is related to the density matrix in phase space $\hat{\rho}(\boldsymbol{x}_r, \boldsymbol{p}_r)$ by a Fourier (or Wigner) transform

$$\hat{\rho}(\boldsymbol{x}_r, \boldsymbol{p}_r) = \int \frac{d^3\boldsymbol{p}_a}{(2\pi)^3}\, e^{i\boldsymbol{p}_a\cdot\boldsymbol{x}_r}\, \hat{\rho}(\boldsymbol{p}_r, \boldsymbol{p}_a)\,. \tag{3.3}$$

We will assume that the density matrix in phase space $\hat{\rho}(\boldsymbol{x},\boldsymbol{p})$ is a slowly varying function on space $\boldsymbol{x}$, compared to a microscopic scale of QCD interactions, usually set by the mean free path $l_{mfp} \sim (\alpha_s^2 T)^{-1}$. This means that we can consider $\boldsymbol{x}_r$ as constant in the computation of relaxation operator Γ in Eq.(3.1). This is translated to a smallness of $\boldsymbol{p}_a \sim \partial_{\boldsymbol{x}} \ll l_{mfp}^{-1}$ by Eq.(3.3), that is, the density matrix in momentum space $(\boldsymbol{p}_1,\boldsymbol{p}_2)$ is nearly diagonal in momentum variables. If we neglected spin degrees of freedom, these diagonal elements would correspond to a usual distribution function $f(\boldsymbol{p})$ in momentum space. In our computation of Γ, we therefore work with diagonal elements in the density matrix in momentum space, defined by $\hat{\rho}(\boldsymbol{p}_1,\boldsymbol{p}_2) \equiv (2\pi)^3\delta(\boldsymbol{p}_1-\boldsymbol{p}_2)\hat{\rho}(\boldsymbol{p}_1)$. This is justified as long as we don't care about the advective terms in $\boldsymbol{x}$ in quantum kinetic equation, but focus only on local "collision terms" of Γ in Eq.(3.1) in the *spatial homogeneous limit*. Note that we still keep a full spin matrix of $\hat{\rho}(\boldsymbol{p})$ in the spin space.

The reason why we need to keep full quantum correlation of spin degrees of freedom in the density matrix $\hat{\rho}(\boldsymbol{p})$ is that the two spin states are degenerate in energy and the quantum correlation time is arbitrarily large $\tau_q \sim \frac{\hbar}{\Delta E} \to \infty$. Even in the presence of background vorticity or magnetic field, the energy shift is $\Delta E \sim \boldsymbol{S}\cdot\boldsymbol{\omega}$ or $\Delta E \sim Q\boldsymbol{S}\cdot\boldsymbol{B}$ (Q is charge) which is $\mathcal{O}(\hbar)$ since $\boldsymbol{S} \sim \mathcal{O}(\hbar)$. The quantum correlation time for spin is $\tau_q \sim \frac{\hbar}{\Delta E} \sim \mathcal{O}(\hbar^0)$, and it is in the classical time scale, that is usually described by a classical Boltzmann kinetic theory. Therefore, quantum correlation of spin should be considered even in a regime of kinetic theory, and hence "*Quantum kinetic theory*".

A more fundamental treatment of Eq.(3.1), that should require a significantly larger effort in the future, would involve a complete analysis of spin density matrix in the full phase space $(\boldsymbol{x}, \boldsymbol{p})$. The free streaming, collision-less quantum kinetic equation for this case was recently studied in Refs.[101; 38; 39; 102]. Our study in this sense can be viewed as providing the collision term in leading log of pQCD. However, our result should be improved in this case, including spatial gradient effects in the collision terms (we are restricting to the homogeneous limit, as described in the previous paragraph). This is because the vorticity is a spatial gradient of background fluids. Another way to understand this is that the orbital angular momentum of background fluids can in general be transferred to spin angular momentum of the massive quarks we are looking at. In this more fundamental picture, since total angular momentum has to be conserved, a loss of spin angular momentum of the massive quark (described by Γ) must be compensated by a gain of angular momentum in the background fluid. This gain term will be shared among all quasi-particles of the background, dominantly light quarks and gluons. Compared to the massive quark we consider, these other degrees of freedom is much larger, and the spin gain is diluted and its back reaction to the equation for $\hat{\rho}$ will be suppressed compared to the loss term. More importantly, the gain in angular momentum of background will be shared between orbital and spin angular momenta. Since spin is smaller than orbital by $\hbar$, the most of gain will go to the orbital angular momentum with a change of vorticity, $\Delta\boldsymbol{\omega}$. Since the spin is $\boldsymbol{S} \sim \mathcal{O}(\hbar)$, the change $\Delta\boldsymbol{\omega} \sim \mathcal{O}(\hbar)$, and its effect to the dynamics of $\boldsymbol{S}$ via $\Delta E = -\boldsymbol{S} \cdot \boldsymbol{\omega} \sim \mathcal{O}(\hbar^2)$ is higher order in small $\hbar$. Based on this consideration, we neglect possible "gain terms" in our quantum kinetic equation Eq.(3.1). In essence, we treat the background as a spin reservoir that can absorb any change of spin angular momentum in $\hat{\rho}$ of "dilute" massive quarks, without any back reaction of the absorbed spin to the evolution of $\hat{\rho}$ itself. This is justified as long as we track the spin polarization of dilute massive quarks only, without caring about those of light quarks and gluons.

The characteristic relaxation rate of spin polarization of massive quarks will be shown to be of order $\Gamma_0 \sim \alpha_s^2 \log(1/\alpha_s)T$ where $\alpha_s = g^2/(4\pi)$[1]. This is of the same microscopic relaxation rate that governs other transport coefficients, such as shear viscosity or charge conductivities. See Refs.[71; 103] for similar observations, but in terms of usual scattering rate picture, i.e. considering only diagonal elements of the density matrix. These contributions to Γ_0 arise from soft t-channel gluon exchange of momentum q in the scatterings with background hard thermal particles, where the log comes from a range $m_D \sim gT \ll q \ll T$. If the quark was light, there would also exist soft t-channel quark exchange contribution of the same leading log order, making conversion of a quark to a gluon[61; 97]. See Figure 8.

The spin polarization of light quarks can be transferred to that of gluons and vice versa by these conversion processes, and a complete picture for light quarks would have to involve the spin density matrices of both light quarks and gluons. For the process of Figure 8 to happen, the exchanged quark should be the same species of the incoming quark. Our assumption of a hard-scale mass $m \gg gT$ for the massive quark implies $q \gtrsim m \gg gT$, which makes a soft

[1]It can be shown that this is in fact true for light quarks and gluons as well, as it is universal for all soft t-channel processes [61].

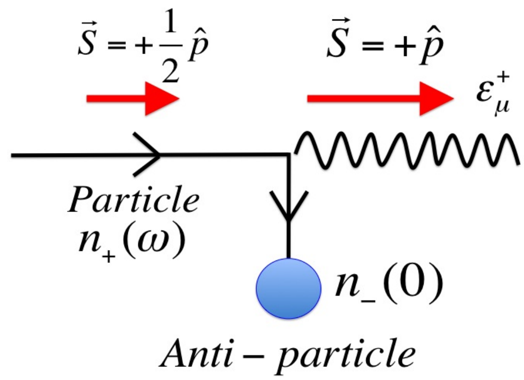

Figure 8: The quark-gluon conversion process that we can neglect for massive quarks in leading log order.

q quark exchange impossible for the massive quark. This justifies the absence of quark-gluon conversion process of Figure 8 for massive quark at leading log in our study.

3.1.2 Time evolution of spin density matrix in Schwinger-Keldysh formalism

We consider the Hilbert space of one-quark state interacting with background QCD plasma degrees of freedom in a finite temperature T. This reduced description is justified as long as the occupation number of quark per unit quantum state (given by $(\mathrm{N}umber\, of\, quarks) \times (2\pi\hbar)^3/(d^3\boldsymbol{x}d^3\boldsymbol{p})$ in phase space, usually called the distribution function $f(\boldsymbol{x},\boldsymbol{p})$) is much less than unity (or "dilute" Boltzmann limit), so that quantum statistics of Pauli blocking is negligible. We assume that our massive quark species satisfies this condition, either by $m \gtrsim T$ due to thermal Boltzmann suppression, or at least in early stages in heavy-ion collisions when the massive quarks are scarce. A convenient basis of states for our purpose is $\{|\boldsymbol{p},\pm\rangle\}$ of a momentum $\boldsymbol{p}$ and helicity $h = \pm 1/2$ (meaning that the spin state is an eigenstate of the spin angular momentum along $\hat{\boldsymbol{p}} = \boldsymbol{p}/p$ ($p \equiv |\boldsymbol{p}|$) with the eigenvalue $\pm\hbar/2$, that is, $(\hat{\boldsymbol{p}} \cdot \boldsymbol{\sigma})|\boldsymbol{p}, \pm\rangle = \pm|\boldsymbol{p}, \pm\rangle$). As explained in the introduction, we consider a density matrix that is (approximately) diagonal in the momentum variable, that is sufficient for describing the local quantum collision term Γ_0 in the quantum kinetic equation. We therefore have the density matrix per unit volume as (we set $\hbar = 1$ from here without much confusion)

$$\hat{\rho} = \int \frac{d^3\boldsymbol{p}}{(2\pi)^3} \hat{\rho}(\boldsymbol{p}) \,, \tag{3.4}$$

where $\hat{\rho}(\boldsymbol{p})$ is a 2×2 spin density matrix at a fixed momentum $\boldsymbol{p}$. More explicitly, we have

$$\hat{\rho}(\boldsymbol{p}) = \sum_{s,s'=\pm} |\boldsymbol{p}, s\rangle \rho_{s,s'}(\boldsymbol{p}) \langle \boldsymbol{p}, s'| \,, \tag{3.5}$$

in bra-ket notation, with a set of four functions in momentum space, $\rho_{s,s'}(\boldsymbol{p})$.

It is important to recall a phase ambiguity of the basis states $|\boldsymbol{p}, s\rangle \to e^{i\phi(\boldsymbol{p},s)}|\boldsymbol{p}, s\rangle$ with an arbitrary choice of $\phi(\boldsymbol{p}, s)$, which is reflected to the compensating phase ambiguity of $\rho_{s,s'}(\boldsymbol{p}) \to e^{-i(\phi(\boldsymbol{p},s)-\phi(\boldsymbol{p},s'))}\rho_{s,s'}(\boldsymbol{p})$, such that the density matrix $\hat{\rho}$ is unambiguous. We will be careful about this ambiguity in our computation, such that our final quantum kinetic equation in terms of physical spin polarization is well defined free of this phase ambiguity.

One way to fix the phase ambiguity is to work universally in the basis of z-component of spin operator. Then, the helicity $s/2$ state has an explicit 2-component spinor representation,

$\xi_s(\boldsymbol{p})$, satisfying $(\hat{\boldsymbol{p}} \cdot \boldsymbol{\sigma})\xi_s(\boldsymbol{p}) = s\xi_s(\boldsymbol{p})$, with normalization $\xi_s^\dagger \xi_s = 1$. The density matrix in this basis is then an explicit 2×2 matrix, given by

$$\hat{\rho}(\boldsymbol{p}) = \sum_{s,s'=\pm} \xi_s(\boldsymbol{p})\rho_{s,s'}(\boldsymbol{p})\xi_{s'}^\dagger(\boldsymbol{p})\,. \tag{3.6}$$

We emphasize again that $\xi_s(\boldsymbol{p})$ and hence $\rho_{s,s'}(\boldsymbol{p})$ are each phase ambiguous, but the net density matrix $\hat{\rho}(\boldsymbol{p})$ is free of ambiguity. The spin operator in this basis is $\boldsymbol{S} = \frac{1}{2}\boldsymbol{\sigma}$ (with $\hbar = 1$), and the spin polarization density in momentum space from $\hat{\rho}(\boldsymbol{p})$ is then given by

$$\boldsymbol{S}(\boldsymbol{p}) = \mathrm{T}r(\boldsymbol{S}\hat{\rho}(\boldsymbol{p})) = \frac{1}{2}\mathrm{T}r(\boldsymbol{\sigma}\hat{\rho}(\boldsymbol{p}))\,. \tag{3.7}$$

Recalling that $\mathrm{T}r(\hat{\rho}(\boldsymbol{p}))$ is the usual number distribution $f(\boldsymbol{p})$ that appears in the conventional semi-classical Boltzmann equation, we can express the density matrix in this basis as

$$\hat{\rho}(\boldsymbol{p}) = \frac{1}{2}f(\boldsymbol{p}) + \boldsymbol{S}(\boldsymbol{p}) \cdot \boldsymbol{\sigma}\,. \tag{3.8}$$

Note that $f(\boldsymbol{p})$ and $\boldsymbol{S}(\boldsymbol{p})$ are physical quantities and are independent of our basis choice: we will present our quantum kinetic equation for $f(\boldsymbol{p}, t)$ and $\boldsymbol{S}(\boldsymbol{p}, t)$ (t is time). The total spin polarization and the number of quarks per unit volume is then given by

$$\boldsymbol{S} = \int \frac{d^3\boldsymbol{p}}{(2\pi)^3}\, \boldsymbol{S}(\boldsymbol{p})\,, \quad n = \int \frac{d^3\boldsymbol{p}}{(2\pi)^3}\, f(\boldsymbol{p})\,. \tag{3.9}$$

The density matrix $\hat{\rho}(t)$ and its time evolution is most naturally described in the Schwinger-Keldysh formalism. The path integral in the time-forward contour (labeled as contour 1) gives the unitary time evolution of the ket part of the density matrix, and that in the time-backward contour (contour 2) gives the complex conjugate evolution of the bra part of the density matrix,

$$\hat{\rho}(t) = \langle U_1(t,t_0)\hat{\rho}(t_0)U_2^\dagger(t,t_0)\rangle_A \,, \tag{3.10}$$

where $U_{1,2}(t,t_0) = \mathcal{P}e^{-i\int_{t_0}^{t} dt'\, H_{1,2}(t')}$ are the unitary time evolutions in the contours 1 and 2 respectively, and $\langle\cdots\rangle_A$ means the thermal path integral average of background degrees of freedom of the QCD plasma. Since our system is an open system and is interacting with background degrees of freedom (more precisely, through the soft-scale color gauge field $A_\mu(x)$ in leading log order), the $H_1(t)$ depends on the operator of the background degrees of freedom in contour 1 that couples our system to the background, and it is time-dependent in general due to time-dependence of that operator (i.e. the color gauge field in contour 1, $A_\mu^{(1)}(\boldsymbol{x},t)$). The same is true for $H_2(t)$ and $A_\mu^{(2)}(\boldsymbol{x},t)$. The average $\langle\cdots\rangle_A$ in the above then involves the thermal correlation functions of $A^{(1)}$ and $A^{(2)}$ in the Schwinger-Keldysh contours (the two-point functions in our leading order computation). In the frequency space, these correlation functions satisfy the KMS relations. More explicitly, defining

$$G_{\mu\nu}^{(ij)}(q^0,\boldsymbol{q}) = \int d^3\boldsymbol{x}dt\, e^{i(q^0t-\boldsymbol{q}\cdot\boldsymbol{x})}\,\langle A_\mu^{(i)}(\boldsymbol{x},t)A_\nu^{(j)}(\boldsymbol{0},0)\rangle_A \,, \quad i,j=1,2\,(\text{SK contours}) \tag{3.11}$$

what we will need later are the relations,

$$G^{(12)}_{\mu\nu}(q^0,\boldsymbol{q}) = n_B(q^0)\rho_{\mu\nu}(q^0,\boldsymbol{q})\,,\quad G^{(21)}_{\mu\nu}(q^0,\boldsymbol{q}) = (n_B(q^0)+1)\rho_{\mu\nu}(q^0,\boldsymbol{q})\,, \tag{3.12}$$

in terms of the gluon spectral density $\rho_{\mu\nu} \equiv i(G^R_{\mu\nu} - (G^R_{\nu\mu})^*) = -2\,\mathrm{Im}[G^R_{\mu\nu}]$, where G^R is the retarded two-point function and the last equality holds only for symmetric case that is true in parity (P)-even background that we assume[1], and $n_B(q^0) = 1/(e^{\beta q^0}-1)$ is the Bose-Einstein distribution. In our leading log computation, these correlation functions include the well-known 1-loop Hard-Thermal-Loop (HTL) self-energy, the imaginary part of which gives the non-vanishing spectral density in soft t-channel space-like momenta, that represents the scatterings with background thermal particles by cutting the 1-loop, while the real part regulates the infrared divergence in these t-channel scatterings by (real-time) screening effects due to background thermal particles (see the Sec.(3.1.3) for a more detailed review on this).

The Hamiltonian in our one-quark picture is a sum of the free kinetic energy, H_0, and the QCD interaction with background gluon fields, H_I. The interaction Hamiltonian arises from the field theory Hamiltonian

$$H_I = g\int d^3\boldsymbol{x}\,\bar\psi(\boldsymbol{x})\gamma^\mu t^a\psi(\boldsymbol{x})A^a_\mu(\boldsymbol{x})\,, \tag{3.13}$$

---

[1]See Ref.[104] for an introduction to a possible anti-symmetric part, that is called “P-odd spectral density”, in the presence of background axial charge.

where $\psi(\boldsymbol{x})$ is the quark field operator, and $A^a_\mu(\boldsymbol{x})$ is the gluon field with color index a (t^a are the color generators). We choose our convention as

$$\gamma^0 = \begin{pmatrix} 0 & i\mathbf{1}_{2\times 2} \\ i\mathbf{1}_{2\times 2} & 0 \end{pmatrix}, \quad \gamma^i = \begin{pmatrix} 0 & i\sigma^i \\ -i\sigma^i & 0 \end{pmatrix}, i = 1, 2, 3\,, \tag{3.14}$$

and $\bar{\psi} \equiv -\psi^\dagger \gamma^0$. In this convention, the quark spinor of momentum $\boldsymbol{p}$ and helicity $h = \pm 1/2$, that shares the same phase ambiguity as the state $|\boldsymbol{p}, \pm\rangle$, is explicitly given by

$$|\boldsymbol{p}, s\rangle \sim u(\boldsymbol{p}, s) = \begin{pmatrix} \sqrt{E_p - sp}\, \xi_s(\boldsymbol{p}) \\ \sqrt{E_p + sp}\, \xi_s(\boldsymbol{p}) \end{pmatrix}, \tag{3.15}$$

where $p = |\boldsymbol{p}|$, $E_p = \sqrt{p^2 + m^2}$ and $(\hat{\boldsymbol{p}} \cdot \boldsymbol{\sigma})\xi_s(\boldsymbol{p}) = s\xi_s(\boldsymbol{p})$ ($s = \pm 1$). This explicit expression will be used in our computation of spin-dependent transition amplitudes. A quick way to see why the (arbitrary) phase of $|\boldsymbol{p}, s\rangle$ is identical to that of $u(\boldsymbol{p}, s)$ is to note the field operator $\psi(\boldsymbol{x})$ expanded as

$$\psi(\boldsymbol{x}) \sim \sum_{\boldsymbol{p}, s} u(\boldsymbol{p}, s) a_{\boldsymbol{p}, s} e^{i\boldsymbol{p}\cdot\boldsymbol{x}} + \mathrm{h.c} \tag{3.16}$$

where $a_{\boldsymbol{p},s}$ is the annihilation operator of one-quark state. Noting that $|\boldsymbol{p}, s\rangle \sim a^\dagger_{\boldsymbol{p},s}|0\rangle$, the phase ambiguity of $|\boldsymbol{p}, s\rangle$ (or equivalently, $a^\dagger_{\boldsymbol{p},s}$) is precisely identical to the phase ambiguity of $u(\boldsymbol{p}, s)$, such that the $\psi(\boldsymbol{x})$ operator and its conjugate entering the interaction Hamiltonian H_I are unambiguous. Ultimately, this phase ambiguity becomes that of the 2-component spinor

$\xi_s(\boldsymbol{p})$ in Eq.(3.15). As we use H_I in our computation with a consistent use of $\xi_s(\boldsymbol{p})$ in both H_I and the definition of density matrix Eq.(3.6), our result for $f(\boldsymbol{p})$ and $\boldsymbol{S}(\boldsymbol{p})$ is free of this ambiguity.

Since we need to keep the normalization of one-quark state correctly when discussing the density matrix, it is most convenient to work in a finite volume V with discrete spectrum of states and then take an infinite volume limit. The momentum space becomes discrete $\boldsymbol{p}_{\boldsymbol{n}}$ with integer-valued label vector $\boldsymbol{n}$, and the infinite volume limit is

$$\sum_{\boldsymbol{n}} \to V \int \frac{d^3\boldsymbol{p}}{(2\pi)^3} \,. \tag{3.17}$$

The fields are expanded as (including only the quark sector, neglecting anti-quarks)

$$\psi(\boldsymbol{x}) = \frac{1}{\sqrt{V}} \sum_{\boldsymbol{n},s} \frac{1}{\sqrt{2E_{p_{\boldsymbol{n}}}}} u(\boldsymbol{p}_{\boldsymbol{n}}, s) e^{i\boldsymbol{p}_{\boldsymbol{n}}\cdot\boldsymbol{x}} a_{\boldsymbol{p}_{\boldsymbol{n}},s} \,, \tag{3.18}$$

and

$$A_\mu(\boldsymbol{x}, t) = \frac{1}{V} \sum_{\boldsymbol{n}} A_\mu(\boldsymbol{p}_{\boldsymbol{n}}, t) e^{i\boldsymbol{p}_{\boldsymbol{n}}\cdot\boldsymbol{x}} + \text{h.}c. \,, \tag{3.19}$$

where $a_{\boldsymbol{p}_{\boldsymbol{n}},s}$ is the annihilation operator of one-quark state $|\boldsymbol{p}_{\boldsymbol{n}}, s\rangle$, with *unit normalization*, that is

$$\{a_{\boldsymbol{p}_{\boldsymbol{n}},s}, a^\dagger_{\boldsymbol{p}_{\boldsymbol{n}'},s'}\} = \delta_{\boldsymbol{n},\boldsymbol{n}'}\delta_{s,s'} \,, \tag{3.20}$$

and $A_\mu(\boldsymbol{p_n}, t)$ is defined such that it has the two-point correlation functions as

$$\langle A_\mu^{(i)}(\boldsymbol{p_n}, t) A_\nu^{(j)}(\boldsymbol{p_{n'}}, t')\rangle_A = V \delta_{\boldsymbol{n}, -\boldsymbol{n'}} G_{\mu\nu}^{(ij)}(\boldsymbol{p_n}, t)\,, \tag{3.21}$$

with the usual infinite volume correlation function $G_{\mu\nu}^{(ij)}(\boldsymbol{p}, t)$, so that $\langle A^{(i)}(\boldsymbol{x}, t) A^{(j)}(\boldsymbol{x'}, t')\rangle_A$ has the correct infinite volume limit (that is, independent of the volume V as a local correlation function). Then, the one-quark Hamiltonian from H_I becomes

$$H_I(t) = \frac{g}{V} \sum_{\boldsymbol{n}, s} \sum_{\boldsymbol{n'}, s'} \frac{1}{\sqrt{2E_{p_{\boldsymbol{n}}}}} \frac{1}{\sqrt{2E_{p_{\boldsymbol{n'}}}}} \bar{u}(\boldsymbol{p_n}, s) \gamma^\mu u(\boldsymbol{p_{n'}}, s') A_\mu(\boldsymbol{p_n} - \boldsymbol{p_{n'}}, t) a^\dagger_{\boldsymbol{p_n}, s} a_{\boldsymbol{p_{n'}}, s'}\,, \tag{3.22}$$

where the color structure is omitted for notation simplicity. The *normalized* one-quark states are created by

$$|\boldsymbol{p_n}, s\rangle \equiv a^\dagger_{\boldsymbol{p_n}, s} |0\rangle\,. \tag{3.23}$$

To obtain the time evolution equation of the density matrix from Eq.(3.10) in perturbation theory of H_I, we work in the interaction picture of H_0 and need to expand $U_{1,2}$ to quadratic order in H_I, since one-point functions of gluon fields vanish, $\langle A\rangle_A = 0$, and the first non-vanishing correlation functions are the two-point functions. Recall the interaction picture: $U(\Delta t, 0) = U_0(\Delta t) U_I(\Delta t, 0)$ where Δt is the time step we are considering, $U_0(\Delta t) = e^{-iH_0 \Delta t}$

is the free evolution, and we set the initial time as $t_0 = 0$ without loss of generality. Then, we have the interaction picture evolution as

$$U_I(\Delta t, 0) \approx 1 - i\int_0^{\Delta t} dt H_I^{\rm int}(t) + (-i)^2 \int_0^{\Delta t} dt \int_0^t dt' H_I^{\rm int}(t) H_I^{\rm int}(t') + \cdots \,, \qquad (3.24)$$

with $H_I^{int}(t) = U_0(t)^\dagger H_I(t) U_0(t)$. Using these in Eq.(3.10), we have

$$\begin{aligned} \hat{\rho}(\Delta t) &= U_0(\Delta t)\hat{\rho}(0)U_0^\dagger(\Delta t) + \int_0^{\Delta t} dt_1 \int_0^{\Delta t} dt_2 U_0(\Delta t)\langle H_I^{\rm int(1)}(t_1)\hat{\rho}(0)H_I^{\rm int(2)}(t_2)\rangle_A U_0^\dagger(\Delta t) \\ &+ (-i)^2 U_0(\Delta t)\int_0^{\Delta t} dt_1 \int_0^{t_1} dt_1' \langle H_I^{\rm int(1)}(t_1) H_I^{\rm int(1)}(t_1')\rangle_A \hat{\rho}(0) U_0^\dagger(\Delta t) \\ &+ (+i)^2 U_0(\Delta t)\hat{\rho}(0)\int_0^{\Delta t} dt_2 \int_0^{t_2} dt_2' \langle H_I^{\rm int(2)}(t_2') H_I^{\rm int(2)}(t_2)\rangle_A U_0^\dagger(\Delta t) \,, \end{aligned} \qquad (3.25)$$

where the second term in the first line comes from "cross" combination obtained by one H_I from U_1 and one from U_2, while the last two lines are "self-energy" contributions coming from quadratic expansions in H_I in each U_1 and U_2. We need the both types of contributions in order to make sure the probability conservation of the density matrix, that is, $\mathrm{T}r(\hat{\rho}(\Delta t)) = \mathrm{T}r(\hat{\rho}(0))$ to this order, that can be checked easily using the definition of correlation functions in Schwinger-Keldysh contours. See Figure 9 for diagrammatic representation of these contributions. The $H_I^{int(1)}$ and $H_I^{int(2)}$ are the Hamiltonians Eq.(3.22) with $A^{(1)}$ and $A^{(2)}$ fields, respectively. As they are linear in A fields, their correlation functions in Eq.(3.25) are proportional to the two-point correlation functions of background gluon fields, defined in Eq.(3.11).

Since our density matrix in Eq.(3.4) is diagonal in momentum space, and hence in energy spectrum of H_0, it commutes with H_0 and the first term in Eq.(3.25) is simply $\hat{\rho}(0)$. Writing

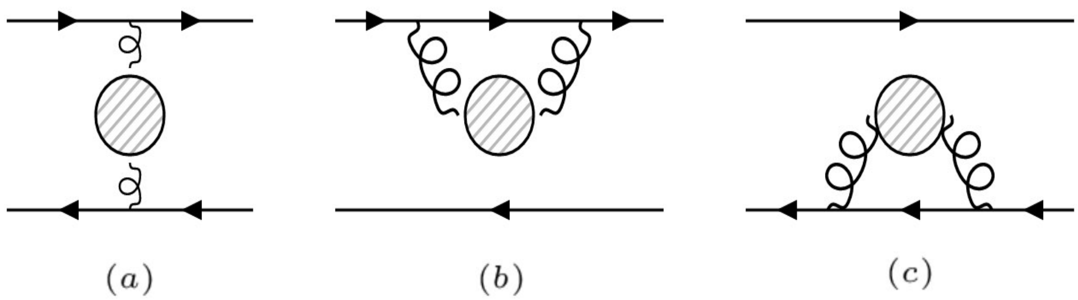

Figure 9: The "cross" contribution (a), and the two self energy contributions (b) and (c).

$\hat{\rho}(\boldsymbol{p_n})$ in the helicity basis Eq.(3.5) in terms of $\rho_{s,s'}(\boldsymbol{p_n}, t)$ (now with time-dependence), and using the explicit form of H_I in Eq.(3.22), the above evolution Eq.(3.25) can easily be translated to those of $\rho_{s,s'}(\boldsymbol{p_n}, t)$. From the identification $|\boldsymbol{p_n}, s\rangle = a^\dagger_{\boldsymbol{p_n},s}|0\rangle$, it can be seen that the phase ambiguity of $\rho_{s,s'}(\boldsymbol{p_n})$ via that of $|\boldsymbol{p_n}, s\rangle$ will cancel in the expression of the physical density matrix Eq.(3.6),

$$\hat{\rho}(\boldsymbol{p_n}) = \sum_{s,s'} \xi_s(\boldsymbol{p_n}) \rho_{s,s'}(\boldsymbol{p_n}) \xi^\dagger_{s'}(\boldsymbol{p_n}) \,, \tag{3.26}$$

due to the fact that $u(\boldsymbol{p_n}, s)$ appearing in H_I is proportional to $\xi_s(\boldsymbol{p_n})$ and it shares the same phase with the $a^\dagger_{\boldsymbol{p_n},s}$ (so that H_I is unambiguous) and hence $|\boldsymbol{p_n}, s\rangle$.

When the time step Δt of evolution is much larger than the correlation time of the gluon two-point functions, the cross and self energy terms in Eq.(3.25) will be linear in Δt, and the resulting evolution equation of density matrix will be of first order in time. In our leading log order, the dominant contribution to these terms come from the HTL contribution to the gluon two-point functions, with soft frequency-momenta in a range $gT \ll q \ll T$. This gives an estimate for the correlation time $\tau_c \lesssim (gT)^{-1}$ for leading log. As long as $\tau_c \ll \Delta t \ll 1/\delta E = \infty$, where δE is the energy difference between the two quantum spin states, this is a valid description of the time evolution.

More explicitly, for the cross term as an example, the two time integrals with the gluon two-point function can be written schematically as

$$\int_0^{\Delta t} dt_1 \int_0^{\Delta t} dt_2\, G^{(12)}(t_1 - t_2) e^{iq^0(t_1-t_2)} = \int_0^{\Delta t} dt_r \int_{-2t_r}^{2t_r} dt_a\, G^{(12)}(t_a) e^{iq^0 t_a}\,, \qquad (3.27)$$

with a change of variable $t_r = (t_1+t_2)/2$ and $t_a = t_1 - t_2$, and q^0 is some combination of energies of states (see the following expressions in this section). As $G^{(12)}(t_a)$ decays fast beyond $t_a > \tau_c$, we can extend the range of t_a integral to $[-\infty, +\infty]$ for most of t_r values in $[0, \Delta t]$ when $\Delta t \gg \tau_c$: this gives the leading term linear in Δt. Then the above becomes $G^{(12)}(q^0)\Delta t$ where $G^{(12)}(q^0)$ is the Fourier transform of $G^{(12)}(t)$. A similar manipulation can be done for self energy terms to get the leading linear term in Δt.

After some algebra with these ingredients, and taking an infinite volume limit, we obtain a well-defined evolution equation for $\rho_{s,s'}(\boldsymbol{p}, t)$. Writing

$$\frac{d}{dt}\rho_{s,s'}(\boldsymbol{p}, t) = g^2 C_2(F)(\Gamma_{cross} + \Gamma_{self\,energy})\,, \quad C_2(F) = \frac{N_c^2 - 1}{2N_c}\,, \qquad (3.28)$$

the cross contribution is given by

$$\Gamma_{cross} = \int \frac{d^3\boldsymbol{p}'}{(2\pi)^3}\frac{1}{4E_pE_{p'}}\sum_{s'',s'''}[\bar{u}(\boldsymbol{p},s)\gamma^\mu u(\boldsymbol{p}',s'')]\rho_{s'',s'''}(\boldsymbol{p}')[\bar{u}(\boldsymbol{p}',s''')\gamma^\nu u(\boldsymbol{p},s')]G^{(12)}_{\mu\nu}(E_p-E_{p'},\boldsymbol{p}-\boldsymbol{p}')\tag{3.29}$$

and the self-energy contribution is a sum

$$\begin{aligned}\Gamma_{self\,energy} = \; & - \int \frac{d^3\boldsymbol{p}'}{(2\pi)^3}\frac{1}{4E_pE_{p'}}\sum_{s'',s'''}[\bar{u}(\boldsymbol{p},s)\gamma^\mu u(\boldsymbol{p}',s'')][\bar{u}(\boldsymbol{p}',s'')\gamma^\nu u(\boldsymbol{p},s''')]\rho_{s''',s'}(\boldsymbol{p}) \\ & \times \int_0^{+\infty} dt_a\, G^{(11)}_{\mu\nu}(\boldsymbol{p}-\boldsymbol{p}',t_a)e^{i(E_p-E_{p'})t_a} \\ & - \int \frac{d^3\boldsymbol{p}'}{(2\pi)^3}\frac{1}{4E_pE_{p'}}\sum_{s'',s'''}\rho_{s,s'''}(\boldsymbol{p})[\bar{u}(\boldsymbol{p},s''')\gamma^\mu u(\boldsymbol{p}',s'')][\bar{u}(\boldsymbol{p}',s'')\gamma^\nu u(\boldsymbol{p},s')] \\ & \times \int_{-\infty}^0 dt_a\, G^{(22)}_{\mu\nu}(\boldsymbol{p}-\boldsymbol{p}',t_a)e^{i(E_p-E_{p'})t_a}\,.\end{aligned}\tag{3.30}$$

In the Appendix.(3.A.1), we prove the following important simplification in the self energy term, due to the rotational symmetry and P-even nature of thermal QCD background: the $\boldsymbol{p}'$ integral appearing in the self energy term

$$\int \frac{d^3\boldsymbol{p}'}{(2\pi)^3}\frac{1}{2E_{p'}}\sum_{s''}[\bar{u}(\boldsymbol{p},s)\gamma^\mu u(\boldsymbol{p}',s'')][\bar{u}(\boldsymbol{p}',s'')\gamma^\nu u(\boldsymbol{p},s''')]G^{(ij)}_{\mu\nu}(\boldsymbol{p}-\boldsymbol{p}',t_a)\tag{3.31}$$

is proportional to $\delta_{s,s'''}$, that is, it is non-zero only when the initial and final spins are the same, $s = s'''$, and moreover, the value doesn't depend on $s = \pm$. Physically, what it means is that the self energy can't flip the longitudinally polarized spin (i.e. helicity, $s/2$) due to rotational invariance of the background, and the self energy can't depend on the sign of helicity $s/2$ either, since s flips under parity transformation. With this, the two terms in the self energy Eq.(3.30) nicely combine to give

$$\begin{aligned}
\Gamma_{self\,energy} = & -\int \frac{d^3\boldsymbol{p}'}{(2\pi)^3}\frac{1}{4E_pE_{p'}}\sum_{s''}[\bar{u}(\boldsymbol{p},s)\gamma^\mu u(\boldsymbol{p}',s'')][\bar{u}(\boldsymbol{p}',s'')\gamma^\nu u(\boldsymbol{p},s)]\rho_{s,s'}(\boldsymbol{p}) \\
& \times \left(\int_0^{+\infty} dt_a\, G^{(11)}_{\mu\nu}(\boldsymbol{p}-\boldsymbol{p}',t_a) + \int_{-\infty}^0 dt_a\, G^{(22)}_{\mu\nu}(\boldsymbol{p}-\boldsymbol{p}',t_a)\right) e^{i(E_p-E_{p'})t_a} \\
= & -\int \frac{d^3\boldsymbol{p}'}{(2\pi)^3}\frac{1}{4E_pE_{p'}}\sum_{s''}[\bar{u}(\boldsymbol{p},s)\gamma^\mu u(\boldsymbol{p}',s'')][\bar{u}(\boldsymbol{p}',s'')\gamma^\nu u(\boldsymbol{p},s)]\rho_{s,s'}(\boldsymbol{p}) \\
& \times G^{(21)}_{\mu\nu}(E_p-E_{p'},\boldsymbol{p}-\boldsymbol{p}')\,, \qquad (3.32)
\end{aligned}$$

in terms of the Fourier transform of the correlation function $G^{(21)}_{\mu\nu}$, where we use an identity for Schwinger-Keldysh two-point functions,

$$G^{(11)}_{\mu\nu}(t)\theta(t) + G^{(22)}_{\mu\nu}(t)\theta(-t) = G^{(21)}_{\mu\nu}(t)\,, \qquad (3.33)$$

to combine the two t_a integrals.

The appearance of $G^{(12)}$ in the cross term and $G^{(21)}$ in the self energy is a reflection of the generic feature that ensures the thermal detailed balance with the KMS relation Eq.(3.12). In fact, using the identity

$$G^{(21)} = \left(\frac{n_B(q^0)+1}{n_B(q^0)}\right) G^{(12)} = e^{q^0/T}G^{(12)}\,, \qquad (3.34)$$

one can easily check from Eq.(3.29) and Eq.(3.32) that the equilibrium thermal density matrix

$$\rho^{\mathrm{eq}}_{s,s'}(\boldsymbol{p}) = \frac{z}{2}\delta_{s,s'}e^{-E_p/T}\,, \tag{3.35}$$

with any fugacity constant $z = e^{\mu/T}$ makes the sum of Γ_{cross} and $\Gamma_{self\,energy}$ terms vanishes. This equilibrium is also equivalently described by

$$\hat{\rho}^{\mathrm{eq}}(\boldsymbol{p}) = \frac{z}{2}e^{-E_p/T}\mathbf{1}\,, \quad f^{\mathrm{eq}}(\boldsymbol{p}) = ze^{-E_p/T}\,, \quad \boldsymbol{S}^{\mathrm{eq}}(\boldsymbol{p}) = 0\,. \tag{3.36}$$

The rest of the paper presents key elements of our computation of the integrals in Eq.(3.29) and Eq.(3.32) in leading log order. Readers who are interested in only the final results can go straight to Sec.(3.1.4).

3.1.3 Leading log integrals with arbitrary quark mass

We first consider the evaluation of the cross term Eq.(3.29). Since the physical density matrix that is free of phase ambiguity that we discussed is $\hat{\rho}(\boldsymbol{p}) = \sum_{s,s'}\xi_s(\boldsymbol{p})\rho(\boldsymbol{p})_{s,s'}\xi^\dagger_{s'}(\boldsymbol{p})$, we consider this object. Using also that

$$\rho_{s,s'}(\boldsymbol{p}) = \xi^\dagger_s(\boldsymbol{p})\hat{\rho}(\boldsymbol{p})\xi_{s'}(\boldsymbol{p})\,, \tag{3.37}$$

we can express Eq.(3.29) in terms of the unambiguous $\hat{\rho}(\boldsymbol{p})$. Since we will focus only on the soft $\boldsymbol{q} = \boldsymbol{p} - \boldsymbol{p}' \sim gT$ regime that produces the leading log, we change the integration variables from $\boldsymbol{p}'$ to $\boldsymbol{q}$,

$$\int \frac{d^3\boldsymbol{p}'}{(2\pi)^3} = \int \frac{d^3\boldsymbol{q}}{(2\pi)^3} \,. \tag{3.38}$$

What needs to be computed in the resulting integrand is the following spinor summation, contracted with the gluon two-point function,

$$\sum_{s,s',s'',s'''} \xi_s(\boldsymbol{p})\bar{u}(\boldsymbol{p},s)\gamma^\mu u(\boldsymbol{p}',s'')\xi^\dagger_{s''}(\boldsymbol{p}')\hat{\rho}(\boldsymbol{p}')\xi_{s'''}(\boldsymbol{p}')\bar{u}(\boldsymbol{p}',s''')\gamma^\nu u(\boldsymbol{p},s')\xi^\dagger_{s'}(\boldsymbol{p})G^{(12)}_{\mu\nu}(E_p - E_{p'},\boldsymbol{q}) \tag{3.39}$$

where $\boldsymbol{p}' = \boldsymbol{p} - \boldsymbol{q}$.

We work in the Coulomb gauge, where the gluon two-point functions are written in terms of the longitudinal and transverse spectral densities, ρ_L and ρ_T respectively, (not to be confused with the density matrix)

$$G^{(12)}_{\mu\nu}(q^0,\boldsymbol{q}) = n_B(q^0)\rho_{\mu\nu}(q^0,\boldsymbol{q}) \,, \tag{3.40}$$

with

$$\rho_{\mu\nu}(q^0,\boldsymbol{q}) = \left(\delta_{\mu 0}\delta_{\nu 0}\, \rho_L(q^0,q) + \Pi^T_{\mu\nu}(\boldsymbol{q})\rho_T(q^0,q)\right) \,, \tag{3.41}$$

where $q \equiv |\boldsymbol{q}|$, and the transverse projection operator has only spatial components as

$$\Pi^T_{ij}(\boldsymbol{q}) = (\delta_{ij} - \hat{\boldsymbol{q}}_i \hat{\boldsymbol{q}}_j)\,, \quad \hat{\boldsymbol{q}} \equiv \boldsymbol{q}/q\,. \tag{3.42}$$

From the explicit expression of spinor Eq.(3.15), we have

$$\bar{u}(\boldsymbol{p},s)\gamma^\mu u(\boldsymbol{p}',s'') = \left(\sqrt{(E_p - sp)(E_{p'} - s''p')}\xi^\dagger_s(\boldsymbol{p})\bar{\sigma}^\mu \xi_{s''}(\boldsymbol{p}') + \sqrt{(E_p + sp)(E_{p'} + s''p'')}\xi^\dagger_s(\boldsymbol{p})\sigma^\mu \xi_{s''}(\boldsymbol{p}')\right), \tag{3.43}$$

where $\sigma^\mu = (\mathbf{1}, \boldsymbol{\sigma})$ and $\bar{\sigma}^\mu = (\mathbf{1}, -\boldsymbol{\sigma})$. Noting that

$$\xi_s(\boldsymbol{p})\xi^\dagger_s(\boldsymbol{p}) = \mathcal{P}_s(\boldsymbol{p}) = \frac{1}{2}\left(\mathbf{1} + s\hat{\boldsymbol{p}}\cdot\boldsymbol{\sigma}\right)\,, \tag{3.44}$$

is the projection operator to the helicity $s/2$ state in spin space, the spinor sum in Eq.(3.39) becomes a summation of various terms of the type,

$$\mathcal{P}_s(\boldsymbol{p})\sigma^\mu \mathcal{P}_{s''}(\boldsymbol{p}')\hat{\rho}(\boldsymbol{p}')\mathcal{P}_{s'''}(\boldsymbol{p}')\sigma^\nu \mathcal{P}_{s'}(\boldsymbol{p})\,. \tag{3.45}$$

The computation of these spinor sum is challenging, but is doable with some efforts utilizing several properties of the projection operators, such as

$$\sum_s \mathcal{P}_s(\boldsymbol{p}) = \mathbf{1}\,, \quad \mathcal{P}_s(\boldsymbol{p})A\mathcal{P}_s(\boldsymbol{p}) = \mathrm{Tr}\left(A\mathcal{P}_s(\boldsymbol{p})\right)\mathcal{P}_s(\boldsymbol{p})\,, \tag{3.46}$$

for any operator A. Note that these expressions are free of phase ambiguity of $\xi_s(\boldsymbol{p})$, due to the reasons as explained before.

Since $G^{(12)}_{\mu\nu}(q^0,\boldsymbol{q}) = n_B(q^0)(\delta_{\mu 0}\delta_{\nu 0}\rho_L(q^0,q) + \Pi^T_{\mu\nu}(\boldsymbol{q})\rho_T(q^0,q))$, we present our results of computation of Eq.(3.39) in terms of longitudinal (that involves ρ_L) and transverse (ρ_T) gluon parts, respectively. The longitudinal part of Eq.(3.39) is given as, omitting the obvious factor of $n_B(q^0)\rho_L(q^0,q)$ ($q^0 \equiv E_p - E_{p'}$), and writing $\hat\rho(\boldsymbol{p})$ in terms of the physical quantities (see Eq.(3.8)), $\hat\rho(\boldsymbol{p}) = \frac{1}{2}f(\boldsymbol{p}) + \boldsymbol{S}(\boldsymbol{p})\cdot\boldsymbol{\sigma}$,

$$\begin{aligned}&\frac{2}{(E_p+m)(E_{p'}+m)}\left(2(\boldsymbol{p}\cdot\boldsymbol{p}')(\boldsymbol{p}'\cdot\boldsymbol{S}(\boldsymbol{p}'))(\boldsymbol{p}\cdot\boldsymbol{\sigma}) - (p')^2(\boldsymbol{p}\cdot\boldsymbol{S}(\boldsymbol{p}'))(\boldsymbol{p}\cdot\boldsymbol{\sigma}) - p^2(\boldsymbol{p}'\cdot\boldsymbol{S}(\boldsymbol{p}'))(\boldsymbol{p}'\cdot\boldsymbol{\sigma})\right)\\ &+2\left((\boldsymbol{p}'\cdot\boldsymbol{S}(\boldsymbol{p}'))(\boldsymbol{p}\cdot\boldsymbol{\sigma}) - (\boldsymbol{p}\cdot\boldsymbol{S}(\boldsymbol{p}'))(\boldsymbol{p}'\cdot\boldsymbol{\sigma})\right) + 2\left(E_pE_{p'} + \boldsymbol{p}\cdot\boldsymbol{p}' + m^2\right)\hat\rho(\boldsymbol{p}')\,. \end{aligned} \tag{3.47}$$

The transverse part of Eq.(3.39), that is proportional to $n_B(q^0)\rho_T(q^0,q)$, is obtained after a long computation as

$$\begin{aligned} &2\left(E_pE_{p'} - (\boldsymbol{p}\cdot\hat{\boldsymbol{q}})(\boldsymbol{p}'\cdot\hat{\boldsymbol{q}}) - m^2\right)f(\boldsymbol{p}') - 4\frac{(E_p+m)}{(E_{p'}+m)}(\boldsymbol{p}'\cdot\boldsymbol{S}(\boldsymbol{p}'))(\boldsymbol{p}'\cdot\hat{\boldsymbol{q}})(\hat{\boldsymbol{q}}\cdot\boldsymbol{\sigma})\\ +\quad &4\left(-\frac{(E_{p'}+m)}{(E_p+m)}(\hat{\boldsymbol{q}}\cdot\boldsymbol{S}(\boldsymbol{p}'))(\boldsymbol{p}\cdot\hat{\boldsymbol{q}}) + \boldsymbol{p}'\cdot\boldsymbol{S}(\boldsymbol{p}')\right)(\boldsymbol{p}\cdot\boldsymbol{\sigma})\\ +\quad &4(E_pE_{p'} - m^2)(\hat{\boldsymbol{q}}\cdot\boldsymbol{S}(\boldsymbol{p}'))(\hat{\boldsymbol{q}}\cdot\boldsymbol{\sigma}) + 4\left((\boldsymbol{p}'\times\hat{\boldsymbol{q}})\cdot\boldsymbol{S}(\boldsymbol{p}')\right)((\boldsymbol{p}\times\hat{\boldsymbol{q}})\cdot\boldsymbol{\sigma})\,. \end{aligned} \tag{3.48}$$

We have checked the validity of the above results at least in two special limits: 1) $\boldsymbol{p}' = \boldsymbol{p}$ limit (treating $\hat{\boldsymbol{q}}$ arbitrary), and 2) massless ($m = 0$) limit. In both limits, the spinor sum Eq.(3.39) reduces to $s'' = s$ and $s''' = s'$ cases only, due to the fact that $\bar u(\boldsymbol{p},s)\gamma^\mu u(\boldsymbol{p}',s'')$

vanishes in these limits unless $s = s''$, which can be easily checked from the explicit spinor expression Eq.(3.15). Using this fact, one can compute Eq.(3.39) in these limits directly, and then can compare with the above results in the same limits. The longitudinal part is easy to compare, but the comparison of the transverse part needs some non-trivial identities. In the limit 1), one needs the following "*dyad*" identity ($\otimes$ is a dyad product of row and column vectors)

$$\hat{\boldsymbol{p}} \otimes \hat{\boldsymbol{p}} - (\hat{\boldsymbol{p}} \cdot \hat{\boldsymbol{q}})\hat{\boldsymbol{q}} \otimes \hat{\boldsymbol{p}} - (\hat{\boldsymbol{p}} \cdot \hat{\boldsymbol{q}})\hat{\boldsymbol{p}} \otimes \hat{\boldsymbol{q}} - \hat{\boldsymbol{q}} \otimes \hat{\boldsymbol{q}} + (\hat{\boldsymbol{p}} \times \hat{\boldsymbol{q}}) \otimes (\hat{\boldsymbol{p}} \times \hat{\boldsymbol{q}}) = (1 - (\hat{\boldsymbol{p}} \cdot \hat{\boldsymbol{q}})^2)\boldsymbol{I} \,, \tag{3.49}$$

for any two unit vectors $\hat{\boldsymbol{p}}$ and $\hat{\boldsymbol{q}}$, where $\boldsymbol{I}$ is the 3×3 identity dyad (matrix). In the case of the limit 2), one needs a more non-trivial identity that we checked by Mathematica,

$$\begin{aligned} & (1 - \hat{\boldsymbol{p}} \cdot \hat{\boldsymbol{p}'})\hat{\boldsymbol{q}} \otimes \hat{\boldsymbol{q}} - (\hat{\boldsymbol{p}} \cdot \hat{\boldsymbol{q}})\hat{\boldsymbol{q}} \otimes (\hat{\boldsymbol{p}} - \hat{\boldsymbol{p}}') + \hat{\boldsymbol{p}}' \otimes \hat{\boldsymbol{p}} - \hat{\boldsymbol{p}} \otimes \hat{\boldsymbol{p}}' + (\hat{\boldsymbol{q}} \cdot \hat{\boldsymbol{p}}')(\hat{\boldsymbol{p}} - \hat{\boldsymbol{p}}') \otimes \hat{\boldsymbol{q}} \\ + \;\; & (\hat{\boldsymbol{p}} \cdot \hat{\boldsymbol{p}}' - (\hat{\boldsymbol{p}} \cdot \hat{\boldsymbol{q}})(\hat{\boldsymbol{p}}' \cdot \hat{\boldsymbol{q}}))\boldsymbol{I} = -(\hat{\boldsymbol{p}} \cdot \hat{\boldsymbol{q}})\hat{\boldsymbol{q}} \otimes \hat{\boldsymbol{p}} + \hat{\boldsymbol{p}}' \otimes \hat{\boldsymbol{p}} - (\hat{\boldsymbol{p}}' \cdot \hat{\boldsymbol{q}})\hat{\boldsymbol{p}}' \otimes \hat{\boldsymbol{q}} + \hat{\boldsymbol{q}} \otimes \hat{\boldsymbol{q}} + (\hat{\boldsymbol{p}}' \times \hat{\boldsymbol{q}}) \otimes (\hat{\boldsymbol{p}} \times \hat{\boldsymbol{q}}) \,, \end{aligned} \tag{3.50}$$

for any three unit vectors $\hat{\boldsymbol{p}}$, $\hat{\boldsymbol{p}}'$ and $\hat{\boldsymbol{q}}$. These agreements give us confidence on the validity of the above spinor sum results.

The computation of spin sum in the self energy Eq.(3.32) is simpler. First note that the self energy term has a simple structure

$$\Gamma_{self\,energy} = -\gamma\, \hat{\rho}(\boldsymbol{p}) \,, \tag{3.51}$$

that is, it is a constant (γ) times of the identity operator in both the spin and momentum space. The "damping rate" γ is (recall $\boldsymbol{p}' = \boldsymbol{p} - \boldsymbol{q}$)

$$\gamma = \int \frac{d^3\boldsymbol{q}}{(2\pi)^3} \frac{1}{4E_p E_{p'}} \sum_{s''} [\bar{u}(\boldsymbol{p}, s)\gamma^\mu u(\boldsymbol{p}', s'')][\bar{u}(\boldsymbol{p}', s'')\gamma^\nu u(\boldsymbol{p}, s)] G^{(21)}_{\mu\nu}(E_p - E_{p'}, \boldsymbol{q}) \,. \quad (3.52)$$

Recalling that this expression doesn't depend on s (due to parity invariance as proved in Appendix.3.A.1), it turns out to be easier to compute the spin sum by expressing it as

$$\gamma = \frac{1}{2} \int \frac{d^3\boldsymbol{q}}{(2\pi)^3} \frac{1}{4E_p E_{p'}} \sum_{s,s''} [\bar{u}(\boldsymbol{p}, s)\gamma^\mu u(\boldsymbol{p}', s'')][\bar{u}(\boldsymbol{p}', s'')\gamma^\nu u(\boldsymbol{p}, s)] G^{(21)}_{\mu\nu}(E_p - E_{p'}, \boldsymbol{q}) \,, \quad (3.53)$$

removing any reference to s. For the longitudinal gluon contribution ($\mu = \nu = 0$), the spin sum becomes (recall $G^{(21)}_{\mu\nu}(q^0, \boldsymbol{q}) = (n_B(q^0) + 1)(\delta_{\mu 0}\delta_{\nu 0}\rho_L(q^0, q) + \Pi^T_{\mu\nu}(\boldsymbol{q})\rho_T(q^0, q)))$

$$\frac{1}{2} \sum_{s,s''} [\bar{u}(\boldsymbol{p}, s)\gamma^0 u(\boldsymbol{p}', s'')][\bar{u}(\boldsymbol{p}', s'')\gamma^0 u(\boldsymbol{p}, s)] = 2\left(E_p E_{p'} + \boldsymbol{p} \cdot \boldsymbol{p}' + m^2\right) \,, \quad (3.54)$$

and for the transverse gluon contribution, we obtain

$$\frac{1}{2} \sum_{s,s''} [\bar{u}(\boldsymbol{p}, s)\gamma^i u(\boldsymbol{p}', s'')][\bar{u}(\boldsymbol{p}', s'')\gamma^j u(\boldsymbol{p}, s)] \Pi^T_{ij}(\boldsymbol{q}) = 4\left(E_p E_{p'} - (\boldsymbol{p} \cdot \hat{\boldsymbol{q}})(\boldsymbol{p}' \cdot \hat{\boldsymbol{q}}) - m^2\right) \,. \quad (3.55)$$

After Eq.(3.39) and the spin sum in Eq.(3.53) is computed, what remains is to compute the $\boldsymbol{q}$ integrations in Eq.(3.29) and Eq.(3.53) to leading log order, with the gluon spectral densities $\rho_{L/T}(q^0, q)$ given by the well-known HTL contributions. For completeness, they are given by

$$\rho_L(q^0, q) = -2\,\mathrm{Im}\left(\frac{1}{q^2 - \Pi_L}\right)\,, \quad \Pi_L = -m_D^2\left(1 + (q^0/2q)\log\left(\frac{q^0 - q + i\epsilon}{q^0 + q + i\epsilon}\right)\right)\,, \tag{3.56}$$

where $m_D \sim gT$ is the Debye mass, and

$$\rho_T(q^0, q) = 2\,\mathrm{Im}\left(\frac{1}{q^2 - (q^0)^2 - \Pi_T}\right)\,, \tag{3.57}$$

where

$$\Pi_T = -\frac{m_D^2}{2}\left((q^0/q)^2 + \left((q^0/q)^2 - 1\right)(q^0/2q)\log\left(\frac{q^0 - q + i\epsilon}{q^0 + q + i\epsilon}\right)\right)\,. \tag{3.58}$$

As in the computations of shear viscosity and conductivities in massless limit [61], as well as in the computation of diffusion constant of heavy quark limit [105], we find that the leading log contribution comes from the same soft q regime, for arbitrary quark mass, where the log arises from the range $gT \ll q \ll T$. Physically, this contribution represents the t-channel scatterings with background thermal particles of hard scale ($p \sim T$) with a soft gluon exchange of momentum $(q^0, \boldsymbol{q})$. We emphasize that these HTL contributions include only the thermal background gluons and light quarks, which means that we don't include the scatterings with the other massive quarks present in the background plasma. This is the same "diluteness" assumption we explained at the beginning of Sec.(3.1.2). The Debye mass in this case is given by

$$m_D^2 = \frac{g^2T^2}{6}(2N_c + N_F)\,, \tag{3.59}$$

where $N_F = 2$ is the number of light flavors.

We follow the known steps of computing $\boldsymbol{q}$ integration in leading log order [61; 106; 107; 97; 104]. A first step in this $\boldsymbol{q}$ integration is to make a change of variable from the azimuthal angle $\cos\theta_{pq}$ between $\boldsymbol{p}$ and $\boldsymbol{q}$ to the energy transfer $q^0 = E_p - E_{p'}$ (recall $\boldsymbol{p}' \equiv \boldsymbol{p} - \boldsymbol{q}$), where they are related by

$$q\cos\theta_{pq} = \hat{\boldsymbol{p}}\cdot\boldsymbol{q} = \frac{E_p}{p}q^0 + \frac{q^2-(q^0)^2}{2p} \equiv q_L\,. \tag{3.60}$$

The q^0 has a maximum $q^0_{\max}$ (minimum $q^0_{\min}$) when $\theta_{pq} = 0$ (π), and

$$q^0_{\max/min} = \sqrt{p^2+m^2} - \sqrt{(p\mp q)^2+m^2} \approx \pm\frac{p}{E_p}q - \frac{m^2q^2}{2E_p^3} + \mathcal{O}(q^3)\,. \tag{3.61}$$

Note that $q^0_{\min}$ is different from $-q^0_{\max}$ by a term proportional to q^2, that is present only in the massive case. We will see that this q^2 correction to the q^0 integration range, that is absent in massless case, gives rise to the same leading log contribution to the final result, so it is important to keep it to this order. From this, we can convert $\boldsymbol{q}$ integration in Eq.(3.29) and Eq.(3.53) into an integration of two variables (q^0, q),

$$\begin{aligned} &\int \frac{d^3\boldsymbol{q}}{(2\pi)^3}\frac{1}{2E_{p'}}\,(spinor\ sum)\,\rho_{L/T}(E_p - E_{p'}, q) \\ = \quad & \frac{1}{2p}\int_0^\infty \frac{dq\,q}{(2\pi)}\int_{q^0_{\min}}^{q^0_{max}} \frac{dq^0}{(2\pi)}\,(spinor\ sum)\,\rho_{L/T}(q^0, q)\bigg|_{\hat{\boldsymbol{p}}\cdot\boldsymbol{q}\to\frac{E_p}{p}q^0+\frac{q^2-(q^0)^2}{2p}}\,, \end{aligned} \tag{3.62}$$

where (spinor sum) is the spinor part that we computed above, and the integration of polar angle around $\hat{\boldsymbol{p}}$ axis gives (2π), after we make the spinor part to be independent of polar angle, exploiting rotational symmetry, since $\rho_{L/T}(q^0, q)$ depends on $\boldsymbol{q}$ only via $q = |\boldsymbol{q}|$. Specifically, we can replace

$$\boldsymbol{q}^i \to q_L\hat{\boldsymbol{p}}^i = (\hat{\boldsymbol{p}}\cdot\boldsymbol{q})\hat{\boldsymbol{p}}^i\,,\quad \boldsymbol{q}^i\boldsymbol{q}^j \to q_L^2\hat{\boldsymbol{p}}^i\hat{\boldsymbol{p}}^j + \frac{1}{2}(\delta^{ij} - \hat{\boldsymbol{p}}^i\hat{\boldsymbol{p}}^j)(q^2 - q_L^2)\,. \tag{3.63}$$

One then computes (q^0, q) integration with the gluon spectral densities $\rho_{L/T}(q^0, q)$ to the desired order that produces the leading log in the final result. Since the leading log comes from soft $(q^0, q) \sim gT$ regime, one expands the (spinor sum) part in power series of soft $(q^0, q) \ll (p, E_p, m) \sim T$: it is sufficient to keep only up to linear order in (q^0, q), as higher powers give higher order terms in g. The total sum of the cross and self energy terms, Eq.(3.29) and Eq.(3.51) respectively, takes a form of Eq.(3.62) after this expansion, where the "spinor sum" part has a structure of

$$(spinor\ sum) = C^0(q^0/q) + q^0 C^1(q^0/q) + \mathcal{O}(q^2)\,, \tag{3.64}$$

with two functions $C^{0,1}(q^0/q)$ on q^0/q. There are two important features in this result, that makes the leading log contribution possible: 1) In principle, since the (spinor sum) contains $n_B(q^0) \sim T/q^0$ for $q^0 \sim gT \ll T$ (see Eq.3.12), the expansion could start from $(1/q^0)C^{-1}(q^0/q)$, instead of $C^0(q^0/q)$. In fact, both the cross and the self energy terms start from this order, but their sum cancels to this order. If this cancellation was absent, the final result of spin evolution rate would have been dominated by this order, which gives $g^2 \log(1/g)$, instead of $g^4 \log(1/g)$ that we find. This contribution would come from the ultra-soft range $g^2T \ll q \ll gT$, which represents "small angle" scatterings, contrary to our range $gT \ll q \ll T$ for $g^4 \log(1/g)$ that represents "large angle" scatterings. This cancellation is important also in computations of shear viscosity and charge conductivities (but not in "color" conductivity [108; 109]), and has been shown to be related to conservation Ward identities of energy-momentum and charge currents [107]. The same cancellation we observe in our spin density matrix suggests it may be related to angular momentum conservation. This cancellation also adds confidence that our computation of spin sum is correct. 2) In principle, the functions $C^{0,1}(q^0/q)$ could be any function on q^0/q, but they turn out to be even functions on q^0/q, which is crucial to have the final $g^4 \log(1/g)$ rate. This feature is important due to the fact that the spectral densities, $\rho_{L/T}$, are odd functions on q^0. If $q^0_{\min}$ was precisely equal to $-q^0_{\max}$ (as in the massless case), the q^0 integral of $C^0(q^0/q)$ would have vanished, and the first non-vanishing result would come from the next order $q^0C^1(q^0/q)$ term, which gives $g^4 \log(1/g)$ rate. Due to the q^2 correction to the q^0 integration range, $q^0_{max/min}$, in our massive case (see Eq.(3.61)), the $C^0(q^0/q)$ integral does contribute, but since this correction is one higher order than the leading range, the result is of the same order as the one from $q^0 C^1(q^0/q)$, that is, the same $g^4 \log(1/g)$ rate.

Let us define q^0 integrals of spectral densities, that are needed in our computation described above,

$$J_n^{L/T} = \int_{q^0_{\min}}^{q^0_{max}} \frac{dq^0}{(2\pi)} (q^0)^{2n-1} \rho_{L/T}(q^0, q)\,. \tag{3.65}$$

In the massless case, only integer n survives due to $q_{min} = -q_{\max}$ in that case, and they can be computed by a sum-rule technique [106; 107; 104], utilizing analytic property of the spectral densities. In our massive case, and only for the range of our interests, $gT \ll q \ll T$, the spectral densities can be simplified to produce the results for $J_n^{L/T}$ to our desired order

$$\rho_L(q^0, q) \approx \frac{\pi m_D^2 q^0}{q^5}\,, \quad \rho_T(q^0, q) \approx \frac{\pi m_D^2 \left(1 - (q^0/q)^2\right)(q^0/2q)}{\left(q^2 - (q^0)^2 + m_D^2/2\right)^2}\,, \tag{3.66}$$

where $m_D \sim gT$ is the Debye mass. One can easily check that in the massless limit, these spectral densities produce the same results for $J_n^{L/T}$ from the sum-rule technique. These expressions are obtained from the full expressions, Eq.(3.56) and Eq.(3.57), by using the hierarchy $m_D \sim gT \ll (q^0, q) \ll T$. It is convenient to write $J_n^{L/T}$ as

$$J_n^{L/T} = \frac{m_D^2}{q^{(4-2n)}} j_n^{L/T} \quad (n = \text{integer})\,, \quad J_n^{L/T} = \frac{m_D^2}{q^{(3-2n)}} \frac{m^2}{E_p^3} j_n^{L/T} \quad (n = half\ integer)\,, \tag{3.67}$$

in terms of the dimensionless coefficient functions $j_n^{L/T}$ on (p, E_p, m), after extracting the dependence on q explicitly as above. By explicit evaluations, we find them as in Table 1. Note

$j_0^L = \frac{p}{E_p}$	$j_0^T = \frac{\eta_p}{2}$
$j_{1/2}^L = -\frac{p}{2E_p}$	$j_{1/2}^T = -\frac{pE_p}{4m^2}$
$j_1^L = \frac{p^3}{3E_p^3}$	$j_1^T = \frac{\eta_p}{2} - \frac{p}{2E_p}$
$j_{3/2}^L = -\frac{2p^3}{E_p^3}$	$j_{3/2}^T = -\frac{p^3}{4m^2 E_p}$
$j_2^L = \frac{p^5}{5E_p^5}$	$j_2^T = \frac{\eta_p}{2} - \frac{p}{2E_p} - \frac{p^3}{6E_p^3}$

TABLE I: The coefficient functions $j_n^{L/T}$ ($\eta_p = \frac{1}{2}\ln\frac{E_p+p}{E_p-p}$ is rapidity).

that the half-integer n cases are needed for the contributions from $C^0(q^0/q)$ as we explained above, which exist only in the massive case. After doing q^0 integration using these formula, one finally performs q integration in Eq.(3.62) to get the leading log result, where q ranges in $m_D \ll q \ll T$: these boundaries come from the fact that our expression for the integrand is valid only in this range. The log arises from

$$\int_{m_D}^{T} \frac{dq}{q} \sim \log(T/m_D) \sim \log(1/g)\,. \tag{3.68}$$

3.1.4 Quantum kinetic equation for spin polarization of massive quarks

After a lengthy, but straightforward computation that we describe in the previous section, we present our final result for the time-evolution of the spin density matrix in momentum space, $\hat{\rho}(\boldsymbol{p}) = \frac{1}{2}f(\boldsymbol{p}) + \boldsymbol{S}(\boldsymbol{p})\cdot\boldsymbol{\sigma}$, in leading log order of $g^4\log(1/g)$. We write these evolution equations as

$$\frac{\partial f(\boldsymbol{p},t)}{\partial t} = C_2(F)\frac{m_D^2 g^2\log(1/g)}{(4\pi)}\,\frac{1}{2pE_p}\,\Gamma_f\,, \quad \frac{\partial \boldsymbol{S}(\boldsymbol{p},t)}{\partial t} = C_2(F)\frac{m_D^2 g^2\log(1/g)}{(4\pi)}\,\frac{1}{2pE_p}\,\boldsymbol{\Gamma}_S\,, \tag{3.69}$$

where Γ_f and $\boldsymbol{\Gamma}_S$ are diffusion-like differential operators in momentum space, that contain up to second order derivatives in $\boldsymbol{p}$. The Γ_f is given by ($\boldsymbol{\nabla}_p \equiv \partial/\partial\boldsymbol{p}$ and $(\boldsymbol{p}\cdot\boldsymbol{\nabla}_p)^2 f \equiv \boldsymbol{p}\cdot\boldsymbol{\nabla}_p\,(\boldsymbol{p}\cdot\boldsymbol{\nabla}_p f)$)

$$\begin{aligned}
\Gamma_f \;=\;& 4\left(-\frac{m^2}{E_p}j^L_{1/2} + E_p j^L_1 - \frac{m^2}{E_p^3}(p^2 j^T_{1/2} - E_p^2 j^T_{3/2}) + E_p(j^T_1 - j^T_2)\right) f(\boldsymbol{p}) \\
+& \left(E_p^2 T\left(j^L_0 - \frac{E_p^2}{p^2}j^L_1\right) + Tp^2 j^T_0 - 2TE_p^2 j^T_1 + \frac{TE_p^4}{p^2}j^T_2\right)\boldsymbol{\nabla}_p^2 f(\boldsymbol{p}) \\
+& \left(-\frac{TE_p^2}{p^2}\left(j^L_0 - \frac{3E_p^2}{p^2}j^L_1\right) - Tj^T_0 + \frac{4TE_p^2}{p^2}j^T_1 - \frac{3TE_p^4}{p^4}j^T_2\right)(\boldsymbol{p}\cdot\boldsymbol{\nabla}_p)^2 f(\boldsymbol{p}) \\
+& \frac{1}{p^2}\Bigg(-4m^2Tj^L_{1/2} - TE_p^2 j^L_0 + \left(6TE_p^2 + 2E_p^3 - \frac{3TE_p^4}{p^2}\right)j^L_1 - \frac{4m^2T}{E_p^2}(p^2 j^T_{1/2} - E_p^2 j^T_{3/2}) \\
& -Tp^2 j^T_0 + 2\left(p^2E_p + Tp^2 + TE_p^2\right)j^T_1 + E_p^2\left(-2E_p - 6T + \frac{3TE_p^2}{p^2}\right)j^T_2\Bigg)(\boldsymbol{p}\cdot\boldsymbol{\nabla}_p)f(\boldsymbol{p})\,.
\end{aligned} \tag{3.70}$$

This result passes a very non-trivial test of the expected detailed balance: one can check that $\Gamma_f = 0$ when $f(\boldsymbol{p}) = f^{\rm eq}(\boldsymbol{p}) = ze^{-E_p/T}$ for any constant z. It should be emphasized that this check is satisfied irrespective of the values of $j_n^{L/T}$, because the detailed balance is independent of details of the spectral densities that determine $j_n^{L/T}$. This gives us confidence that our computation is correct. We also note that our result for Γ_f that provides the local collision term in leading log order, together with free streaming advection term in Boltzmann equation, can be used to compute several conventional transport coefficients, such as shear viscosity and electric conductivity, arising from dilute massive quarks.

For the spin polarization part, we obtain ($i = 1, 2, 3$ denotes a spatial index for vector)

$$
\begin{aligned}
\boldsymbol{\Gamma}_S^i \;=\;& \left(-\frac{4m^2}{E_p} j^L_{1/2} + T j^L_0 + \left(4E_p - \frac{TE_p^2}{p^2}\right) j^L_1 - \frac{4m^2}{E_p^3}(p^2 j^T_{1/2} - E_p^2 j^T_{3/2}) + T j^T_0 \right.\\
& \left. + \left(4E_p + T - \frac{3TE_p^2}{p^2}\right) j^T_1 + \left(-4E_p + \frac{TE_p^2}{p^2}\right) j^T_2 \right) \boldsymbol{S}^i(\boldsymbol{p})\\
+\;& \left(E_p^2 T \left(j^L_0 - \frac{E_p^2}{p^2} j^L_1\right) + Tp^2 j^T_0 - 2TE_p^2 j^T_1 + \frac{TE_p^4}{p^2} j^T_2\right) \boldsymbol{\nabla}_p^2 \boldsymbol{S}^i(\boldsymbol{p})\\
+\;& \left(-\frac{TE_p^2}{p^2}\left(j^L_0 - \frac{3E_p^2}{p^2} j^L_1\right) - T j^T_0 + \frac{4TE_p^2}{p^2} j^T_1 - \frac{3TE_p^4}{p^4} j^T_2\right) (\boldsymbol{p}\cdot\boldsymbol{\nabla}_p)^2 \boldsymbol{S}^i(\boldsymbol{p})\\
+\;& \frac{1}{p^2}\left(-4m^2 T j^L_{1/2} - TE_p^2 j^L_0 + \left(6TE_p^2 + 2E_p^3 - \frac{3TE_p^4}{p^2}\right) j^L_1 - \frac{4m^2 T}{E_p^2}(p^2 j^T_{1/2} - E_p^2 j^T_{3/2}) \right.\\
& \left. -Tp^2 j^T_0 + 2\left(p^2 E_p + Tp^2 + TE_p^2\right) j^T_1 + E_p^2 \left(-2E_p - 6T + \frac{3TE_p^2}{p^2}\right) j^T_2 \right) (\boldsymbol{p}\cdot\boldsymbol{\nabla}_p) \boldsymbol{S}^i(\boldsymbol{p})\\
+\;& 2T\left(\frac{E_p}{E_p+m}\left(j^L_0 - \frac{E_p^2}{p^2} j^L_1\right) + j^T_0 - \frac{E_p}{p^2}(2E_p - m) j^T_1 + \frac{E_p^3}{p^2(E_p+m)} j^T_2\right) \boldsymbol{p}^i (\boldsymbol{\nabla}_p \cdot \boldsymbol{S}(\boldsymbol{p}))\\
-\;& 2T\left(\frac{E_p}{E_p+m}\left(j^L_0 - \frac{E_p^2}{p^2} j^L_1\right) + j^T_0 - \frac{E_p}{p^2}(2E_p - m) j^T_1 + \frac{E_p^3}{p^2(E_p+m)} j^T_2\right) \boldsymbol{\nabla}_p^i (\boldsymbol{p} \cdot \boldsymbol{S}(\boldsymbol{p}))\\
-\;& \frac{T}{p^2}\left(\frac{E_p - m}{E_p + m}\left(j^L_0 - \frac{E_p^2}{p^2} j^L_1\right) + j^T_0 - \left(1 + \frac{3E_p^2}{p^2} - \frac{2E_p}{E_p+m}\right) j^T_1 \right.\\
& \left. + \frac{E_p^2}{p^2}\left(3 + \frac{4p^2}{(E_p+m)^2} - \frac{6E_p}{E_p+m}\right) j^T_2 \right) \boldsymbol{p}^i (\boldsymbol{p}\cdot\boldsymbol{S}(\boldsymbol{p}))\,.
\end{aligned} \tag{3.71}
$$

Note that $f(\boldsymbol{p})$ and $\boldsymbol{S}(\boldsymbol{p})$ do not mix with each other in these equations.

There is a highly non-trivial test of the above result in the massless limit. Note that our computation doesn't include the quark-gluon conversion processes that becomes of the same order in the massless limit, and also our values of $J_n^{L/T}$ do not have the correct massless limit, so the massless limit of the above result should not be taken as the true result for the massless case. What we are testing is the "consistency" of the above equations with the "chirality conservation" in the massless limit, and this test is a *kinematical* one, and should hold true for each scattering processes included, independent of details of spectral densities, that is, the values of $J_n^{L/T}$. In the massless limit, the negative helicity state ($s=-1$, left-handed) and positive helicity state ($s=+1$, right-handed) are decoupled, and do not mix by gauge interactions. The spin density matrix should then take the following decoupled form

$$\hat{\rho}(\boldsymbol{p}) = f_+(\boldsymbol{p})\mathcal{P}_+(\boldsymbol{p}) + f_-(\boldsymbol{p})\mathcal{P}_-(\boldsymbol{p})\,, \quad \mathcal{P}_\pm(\boldsymbol{p}) = \frac{1}{2}\left(\mathbf{1} \pm \hat{\boldsymbol{p}}\cdot\boldsymbol{\sigma}\right)\,, \tag{3.72}$$

as a sum of positive and negative helicity chiral quark contributions, where $\mathcal{P}_\pm$ are nothing but the spin projection operators to the two decoupled helicity states. The $f_\pm(\boldsymbol{p})$ are the number distribution functions of chiral quarks of helicity $s/2 = \pm 1/2$ in momentum space. In a parity-even background that we are considering, f_+ and f_- should satisfy the same evolution equation. Writing the above density matrix as

$$\hat{\rho}(\boldsymbol{p}) = \frac{1}{2}\left(f_+(\boldsymbol{p}) + f_-(\boldsymbol{p})\right) + \frac{1}{2}\left(f_+(\boldsymbol{p}) - f_-(\boldsymbol{p})\right)\hat{\boldsymbol{p}}\cdot\boldsymbol{\sigma}\,, \tag{3.73}$$

we see the correspondence to our variables $f(\boldsymbol{p})$ and $\boldsymbol{S}(\boldsymbol{p})$ as,

$$f(\boldsymbol{p}) = f_+(\boldsymbol{p}) + f_-(\boldsymbol{p}) \,, \quad \boldsymbol{S} = \frac{1}{2}\left(f_+(\boldsymbol{p}) - f_-(\boldsymbol{p})\right)\hat{\boldsymbol{p}} \equiv f_s(\boldsymbol{p})\hat{\boldsymbol{p}} \,. \tag{3.74}$$

Since f_+ and f_- satisfy the same evolution equation, the two functions $f(\boldsymbol{p})$ and $f_s(\boldsymbol{p})$ should satisfy the same equation as well. This means that our above result, when we take the massless limit while keeping $J_n^{L/T}$ arbitrary, should pass the following non-trivial tests: 1) the evolution equation for $\boldsymbol{S}(\boldsymbol{p})$ must admit a consistent Ansatz, $\boldsymbol{S}(\boldsymbol{p}) = f_s(\boldsymbol{p})\hat{\boldsymbol{p}}$, and 2) the resulting evolution equation for $f_s(\boldsymbol{p})$ must be the same as the one for $f(\boldsymbol{p})$ in the massless limit. Both tests require non-trivial cancellations between various terms in Eq.(3.71), and it is amusing to check that the tests are satisfied by our results Eq.(3.70) and Eq.(3.71): the $f(\boldsymbol{p})$ and $f_s(\boldsymbol{p})$ satisfy the same evolution equation in the massless limit with

$$\begin{aligned}
\Gamma_f^{m=0} \;&=\; 4p\left(j_1^L + j_1^T - j_2^T)\right) f(\boldsymbol{p}) + p^2 T\left(j_0^L - j_1^L + j_0^T - 2j_1^T + j_2^T\right)\boldsymbol{\nabla}_p^2 f(\boldsymbol{p}) \\
&+\; T\left(-j_0^L + 3j_1^L - j_0^T + 4j_1^T - 3j_2^T\right)(\boldsymbol{p}\cdot\boldsymbol{\nabla}_p)^2 f(\boldsymbol{p}) \\
&+\; \left(-Tj_0^L + (3T+2p)j_1^L - j_0^T + 2(p+2T)j_1^T - (3T+2p)j_2^T\right)(\boldsymbol{p}\cdot\boldsymbol{\nabla}_p) f(\boldsymbol{p}) \,.
\end{aligned} \tag{3.75}$$

This also means that the massless limit allows a broader set of equilibria as

$$\hat{\rho}^{\rm eq}(\boldsymbol{p}) = z_+ e^{-p/T}\mathcal{P}_+(\boldsymbol{p}) + z_- e^{-p/T}\mathcal{P}_-(\boldsymbol{p}) \,, \tag{3.76}$$

with arbitrary chiral fugacity constants $z_\pm = e^{\mu_\pm/T}$. With these remarkable checks satisfied, we become confident that the results Eq.(3.70) and Eq.(3.71) are correct.

Using the explicit values of $j_n^{L/T}$ given in Table 1, we have the following expression for the Γ_f,

$$\begin{aligned}\Gamma_f &= 2pf(\boldsymbol{p}) + \left(\frac{3}{2}TE_p p - \frac{TE_p^3}{2p} + \frac{\eta_p T m^4}{2p^2}\right)\boldsymbol{\nabla}_p^2 f(\boldsymbol{p}) + \frac{Tm^2}{2p^2}\left(\eta_p + \frac{3E_p}{p} - \eta_p\frac{3E_p^2}{p^2}\right)(\boldsymbol{p}\cdot\boldsymbol{\nabla}_p)^2 f(\boldsymbol{p}) \\ &+ \frac{1}{p^2}\left(pE_p^2 - \frac{\eta_p T m^2}{2} - \eta_p E_p m^2 - \frac{3TE_p m^2}{2p} + \frac{3\eta_p T m^2 E_p^2}{2p^2}\right)(\boldsymbol{p}\cdot\boldsymbol{\nabla}_p) f(\boldsymbol{p})\,. \qquad (3.77)\end{aligned}$$

It can be shown that after some tedious calculation one can rewrite $\frac{1}{2pE_p}\Gamma_f$ as a total divergence term so that total number of massive quarks are clearly conserved.

$$\begin{aligned}\frac{\Gamma_f}{2pE_p} &= \boldsymbol{\nabla}_{p^i}\Big(T(\frac{3}{4} - \frac{E_p^2}{4p^2} + \frac{\eta_p m^4}{4p^3 E_p})\boldsymbol{\nabla}_{p^i} f(\boldsymbol{p}) + \boldsymbol{p}^i\frac{Tm^2}{4p^3E_p}(\eta_p + \frac{3E_p}{p} - \frac{3\eta_p E_p^2}{p^2})\boldsymbol{p}\cdot\boldsymbol{\nabla}_p f(\boldsymbol{p}) \\ &+ \frac{\boldsymbol{p}^i}{2p^2}(E_p - \frac{\eta_p m^2}{p}) f(\boldsymbol{p})\Big) \qquad (3.78)\end{aligned}$$

It can be checked again that the detailed balance condition is satisfied with $f^{\rm eq}(\boldsymbol{p}) = ze^{-E_p/T}$. For $\boldsymbol{\Gamma}^i_S$, we have

$$\begin{aligned}
\boldsymbol{\Gamma}^i_S &= \left(2p + \frac{TE_p}{p} - \frac{\eta_p m^2 T}{p^2}\right)\boldsymbol{S}^i(p) + \left(pTE_p - \frac{m^2 TE_p}{2p} + \frac{\eta_p m^4 T}{2p^2}\right)\boldsymbol{\nabla}_p^2 \boldsymbol{S}^i(\boldsymbol{p}) \\
&+ \left(\frac{\eta_p m^2 T}{2p^2}\left(1 - \frac{3E_p^2}{p^2}\right) + \frac{3m^2 TE_p}{2p^3}\right)(\boldsymbol{p}\cdot\boldsymbol{\nabla}_p)^2 \boldsymbol{S}^i(\boldsymbol{p}) \\
&+ \frac{1}{p^2}\left(pE_p^2 - \frac{3m^2 TE_p}{2p} + \eta_p m^2\left(-E_p - \frac{T}{2} + \frac{3TE_p^2}{2p^2}\right)\right)(\boldsymbol{p}\cdot\boldsymbol{\nabla}_p)\boldsymbol{S}^i(\boldsymbol{p}) \\
&+ 2T\left(\eta_p\left(\frac{1}{2} - \frac{E_p^2}{p^2} + \frac{mE_p}{2p^2} + \frac{E_p^3}{2p^2(E_p+m)}\right) + \frac{E_p}{p} - \frac{m}{2p} - \frac{m^2}{2p(E_p+m)}\right)\boldsymbol{p}^i(\boldsymbol{\nabla}_p\cdot\boldsymbol{S}(\boldsymbol{p})) \\
&- 2T\left(\eta_p\left(\frac{1}{2} - \frac{E_p^2}{p^2} + \frac{mE_p}{2p^2} + \frac{E_p^3}{2p^2(E_p+m)}\right) + \frac{E_p}{p} - \frac{m}{2p} - \frac{m^2}{2p(E_p+m)}\right)\boldsymbol{\nabla}_p^i(\boldsymbol{p}\cdot\boldsymbol{S}(\boldsymbol{p})) \\
&- \frac{T}{p^2}\left(\frac{E_p(E_p+2m)}{p(E_p+m)} + \frac{\eta_p m E_p}{E_p+m}\left(-\frac{3E_p}{p^2} + \frac{1}{E_p+m}\right)\right)\boldsymbol{p}^i(\boldsymbol{p}\cdot\boldsymbol{S}(\boldsymbol{p}))\,. \qquad (3.79)
\end{aligned}$$

Discussion

Our work is a small step toward a more complete picture of quantum kinetic theory of spin dynamics in perturbative QCD plasma. It is important to extend our work, going beyond the spatial homogeneous limit. This would introduce a spin density matrix $\hat\rho(\boldsymbol{x},\boldsymbol{p})$ that depends on both position and momentum, or equivalently $\hat\rho(\boldsymbol{p}_1,\boldsymbol{p}_2)$ which is non-diagonal in momentum space, as explained in the introduction. One could expect that the resulting quantum kinetic equation would look like

$$\left(\frac{\partial}{\partial t} + \boldsymbol{v}_p\cdot\frac{\partial}{\partial\boldsymbol{x}}\right)\hat\rho(\boldsymbol{x},\boldsymbol{p}) = \Gamma\cdot\hat\rho(\boldsymbol{x},\boldsymbol{p})\,,\quad \boldsymbol{v}_p \equiv \frac{\boldsymbol{p}}{E_p}\,, \qquad (3.80)$$

where Γ, the quantum kinetic collision term, is what we compute in this work. As discussed in the motivation, this picture has to be improved by including, either the gradient corrections to the collision term Γ (that is, corrections that involve $\partial_{\boldsymbol{x}}\hat{\rho}$), in order to allow spin-orbital angular momentum exchange, or the effects of background electromagnetic fields in both free streaming and collision terms. The latter part for the free streaming case was recently studied in Refs.[101; 38; 39; 102] for massive quarks, extending the recent development of chiral kinetic theory for massless chiral quarks [110; 111; 112; 113; 40; 114; 115], for which a Berry's curvature in momentum space due to spin projection plays a critical role. The former part is also expected to be intimately related to the "side-jump" phenomenon in chiral kinetic theory [116; 117; 118]. We hope to make further progress on these important goals in a near future.

The spin polarization in local equilibrium of conventional hydrodynamics description is fixed by hydrodynamic variables, such as temperature and vorticity, and it is not an independent hydrodynamic variable. However, since the total angular momentum including spin has to be conserved, one may think of formulating a hydrodynamics description of possible interplay between spin and orbital angular momenta. There has been recent development in this "spin hydrodynamics" in relativistic regime [41; 119; 42]. Since spin is of order $\hbar$, one can think of this as a $\mathcal{O}(\hbar)$ quantum correction to the conventional classical hydrodynamics description. Some of the transport coefficients in this spin hydrodynamics [42] should in principle be determined by the quantum kinetic theory that we aim to construct. We shall discuss more about our recent development about the "spin hydrodynamics" in the next section.

3.2 Non-dissipative second-order transport, spin, and pseudo-gauge transformations in hydrodynamics

(Previously published as: S. Li, M. A. Stephanov, and H.-U. Yee, Non-dissipative second-order transport, spin, and pseudo-gauge transformations in hydrodynamics, arXiv:2011.12318)

3.2.1 Motivation

Recent developments include interesting attempts to incorporate spin polarization of microscopic constituents as an additional hydrodynamic variable characterizing the system, which led to consideration of "spin hydrodynamics"[41; 42; 120]. This is motivated by importance of spin observables in many applications of hydrodynamics in condensed matter as well as nuclear physics. Specifically, each event in non-central RHIC carries a significant amount of initial orbital angular momentum $\sim 10^5\hbar$, some of which is transferred to the spin polarization of observed hadrons [36; 21; 23; 24; 25; 28; 29]. However, in the strict sense of hydrodynamics, spin polarization of plasma constituents should also be in local equilibrium, and must be determined by conventional hydrodynamic variables. [1]

In this section we assume the standard local equilibrium, and construct the spin hydrodynamics. We further show that the conventional hydrodynamics and spin hydrodynamics are two equivalent descriptions of the same system. This not only reconciles the two formula-

[1] Certain variants of spin hydrodynamics [42] could describe off-equilibrium dynamics of spin polarization in a system where relaxation time of spin polarization is much slower than other microscopic time scales. Similar extensions of hydrodynamics by non-hydrodynamic, but nevertheless *parametrically* slow, variables have been termed Hydro+ [121].

tions, but also leads us to find new constraints for certain transport coefficients in conventional second-order hydrodynamics.

The central question we answer in this work is the meaning of pseudo-gauge transformations [122; 119; 123] in spin hydrodynamics. Since hydrodynamics is based on local thermodynamics, this question can only be answered after properly addressing how thermodynamics transform under pseudo-gauge transformations. We show the equivalence of local thermodynamics between the spin and conventional hydrodynamics, which requires us to generalize pseudo-gauge transformation to currents of entropy and conserved charge. We use these results to prove the equivalence between the spin hydrodynamics and the conventional hydrodynamics. In particular, we find that the ideal limit of spin hydrodynamics is equivalent to the conventional hydrodynamics with certain non-dissipative second-order transport coefficients. Moreover, five of these second-order transport coefficients are uniquely determined by two thermodynamic functions, one of which appears as the spin susceptibility in the spin hydrodynamics description.

The existence of such constraints on certain second-order transport coefficients is an interesting fact by itself, independent of its physics connection to the spin hydrodynamics. Within the conventional hydrodynamics, we show that the same constraints can be derived directly using the second law of thermodynamics, and are therefore universal. Our derivation is based on a new power counting scheme for gradients of hydrodynamic variables, motivated by considering small deviations from one of the equilibrium states of uniformly rotating fluid, which exist due to conservation of total angular momentum.

We consider *dissipative* gradients of fluid velocity and of $\alpha = \mu/T$, as being much smaller than the vorticity and the temperature gradients neither of which appear in the entropy production rate at leading order in gradients. This allows us to reorganize the naive gradient expansion in the entropy production rate and to derive a set of nontrivial constraints on certain second-order transport coefficients by applying the second law of thermodynamics. Our method should be more generally applicable to some higher-order transport coefficients, as well as to transport coefficients involving external electromagnetic fields, but we leave such generalizations to future work.

Although similar constraints have been found for chargless fluid [124; 125; 126] and charged fluid in Ref.[127] using different approach, the constraints in Ref. [127] appear to be less stringent, leaving four unconstrained parameters in constrast to the two coefficients we find. It would be interesting to establish relationship between the constraints we derive and the ones in Ref. [127], which appears to be a nontrival task due to difference in choices of variables and frames (we use conventional Landau frame).

3.2.2 Non-dissipative second-order hydrodynamics

Guided by the observation that vorticity in a uniformly rotating fluid can take arbitrary values without entropy production, we consider fluid states where vorticity and temperature gradients, $\omega_{\mu\nu} = \frac{1}{2}(\partial^{\perp}_{\mu} u_{\nu} - \partial^{\perp}_{\nu} u_{\mu})$, $\partial^{\perp}_{\mu}\beta$, while still being small, are larger than other, dissipative gradients, $\theta_{\mu\nu} = \frac{1}{2}(\partial^{\perp}_{\mu} u_{\nu} + \partial^{\perp}_{\nu} u_{\mu})$ and $\partial^{\perp}_{\mu}\alpha$, where $\partial^{\perp}_{\mu} \equiv \Delta_{\mu\nu}\partial^{\nu}$ with $\Delta_{\mu\nu} = u_{\mu}u_{\nu} + g_{\mu\nu}$. To this end, we introduce the following power counting scheme: $\omega_{\mu\nu} \sim \epsilon_{\omega}$, $\partial^{\perp}_{\mu}\beta \sim \epsilon'$, $\theta_{\mu\nu} \sim \partial^{\perp}_{\mu}\alpha \sim \epsilon$, while any further spatial derivative on $(\omega_{\mu\nu}, \beta)$ and $(\theta_{\mu\nu}, \alpha)$ brings an extra ϵ' and ϵ, respectively.

For example, $\partial^{\perp}_{\rho}\omega_{\mu\nu} \sim \epsilon_{\omega}\epsilon'$, $\partial^{\perp}_{\mu}\partial^{\perp}_{\nu}\beta \sim \epsilon'^2$, and $\partial^{\perp}_{\rho}\theta_{\mu\nu} \sim \partial^{\perp}_{\mu}\partial^{\perp}_{\nu}\alpha \sim \epsilon^2$. In addition, we consider spatial gradients of thermal vorticity to be of the same order as the dissipative gradients, i.e. $\partial^{\perp}_{\nu}(\beta\omega^{\mu}) \sim \epsilon_{\omega}\epsilon$ rather than $\epsilon_{\omega}\epsilon'$, which means $\partial^{\perp}_{\nu}\omega^{\mu} = -(\partial^{\perp}_{\nu}\beta)\omega^{\mu}/\beta + \mathcal{O}(\epsilon_{\omega}\epsilon)$. From this and the ideal equation of motion, one can show that $\partial_{\mu}\omega^{\mu} \sim \omega^{\mu}\partial_{\mu}\beta \sim \epsilon_{\omega}\epsilon$.

We then invoke the hierarchy, $\epsilon'^2 \ll \epsilon \ll \epsilon_{\omega}\epsilon' \ll \epsilon_{\omega}^2 \ll \epsilon' \ll \epsilon_{\omega} \ll 1$. As we will see, this allows us to focus on the vorticity related terms arising from certain second-order transport coefficients as the leading contributions to the entropy production rate up to order $\epsilon_{\omega}\epsilon'\epsilon$, while the dissipative terms from first-order transport coefficients are of order $\epsilon^2 \ll \epsilon_{\omega}\epsilon'\epsilon$, and are thus sub-leading. Note that $\epsilon_{\omega}\epsilon'\epsilon$ would naively be of higher order than ϵ^2 in the conventional gradient expansion. By careful inspection of all possible terms in the entropy production rate, potentially larger terms of ϵ_{ω}^4, $\epsilon_{\omega}^3\epsilon'$ and $\epsilon_{\omega}^2\epsilon'^2$ can be shown to be absent in parity($\mathcal{P}$-) even plasma that we focus on in this work. Then the second law of thermodynamics, i.e. the non-negativity of entropy production, should be applied to these leading contributions involving second-order transport coefficients.

We write the general parity($\mathcal{P}$-) even constitutive relations for symmetric energy-momentum tensor, as well as for charge and entropy currents:

$$T^{\mu\nu} = (\varepsilon + p)u^{\mu}u^{\nu} + pg^{\mu\nu} + \Delta T^{\mu\nu}, \tag{3.81}$$

$$j^{\mu} = nu^{\mu} + \Delta j^{\mu}, \tag{3.82}$$

$$s^{\mu} = su^{\mu} + \Delta s^{\mu}, \tag{3.83}$$

where $\Delta T^{\mu\nu}$, Δj^μ and Δs^μ contain all relevant second order terms in our hierarchy,

$$\Delta T^{\mu\nu} = a_0 \Delta^{\mu\nu}\omega^{\lambda\rho}\omega_{\lambda\rho} + a_1 \omega^{\mu}{}_{\lambda}\omega^{\lambda\nu}, \tag{3.84}$$

$$\Delta j^\mu = c_1 \Delta^\mu_\rho \partial_\nu \omega^{\nu\rho} + c_2 \omega^{\mu\nu}\partial_\nu \beta, \tag{3.85}$$

$$\Delta s^\mu + \alpha \Delta j^\mu = b_1 \Delta^\mu_\rho \partial_\nu \omega^{\nu\rho} + b_2 \omega^{\mu\nu}\partial_\nu\beta + b_3 \omega^{\mu\nu}\partial_\nu \alpha, \tag{3.86}$$

with seven second-order transport coefficients $\{a_i, b_i, c_i\}$. We do not need to include the first-order transport terms as explained above, and we omit other possible second-order terms, such as $\partial^\perp_\mu \beta \partial^\perp_\nu \beta$ in $\Delta T^{\mu\nu}$ and $\omega^{\mu\nu}\partial_\nu\alpha$ in Δj^μ, that do not contribute to the entropy production rate to order $\epsilon_\omega \epsilon' \epsilon$, and whose coefficients are thus not constrained by our method. We also remark that one could put a purely spatial gradient $\Delta^\mu_\rho \Delta^\gamma_\nu \partial_\gamma \omega^{\nu\rho}$ in place of $\Delta^\mu_\rho \partial_\nu \omega^{\nu\rho}$ in Eq.(3.85), but this would be equivalent up to a redefinition of $\{b_2, c_2\}$ due to the ideal equations of motion and the thermodynamic relation $\beta dp = -w d\beta + n d\alpha$.

Adding $\beta u_\nu \partial_\mu T^{\mu\nu} + \alpha \partial_\mu j^\mu = 0$ to the entropy production and using the following identity which follow from the ideal hydrodynamic equations of motion,

$$\Delta^\mu_\alpha \partial_\nu \omega^{\nu\alpha} = -2u^\mu \omega_\nu \omega^\nu + \partial_\nu \omega^{\nu\mu}\,, \tag{3.87}$$

$$\omega_\mu D\omega^\mu = \omega^{\mu\nu}\frac{(\partial_\mu \varepsilon)(\partial_\nu p)}{2w^2} - \omega_\mu \omega^\mu \frac{Dp}{w} - \omega_\alpha^{\ \mu}\omega^{\alpha\nu}\theta_{\mu\nu}\,, \tag{3.88}$$

where $\omega^\mu \equiv \frac{1}{2}\epsilon^{\mu\nu\alpha\beta}u_\nu \omega_{\alpha\beta}$, $w = \varepsilon + p$ and $D \equiv u\cdot\partial$, one finds the entropy production rate up to $O(\epsilon_\omega \epsilon' \epsilon)$ given by

$$\partial_\mu s^\mu = C^{(1)}\omega_\nu\omega^\nu\theta + C^{(2)}(\partial_\nu^\perp\omega^{\nu\mu})\partial_\mu^\perp\alpha + C^{(3)}(\partial_\nu^\perp\omega^{\nu\mu})\partial_\mu^\perp\beta + C^{(4)}(\partial_\mu\beta)\omega^{\mu\nu}(\partial_\nu\alpha) + C^{(5)}\theta_{\mu\nu}\omega_\alpha{}^\mu\omega^{\alpha\nu}, \tag{3.89}$$

where $\theta \equiv \theta^\mu_\mu = \partial \cdot u$ and $C^{(i)}$ are given by

$$\begin{aligned}
C^{(1)} &= -2(a_0\beta + b_1 + 2b_1c_s^2 + b_2 w\beta_\varepsilon + b_3\alpha_p w c_s^2),\\
C^{(2)} &= \left(\frac{\partial b_1}{\partial\alpha}\right)_\beta + b_3 - c_1, \quad C^{(3)} = \left(\frac{\partial b_1}{\partial\beta}\right)_\alpha + b_2,\\
C^{(4)} &= \frac{b_3}{\beta} + \left(\frac{\partial b_3}{\partial\beta}\right)_\alpha + \frac{n}{\beta w}\left(\frac{\partial b_1}{\partial\beta}\right)_\alpha + \frac{1}{\beta}\left(\frac{\partial b_1}{\partial\alpha}\right)_\beta\\
&\quad + 2b_1\frac{\partial}{\partial\beta}\left(\frac{n}{\beta w}\right)_\alpha + \frac{b_2 n}{\beta w} - \left(\frac{\partial b_2}{\partial\alpha}\right)_\beta - \frac{c_1}{\beta} + c_2,\\
C^{(5)} &= a_1\beta + 4b_1,
\end{aligned}$$

where $c_s^2 = (\partial p/\partial\varepsilon)_{s/n}$, $\alpha_p = (\partial\alpha/\partial p)_{s/n}$ and $\beta_\varepsilon = (\partial\beta/\partial\varepsilon)_{s/n}$ are thermodynamic derivatives taken with s/n fixed, which appear naturally due to the ideal equations of motion, $(u\cdot\partial)(s/n) = 0$.

All five terms in Eq.(3.89) are independent and can have either sign for generic initial conditions. The second law of thermodynamics thus requires that all $C^{(i)}(i = 1, \ldots, 5)$ vanish. This gives five constraints for seven unknowns $\{a_i, b_i, c_i\}$, which determines them up to two free functions. Choosing a_0(which is nothing but the correction to the pressure) and a_1(which is interpreted as the spin susceptibility) as two given free functions, one can solve for the other five transport coefficients without any integration, proceeding in the following order:

$$b_1 = -\frac{\beta a_1}{4}, \quad b_2 = -\left(\frac{\partial b_1}{\partial \beta}\right)_\alpha, \tag{3.91a}$$

$$b_3 = \frac{1}{\alpha_p w c_s^2}\left[w\beta_\epsilon \left(\frac{\partial b_1}{\partial \beta}\right)_\alpha - b_1 - 2b_1 c_s^2 - \beta a_0\right], \tag{3.91b}$$

$$c_1 = b_3 + \left(\frac{\partial b_1}{\partial \alpha}\right)_\beta, \quad c_2 = -\left(\frac{\partial c_1}{\partial \beta}\right)_\alpha - 2b_1 \frac{\partial}{\partial \beta}\left(\frac{n}{\beta w}\right)_\alpha. \tag{3.91c}$$

As a nontrivial check of these relations we can consider conformal theory, such as the strongly coupled conformal plasma described by AdS/CFT correspondence for which some of the coefficients have been calculated in Ref. [128]. Conformal invariance imposes certain constraints on some of the thermodynamic quantities, such as $w = 4\varepsilon/3$, $c_s^2 = 1/3$, $\beta_\varepsilon = -\beta/(4\varepsilon)$, $\alpha_p = 0$, as well on transport coefficients: $a_1 = 3a_0$ and $(\partial b_1/\partial \beta)_\alpha = -b_1/\beta$. Substituting into Eq.(3.91b) we find that it is satisfied for any b_3 because, while $\alpha_p = 0$, also the expression in the square brackets nontrivially vanishes, provided b_1 is given by Eq.(3.91a). Furthermore, conformal invariance requires $\left(\partial\left(n/\beta w\right)/\partial \beta\right)_\alpha = 0$. Substituting into Eq.(3.91c), we find a relationship between c_1 and c_2 which coincides with a nontrivial constraint imposed by conformal Weyl symmetry [129; 128]. Finally, solving Eq.(3.91a) and Eq.(3.91c) we can now predict the values of b_1, b_2 and b_3 which have not been calculated in Ref. [128], in terms of a_1 and c_1 which have been calculated.

3.2.3 Hydrodynamics with spin degrees of freedom

Spin hydrodynamics is based on the canonical energy-momentum tensor $T_c^{\mu\nu}$ and the rank-3 tensor $S^{\mu\alpha\beta} = -S^{\mu\beta\alpha}$ of spin current, which have microscopic field theory definitions, the review of canonical construction of energy momentum and angular momentum tensor are reviewed in the Appendix.(3.B.1). The total angular momentum tensor consists of the orbital and the spin parts, $J^{\mu\alpha\beta} = (x^\alpha T_c^{\mu\beta} - x^\beta T_c^{\mu\alpha}) + S^{\mu\alpha\beta}$, and the formalism needs the additional conservation law, $\partial_\mu J^{\mu\alpha\beta} = 0$, corresponding to the introduction of additional spin degrees of freedom. This relates the anti-symmetric part of $T_c^{\mu\nu}$ to non-conservation of spin due to spin-orbit exchange of angular momentum: $T_c^{\mu\nu} - T_c^{\nu\mu} = -\partial_\alpha S^{\alpha\mu\nu}$.

The constitutive relations are given by

$$T_c^{\mu\nu} = \varepsilon u^\mu u^\nu + p\Delta^{\mu\nu} + (u^\mu q^\nu + u^\nu q^\mu) + \tau^{\mu\nu} - \frac{1}{2}\partial_\alpha S^{\alpha\mu\nu}, \tag{3.92}$$

$$j^\mu = n u^\mu + \tau^\mu, \quad S^{\mu\alpha\beta} = u^\mu S^{\alpha\beta} + \sigma^{\mu\alpha\beta}, \tag{3.93}$$

where we do not assume that u^μ is the Landau frame, q^μ $(u \cdot q = 0)$ is a contribution to energy current, $S^{\mu\nu}$ is the spin density in local rest frame satisfying the Frenkel condition $u_\mu S^{\mu\nu} = 0$, and $(\tau^{\mu\nu}, \tau^\mu, \sigma^{\mu\alpha\beta})$ are dissipative gradient corrections. We will not be concerned with these dissipative terms in our subsequent discussion of an ideal limit, because their inclusion will not affect our main conclusion.

Writing the entropy current as $s^\mu = su^\mu + \Delta s^\mu$, $(u_\mu \Delta s^\mu = 0)$ and adding $0 = \beta_\nu \partial_\mu T_c^{\mu\nu} + \alpha \partial_\mu j^\mu$ to $\partial_\mu s^\mu$ we obtain the following expression for the entropy production rate:

$$\begin{aligned}\partial_\mu s^\mu = [Ds - \beta D\varepsilon + \alpha Dn + \frac{1}{2}\beta\omega_{\mu\nu}DS^{\mu\nu}] + \theta[s - \beta(\varepsilon + p) + \alpha n + \frac{1}{2}\beta\omega_{\mu\nu}S^{\mu\nu}] \\ -\beta\tau^{\mu\nu}\theta_{\mu\nu} - \tau^\mu\partial_\mu\alpha + \partial_\mu[\Delta s^\mu - \frac{1}{2}\beta_\nu\partial_\alpha S^{\alpha\mu\nu} - \beta q^\mu + \alpha\tau^\mu + \frac{1}{2}(\partial_\rho\beta_\delta)\sigma^{\mu\rho\delta}] \\ +[(-\beta Du_\nu + \partial_\nu\beta)(q^\nu - \frac{1}{2\beta}S^{\nu\rho}\partial_\rho\beta)] - \frac{1}{2}(\partial_\alpha\partial_\mu\beta_\nu)\sigma^{\alpha\mu\nu},\end{aligned} \tag{3.94}$$

where $\beta_\nu \equiv \beta u_\nu$.

There exists an ideal limit of spin hydrodynamics where the right hand side of Eq.(3.94) vanishes. The vanishing of the first two square brackets leads to the following thermodynamics relations [130],

$$ds = \beta d\varepsilon - \alpha dn - \frac{\beta}{2}\gamma_{\mu\nu}dS^{\mu\nu},\; s = \beta(\varepsilon + p) - \alpha n - \frac{\beta}{2}\gamma_{\mu\nu}S^{\mu\nu}, \tag{3.95}$$

where the entropy density is a function of ε, n and $S^{\mu\nu}$, with the spin potential being equal to the fluid vorticity in local equilibrium: $\gamma_{\mu\nu} = \omega_{\mu\nu}$. We emphasize that the spin density should be fixed by the spin potential as a thermodynamic relation in equilibrium, i.e. $S^{\mu\nu} = \chi\gamma^{\mu\nu}$ with the spin susceptibility χ [131]. This determines the spin density in terms of hydrodynamic variables, $S^{\mu\nu} = \chi\omega^{\mu\nu}$.

Vanishing of other terms requires

$$\Delta s^\mu = \frac{1}{2}\beta_\nu\partial_\alpha(u^\alpha S^{\mu\nu}) + \beta q^\mu - \alpha\tau^\mu - \frac{1}{2}(\partial_\rho\beta_\delta)\sigma^{\mu\rho\delta},$$

and the following relation

$$q^{\mu} - \frac{w}{n}\tau^{\mu} = \frac{1}{2\beta}S^{\mu\nu}\partial_{\nu}\beta = \frac{\chi}{2\beta}\omega^{\mu\nu}\partial_{\nu}\beta. \tag{3.96}$$

Note that Eq.(3.96) is independent of the choice of the hydrodynamic frame u^{μ}. However, one can show, by introducing an impurity as in Ref.[132], that is $\partial_{\mu}T^{\mu\nu} = -\mathcal{F}^{\nu}$, then τ^{μ} vanishes in the "no-drag frame". This is a non-trivial example, similar to Chiral Vortical Effect [132], where the entropy flows past a static impurity without generating a drag. One could refer to this non-dissipative heat current we find as the vorticity driven thermal Hall effect.

As a nontrivial check of Eq.(3.96) we can calculate the heat current in the no-drag frame for the microscopic chiral kinetic theory of massless Dirac fermion. As detailed in Ref. [116], we choose the fluid rest frame as the spin frame $n_{\mu} = u_{\mu}$ so that the Frenkel condition is satisfied. With $n^{\mu} = (1, 0, 0, 0)$, the spin density $\boldsymbol{s}$ is proportional to the axial current, $s^i = \hbar j_5^i = \hbar\bar{\psi}\gamma^i\gamma_5\psi$. Therefore, $\boldsymbol{s} = \int_{\boldsymbol{p},\lambda} \hbar\lambda \boldsymbol{j}_p$, where $\boldsymbol{j}_p$ is the phase space (Liouville) current and $\int_{\boldsymbol{p},\lambda} \equiv \sum_{\lambda=\pm 1/2}\int d^3\boldsymbol{p}/(2\pi\hbar)^3$ includes the sum over helicities λ. According to Ref. [116], to order $\mathcal{O}(\hbar)$, $\boldsymbol{j}_p = (\hat{\boldsymbol{p}} - (\hbar\lambda/p_0)\hat{\boldsymbol{p}} \times \boldsymbol{\nabla})\, f_{\text{eq}}$, where $p_0 = |\boldsymbol{p}|$. The second term in $\boldsymbol{j}_p$ not only accounts for 2/3 of the Chiral Vortical Effect [35], but also plays an important role below to give the correct spin density. For uniformly rotating (shear-free) fluid in thermodynamic equilibrium, the particle distribution function in the no-drag frame takes the form [116; 132],

$f_{\rm eq} = 1/(\exp\{\beta(-p\cdot u + (1/2)S^{\mu\nu}_n\omega_{\mu\nu})\}+1)$, where $S^{\mu\nu}_n = \lambda\epsilon^{\mu\nu\alpha\beta}p_\alpha n_\beta/(p\cdot n)$ and $\mu = 0$ for simplicity. The spin density S^{ij} can then be computed as

$$S^{ij} = \epsilon^{ijk}s_k = \frac{\omega^{ij}}{24\hbar\beta^2} + O(\hbar^0)\,. \tag{3.97}$$

On the other hand, the canonical energy-momentum tensor is given by $T_c^{\mu\nu} = \int_{\boldsymbol{p},\lambda} j_p^\mu p^\nu$. Using the known result for j_p^μ, now up to $O(\hbar^2)$ from Ref. [133],

$$\boldsymbol{j}_p = \left(\hat{\boldsymbol{p}} - \frac{\hbar\lambda}{p_0}\hat{\boldsymbol{p}}\times\boldsymbol{\nabla} + \frac{(\hbar\lambda)^2}{p_0^2}(\hat{\boldsymbol{p}}\times\boldsymbol{\nabla})\times\boldsymbol{\nabla}\right)f_{\rm eq} + (\hbar\lambda)^2\boldsymbol{p}\left\{\boldsymbol{p}\cdot[(\hat{\boldsymbol{p}}\times\boldsymbol{\nabla})\times\boldsymbol{\nabla}]\right\}\frac{\partial}{\partial p_0}\left(\frac{f_{\rm eq}}{2p_0^3}\right),$$

and $j_p^0 = \hat{\boldsymbol{p}}\cdot\boldsymbol{j}_p$, we find that the symmetric part of T_c^{0i} contains the vorticity driven thermal Hall effect

$$q^i = \frac{1}{2}\int_{\boldsymbol{p},\lambda}(j_p^0p^i + j_p^ip^0) = \frac{\omega^{ij}\partial_j\beta}{48\hbar\beta^3} + \mathcal{O}(\hbar^0).$$

Combined with Eq.(3.97), this agrees with Eq.(3.96). It can also be checked that a similar term in the charge current $\boldsymbol{\tau} = \int_{\boldsymbol{p},\lambda}\boldsymbol{j}_p$ vanishes, in accordance with our expectation in the no-drag frame.

3.2.4 Equivalence between spin hydrodynamics and non-dissipative second-order hydrodynamics

It is well known that the canonical energy-momentum tensor can be transformed into the symmetric Belinfante-Rosenfeld energy-momentum tensor by a specific pseudo-gauge transformation with $\Sigma^{\alpha\mu\nu} = S^{\alpha\mu\nu}$ [122; 119; 123],

$$\tilde{T}^{\mu\nu} = T_c^{\mu\nu} + \frac{1}{2}\partial_\alpha \left(\Sigma^{\alpha\mu\nu} - \Sigma^{\mu\alpha\nu} - \Sigma^{\nu\alpha\mu}\right) = \frac{1}{2}\left(T_c^{\mu\nu} + T_c^{\nu\mu}\right) - \frac{1}{2}\partial_\alpha \left(S^{\mu\alpha\nu} + S^{\nu\alpha\mu}\right). \tag{3.98}$$

As a result, the spin tensor no longer appears in the total angular momentum tensor, i.e., $\tilde{S}^{\alpha\mu\nu} = S^{\alpha\mu\nu} - \Sigma^{\alpha\mu\nu} = 0$. This leaves the conservation of energy and momentum unchanged, $\partial_\mu \tilde{T}^{\mu\nu} = \partial_\mu T_c^{\mu\nu} = 0$, and the two descriptions of the system based on each energy-momentum tensor should be equivalent. This suggests that the corresponding hydrodynamic descriptions based on the same premise of local equilibrium, i.e. the spin hydrodynamics and the conventional hydrodynamics, should also be equivalent to each other. We will establish this equivalence and show that the hydrodynamic variables between the two descriptions are related quite non-trivially. In the following, quantities in the spin hydrodynamics will be denoted without tilde symbol, while those in the conventional hydrodynamics will be written with tilde symbol.

A central question in showing the equivalence is how the first law of thermodynamics used in hydrodynamics transforms under the pseudo-gauge transformation. The observation crucial for answering this question is that we can generalize the pseudo-gauge transformation to the currents of charge and entropy, without affecting their conservation

$$\tilde{j}^{\mu} = j^{\mu} - \partial_{\nu}\left(\frac{a}{2\chi}S^{\mu\nu}\right) = j^{\mu} - \frac{1}{2}\partial_{\nu}(a\omega^{\mu\nu}), \tag{3.99a}$$

$$\tilde{s}^{\mu} = s^{\mu} - \partial_{\nu}\left(\frac{b}{2\chi}S^{\mu\nu}\right) = s^{\mu} - \frac{1}{2}\partial_{\nu}(b\omega^{\mu\nu}), \tag{3.99b}$$

with thermodynamic functions $a(\varepsilon, n)$, $b(\varepsilon, n)$. An intuitive understanding of physics of these transformations is obtained by noting that the spatial part of $-\partial_{\nu}(a\omega^{\mu\nu})/2$ can be interpreted as the magnetization current $\boldsymbol{\nabla} \times \boldsymbol{M}$ with vorticity induced magnetization $\boldsymbol{M} = -a\boldsymbol{\omega}/2$, i.e. the Barnett effect.

Since the local charge and entropy densities, (n, s), are defined by $n = -u_{\mu}j^{\mu}$ and $s = -u_{\mu}s^{\mu}$ respectively, transformations in Eq.(3.99) redefine them $\tilde{n} = n - \Delta n$, $\tilde{s} = s - \Delta s$, where

$$\Delta n = -\frac{1}{2}u_{\mu}\partial_{\nu}(a\omega^{\mu\nu}) = -a\omega_{\mu}\omega^{\mu}, \quad \Delta s = -b\omega_{\mu}\omega^{\mu}. \tag{3.100}$$

Taking $\tilde{T}^{\mu\nu}$ in Eq.(3.98) obtained from $T_c^{\mu\nu}$ in the ideal spin hydrodynamics in the previous section with $S^{\alpha\mu\nu} = u^{\alpha}S^{\mu\nu} = \chi u^{\alpha}\omega^{\mu\nu}$, we work out the Landau's condition(So that we can easily match to the previous work on the conventional non-dissipative second order hydrodynamics in some later part of this subsection.) for the local energy density and the fluid velocity, $\tilde{T}^{\mu\nu}\tilde{u}_{\nu} = -\tilde{\varepsilon}\tilde{u}^{\mu}$, to obtain $\tilde{\varepsilon}$ and $\tilde{u}^{\mu}$ as $\tilde{\varepsilon} = \varepsilon - \Delta\varepsilon$, $\tilde{u}^{\mu} = u^{\mu} - \Delta u^{\mu}$ with

$$\Delta\varepsilon = 2\chi\omega_{\mu}\omega^{\mu}, \quad \Delta u^{\mu} = -\frac{1}{2\beta w}\Delta^{\mu}_{\alpha}\partial_{\lambda}(\beta\chi\omega^{\alpha\lambda}). \tag{3.101}$$

In addition, we allow a redefinition of pressure $\tilde{p} = p - \Delta p$ with $\Delta p = 2a_0\omega_\mu\omega^\mu$, where a_0 is a free thermodynamic function, and whose physics meaning now is clearly, it is just a correction to the pressure. In terms of these variables, the energy-momentum tensor in conventional hydrodynamics reads

$$\tilde{T}^{\mu\nu} = \tilde{\varepsilon}\tilde{u}^\mu\tilde{u}^\nu + \tilde{p}\tilde{\Delta}^{\mu\nu} + \tilde{\tau}^{\mu\nu}, \tag{3.102}$$

where $\tilde{\tau}^{\mu\nu}$ denotes certain second-order transport terms

$$\tilde{\tau}^{\mu\nu} = \frac{1}{2}\chi\left((\theta^\mu{}_\alpha + \omega^\mu{}_\alpha)\omega^{\alpha\nu} + (\mu \leftrightarrow \nu)\right) + 2a_0\Delta^{\mu\nu}\omega_\lambda\omega^\lambda. \tag{3.103}$$

Similarly, the charge and the entropy currents in the conventional hydrodynamics are given by

$$\tilde{j}^\mu = \tilde{n}\tilde{u}^\mu - \frac{n}{2\beta w}\Delta^\mu_\lambda\partial_\nu(\beta\chi\omega^{\lambda\nu}) - \frac{1}{2}\Delta^\mu_\lambda\partial_\nu(a\omega^{\lambda\nu}), \tag{3.104}$$

$$\tilde{s}^\mu = \tilde{s}\tilde{u}^\mu - \frac{s\Delta^\mu_\lambda\partial_\nu(\beta\chi\omega^{\lambda\nu})}{2\beta w} + \frac{n\chi\omega^{\mu\nu}\partial_\nu\alpha}{2w} - \frac{\Delta^\mu_\lambda\partial_\nu(b\omega^{\lambda\nu})}{2}, \tag{3.105}$$

with other second-order transport terms. A similar observation was made in Ref.[134]. It should be emphasized that the ideal limit of spin hydrodynamics with $\partial_\mu s^\mu = 0$ that we start with guarantees that the conventional hydrodynamics with the above second order transport terms is also ideal, i.e. $\partial_\mu\tilde{s}^\mu = 0$.

However, to make the conventional hydrodynamics truly conventional, the thermodynamics relation of spin hydrodynamics in Eq.(3.95) should transform into conventional thermodynamic relations,

$$d\tilde{s} = \tilde{\beta} d\tilde{\varepsilon} - \tilde{\alpha} d\tilde{n}, \quad \tilde{s} = \tilde{\beta}(\tilde{\varepsilon} + \tilde{p}) - \tilde{\alpha}\tilde{n}. \tag{3.106}$$

We now show that there exists unique choice of (a, b) to achieve this equivalence, with (a, b) expressed in terms of (χ, a_0) without any integrations.

We start from the entropy density s in the spin hydrodynamics as a function of density variables, $s(\varepsilon, n, \sigma)$, where $S^\mu \equiv \epsilon^{\mu\nu\alpha\beta} u_\nu S_{\alpha\beta}/2$ and $\sigma \equiv S_\mu S^\mu/2$. The first law of thermodynamics in Eq.(3.95), $ds = \beta d\varepsilon - \alpha dn - \beta\gamma_{\mu\nu} dS^{\mu\nu}/2 = \beta d\varepsilon - \alpha dn - \beta\gamma_\mu dS^\mu$, then gives us $\beta \equiv (\partial s/\partial\varepsilon)_{n,\sigma}$, $\alpha \equiv -(\partial s/\partial n)_{\varepsilon,\sigma}$ and $\beta\gamma_\mu \equiv -(\partial s/\partial\sigma)_{\varepsilon,n} S^\mu$. In local equilibrium, $\gamma_\mu = \omega_\mu$, and the spin susceptibility is identified as $\chi \equiv -\beta(\partial s/\partial\sigma)^{-1}_{\varepsilon,n}$ from $S^\mu = \chi\omega^\mu$.

To find the first law of thermodynamics in the conventional hydrodynamics, we express $\tilde{s}$ in terms of the variables in the conventional hydrodynamics as

$$\tilde{s}(\tilde{\varepsilon}, \tilde{n}, \omega_\mu\omega^\mu) = s(\tilde{\varepsilon} + \Delta\varepsilon, \tilde{n} + \Delta n, \sigma) - \Delta s \tag{3.107}$$

where $\sigma = \chi^2\omega_\mu\omega^\mu/2$, with the same function s and $(\Delta\varepsilon, \Delta n, \Delta s)$ given by Eq.(3.100) and Eq.(3.101).

It is now straightforward to find the first law of thermodynamics

$$d\tilde{s} = \tilde{\beta} d\tilde{\varepsilon} - \tilde{\alpha} d\tilde{n} + A\omega_\mu d\omega^\mu \tag{3.108}$$

with

$$\tilde{\beta} = \beta + \left(\beta\chi_\varepsilon + b_\varepsilon + \alpha a_\varepsilon\right)\omega_\mu\omega^\mu, \quad (3.109)$$

$$\tilde{\alpha} = \alpha - \left(\beta\chi_n + b_n + \alpha a_n\right)\omega_\mu\omega^\mu, \quad (3.110)$$

$$A = 3\beta\chi + 2\alpha a + 2b, \quad (3.111)$$

where $f_n \equiv (\partial f/\partial n)_\varepsilon$ and $f_\varepsilon \equiv (\partial f/\partial \varepsilon)_n$. From $s = \beta(\varepsilon + p) - \alpha n - \beta\chi\omega_\mu\omega^\mu$ in Eq.(3.95), we also find straightforwardly

$$\tilde{s} = \tilde{\beta}(\tilde{\varepsilon} + \tilde{p}) - \tilde{\alpha}\tilde{n} + B\omega_\mu\omega^\mu,$$

with

$$\begin{aligned} B &= \beta\chi + \alpha a + b - w\left(\beta\chi_\varepsilon + b_\varepsilon + \alpha a_\varepsilon\right) \\ &\quad - n\left(\beta\chi_n + b_n + \alpha a_n\right) + 2\beta a_0, \end{aligned} \quad (3.112)$$

The conventional thermodynamics relations in Eq.(3.106) are obtained by imposing the conditions $A = B = 0$. It is easy to see that these conditions determine (a, b) in terms of (χ, a_0) without any integrations, and their are given by

$$a = \frac{\beta}{2\alpha_p c_s^2}\left(\frac{\chi}{w} - \beta_\varepsilon\left(\frac{3\chi}{\beta} + \left(\frac{\partial\chi}{\partial\beta}\right)_\alpha\right) - \frac{4a_0}{w}\right) - \frac{\beta}{2}\left(\frac{\partial\chi}{\partial\alpha}\right)_\beta \quad (3.113)$$

$$b = -\alpha a - \frac{3}{2}\beta\chi\,. \quad (3.114)$$

With (a,b) given in terms of (χ, a_0), we see that all second-order transport coefficients in the energy-momentum tensor, Eq.(3.103), in the charge current Eq.(3.104) and in the entropy current, Eq.(3.105), can be expressed in terms of two free thermodynamic functions (χ, a_0). With the identification of $a_1 = \chi$, one can non-trivially check that these second-order transport coefficients agree precisely with those we find in the non-dissipative second-order hydrodynamics in the previous section once they are also expressed in terms of (a_1, a_0). The conditions $A = 0$ and $B = 0$ correspond to the constraint $C^{(5)} = 0$ and a linear combination of $C^{(i)} = 0$, respectively. In the special case of conformal system, condition $B = 0$ follows from $A = 0$ and conformality. This completes the proof that the ideal spin hydrodynamics is equivalent to the non-dissipative second-order hydrodynamics by pseudo-gauge transformation.

3.2.5 Discussion

In this section, we introduce a novel power counting scheme for gradients of hydrodynamic variables and discover nontrivial constraints on certain non-dissipative second-order transport coefficients imposed by the second law of thermodynamics. We also show that the spin hydrodynamics and the conventional hydrodynamics with these second-order transport coefficients are two equivalent descriptions of the same system related by pseudo-gauge transformation. In a more concrete form, one can express the hydrodynamic variables in one description in terms of those in the other description.

Furthermore, one can construct infinitely many equivalent spin hydrodynamics descriptions for the same system by performing pseudo-gauge transformations using an arbitrary fraction of the spin tensor, i.e., with $\Sigma^{\alpha\mu\nu} = tS^{\alpha\mu\nu}$, where $t \neq 1$. This transformation changes the spin susceptibility $\chi \to (1-t)\chi \equiv \chi(t)$ in thermodynamic relations, while $a_1(t) + \chi(t)$ remains invariant. The other second-order transport coefficients are related to $a_1(t)$ by Eq.(3.91). The conventional hydrodynamics is a special choice in this infinite family corresponding to $t = 1$. In general, the vorticity driven thermal Hall effect is given by Eq.(3.96) with $\chi \to a_1(t) + \chi(t)$.

What meaning should one then assign to the spin density in a given spin hydrodynamics description? Our conclusion naturally suggests that the answer to this question cannot be found within hydrodynamics itself. For example, a plasma may contain different microscopic constituents carrying their own spins, and it is a matter of choice what to include in the hydrodynamic description. All different choices are equivalent and describe the same system, while the non-dissipative second-order transport coefficients corresponding to each choice are related in the specific way we described.

3.3 Summary

In the first part of this Chapter, in Sec.(3.1), we have formulated the "*Quantum kinetic*" description of the spin polarization of massive spin-1/2 quarks in the leading-log order of pQCD. We obtain the time evolution equations of the spin density matrix in the momentum space of a massive quark interacting with a homogeneous background QCD plasma. Our time evolution operator of spin density matrix or quantum kinetic collision terms are universally of order $\alpha_s^2 \log(1/\alpha_s)$ in terms of the QCD coupling constant $\alpha_s = g^2/(4\pi)$. Our framework is applicable to studying the relaxation dynamics of spin polarization of massive(by massive we mean that quark mass $m \gg m_d \sim gT$, where m_D is the Debye screen mass) quark in the pQCD regime. Our framework is constructed in the momentum space, which is equivalent to the other formulation [38; 135] by Wigner's transformation. Our Quantum kinetic framework can be further improved by going beyond the homogeneity limit to include the spatial gradient and to consider the spin coupling with the vorticity as well as the magnetic field in the collision integral. We leave this for future work.

In the second part of this Chapter, in Sec.(3.2), we have considered the system that is not far away from the uniform rotation of the fluid and formulated the non-dissipative second-order hydrodynamics with certain non-trivial relations for the seven transport coefficients appearing in the constitutive relations follow from non-negative entropy production. We also generalize the hydrodynamics to take into account the spin variable. We demonstrate that the extension of hydrodynamics by the spin variable is equivalent to this non-dissipative second-order conventional hydrodynamics. We also point out the arising of vorticity driven thermal hall effect due to vorticity coupling with temperature gradient in the "no-drag" frame.

3.A.1: A simplification by rotational symmetry

In this appendix, we show that the following integral is non-zero only when $s = s'$, and the value doesn't depend on s either,

$$\int \frac{d^3\boldsymbol{p'}}{(2\pi)^3} \frac{1}{2E_{p'}} \sum_{s''} [\bar{u}(\boldsymbol{p}, s)\gamma^\mu u(\boldsymbol{p'}, s'')][\bar{u}(\boldsymbol{p'}, s'')\gamma^\nu u(\boldsymbol{p}, s')] G_{\mu\nu}(\boldsymbol{p} - \boldsymbol{p'}, t_a) e^{i(E_p - E_{p'})t_a} \,, \quad (3.115)$$

when the gluon two-point function, $G_{\mu\nu}$, has a decomposition to longitudinal and transverse parts in Coulomb gauge,

$$G_{\mu\nu}(t, \boldsymbol{q}) = \delta_{\mu 0}\delta_{\nu 0} G_L(t, q) + \Pi^T_{\mu\nu}(\boldsymbol{q}) G_T(t, q) \,, \quad q \equiv |\boldsymbol{q}| \,, \quad (3.116)$$

where the only non-zero elements of $\Pi^T_{\mu\nu}(\boldsymbol{q})$ is

$$\Pi^T_{ij}(\boldsymbol{q}) = (\delta_{ij} - \boldsymbol{q}^i \boldsymbol{q}^j / q^2) \,, \quad i, j = 1, 2, 3 \,. \quad (3.117)$$

Let us first show this for the longitudinal case. From the explicit expressions for γ^μ in Eq.(3.14), and the spinor in Eq.(3.15) that we reproduce here

$$u(\boldsymbol{p}, s) = \begin{pmatrix} \sqrt{E_p - sp}\, \xi_s(\boldsymbol{p}) \\ \sqrt{E_p + sp}\, \xi_s(\boldsymbol{p}) \end{pmatrix} , \quad (3.118)$$

we have (recall $\bar{u} = -u^\dagger\gamma^0$)

$$\begin{aligned}
\sum_{s''} u(\boldsymbol{p}', s'')\bar{u}(\boldsymbol{p}', s'')\gamma^0 &= \sum_{s''} u(\boldsymbol{p}', s'')u^\dagger(\boldsymbol{p}', s'') \\
= \quad & \sum_{s''} \begin{pmatrix} (E_{p'} - s''p')\xi_{s''}(\boldsymbol{p}')\xi^\dagger_{s''}(\boldsymbol{p}') & m\xi_{s''}(\boldsymbol{p}')\xi^\dagger_{s''}(\boldsymbol{p}') \\ m\xi_{s''}(\boldsymbol{p}')\xi^\dagger_{s''}(\boldsymbol{p}') & (E_{p'} + s''p')\xi_{s''}(\boldsymbol{p}')\xi^\dagger_{s''}(\boldsymbol{p}') \end{pmatrix} \\
= \quad & \begin{pmatrix} E_{p'} - \boldsymbol{p}' \cdot \boldsymbol{\sigma} & m \\ m & E_{p'} + \boldsymbol{p}' \cdot \boldsymbol{\sigma} \end{pmatrix}, \qquad (3.119)
\end{aligned}$$

where we use

$$\xi_{s''}(\boldsymbol{p}')\xi^\dagger_{s''}(\boldsymbol{p}') = \mathcal{P}_{s''}(\boldsymbol{p}') = \frac{1}{2}\left(1 + s''\frac{\boldsymbol{p}' \cdot \boldsymbol{\sigma}}{p'}\right). \qquad (3.120)$$

Now, consider the $\boldsymbol{p}'$ integral in Eq.(3.115), and introduce spherical coordinates (p', θ', ϕ'), where θ' is the azimuthal angle between $\boldsymbol{p}'$ and $\boldsymbol{p}$, and ϕ' is the polar angle around the perpendicular plane to $\boldsymbol{p}$. It is easy to see, due to rotational symmetry of other parts in the integrand around ϕ', that only ϕ' dependence appears in the spinor sum Eq.(3.119), as transverse components of $\boldsymbol{p}'$ with respect to $\boldsymbol{p}$. Since these transverse part of $\boldsymbol{p}'$ will integrate to zero after ϕ' integration, it is clear that $\boldsymbol{p}' \cdot \boldsymbol{\sigma}$ in Eq.(3.119) will be replaced by something proportional to $\boldsymbol{p} \cdot \boldsymbol{\sigma}$ after ϕ' integration. Therefore, Eq.(3.115) becomes after $\boldsymbol{p}'$ integration

$$u^\dagger(\boldsymbol{p}, s) \begin{pmatrix} A + B(\boldsymbol{p} \cdot \boldsymbol{\sigma}) & C \\ C & A - B(\boldsymbol{p} \cdot \boldsymbol{\sigma}) \end{pmatrix} u(\boldsymbol{p}, s'), \qquad (3.121)$$

with some constants A, B, C. As $u(\boldsymbol{p}, s) \propto \xi_s(\boldsymbol{p})$ and $(\boldsymbol{p} \cdot \boldsymbol{\sigma})\xi_s(\boldsymbol{p}) = sp\xi_s(\boldsymbol{p})$, and $\xi_s^\dagger(\boldsymbol{p})\xi_{s'}(\boldsymbol{p}) = \delta_{s,s'}$, we conclude that Eq.(3.115), that is Eq.(3.121), is non-zero only when $s = s'$. To show that the value doesn't depend on $s = s'$, we use the explicit spinor Eq.(3.118) to evaluate Eq.(3.121) to obtain

$$(E_p - sp)(A + spB) + (E_p + sp)(A - spB) + 2mC = 2(E_p A - p^2 B + mC)\,, \tag{3.122}$$

which is indeed independent of the choice of s.

The proof in the transverse case is more complicated, but the idea is the same.

$$\begin{aligned}
&-\sum_{s''} \gamma^0 \gamma^i u(\boldsymbol{p}', s'')\bar{u}(\boldsymbol{p}', s'')\gamma^j \Pi^T_{ij}(\boldsymbol{q}) \\
=\;& \sum_{s''} \begin{pmatrix} \sigma^i & 0 \\ 0 & -\sigma^i \end{pmatrix} u(\boldsymbol{p}', s'')u^\dagger(\boldsymbol{p}', s'') \begin{pmatrix} \sigma^j & 0 \\ 0 & -\sigma^j \end{pmatrix} \left(\delta_{ij} - \hat{\boldsymbol{q}}^i \hat{\boldsymbol{q}}^j\right) \\
=\;& \begin{pmatrix} \sigma^i & 0 \\ 0 & -\sigma^i \end{pmatrix} \begin{pmatrix} E_{p'} - \boldsymbol{p}' \cdot \boldsymbol{\sigma} & m \\ m & E_{p'} + \boldsymbol{p}' \cdot \boldsymbol{\sigma} \end{pmatrix} \begin{pmatrix} \sigma^j & 0 \\ 0 & -\sigma^j \end{pmatrix} \left(\delta_{ij} - \hat{\boldsymbol{q}}^i \hat{\boldsymbol{q}}^j\right) \\
=\;& \begin{pmatrix} 2E_{p'} + 2\boldsymbol{p}' \cdot \boldsymbol{\sigma} - 2i(\hat{\boldsymbol{q}} \cdot \boldsymbol{\sigma})((\hat{\boldsymbol{q}} \times \boldsymbol{p}') \cdot \boldsymbol{\sigma}) & -2m \\ -2m & 2E_{p'} - 2\boldsymbol{p}' \cdot \boldsymbol{\sigma} + 2i(\hat{\boldsymbol{q}} \cdot \boldsymbol{\sigma})((\hat{\boldsymbol{q}} \times \boldsymbol{p}') \cdot \boldsymbol{\sigma}) \end{pmatrix}.
\end{aligned} \tag{3.123}$$

Upon $\boldsymbol{p}'$ integration, we again have $\boldsymbol{p}' \cdot \boldsymbol{\sigma}$ become proportional to $\boldsymbol{p} \cdot \boldsymbol{\sigma}$, and recalling that $\boldsymbol{q} = \boldsymbol{p} - \boldsymbol{p}'$, we have

$$(\hat{\boldsymbol{q}} \cdot \boldsymbol{\sigma})((\hat{\boldsymbol{q}} \times \boldsymbol{p}') \cdot \boldsymbol{\sigma}) = (\hat{\boldsymbol{q}} \cdot \boldsymbol{\sigma})((\hat{\boldsymbol{q}} \times \boldsymbol{p}) \cdot \boldsymbol{\sigma}) = \epsilon^{jkl} \hat{\boldsymbol{q}}^i \hat{\boldsymbol{q}}^k \boldsymbol{p}^l \sigma^i \sigma^j \, . \tag{3.124}$$

Due to symmetry of ϕ' and $\boldsymbol{q} = \boldsymbol{p} - \boldsymbol{p}'$, the $\hat{\boldsymbol{q}}^i \hat{\boldsymbol{q}}^k$ part will become, after ϕ' integration, a linear combination of δ^{ik} and $\boldsymbol{p}^i \boldsymbol{p}^k$. Obviously, these two structures are the only possible rank-2 structures with $\boldsymbol{p}$, since the only available vector after $\boldsymbol{p}'$ integration is $\boldsymbol{p}$. The $\boldsymbol{p}^i \boldsymbol{p}^k$ piece doesn't contribute to the above due to $\epsilon^{jkl} \boldsymbol{p}^l$, while the δ^{ik} piece results in

$$\epsilon^{ijl} \sigma^i \sigma^j \boldsymbol{p}^l \sim \boldsymbol{p} \cdot \boldsymbol{\sigma} \, , \tag{3.125}$$

that is, the same $\boldsymbol{p} \cdot \boldsymbol{\sigma}$ structure. Therefore, Eq.(3.123) becomes, after $\boldsymbol{p}'$ integration in Eq.(3.115),

$$\begin{pmatrix} A' + B'(\boldsymbol{p} \cdot \boldsymbol{\sigma}) & C' \\ C' & A' - B'(\boldsymbol{p} \cdot \boldsymbol{\sigma}) \end{pmatrix} , \tag{3.126}$$

with constants A', B', C', that is the same structure we obtain in the longitudinal polarization case (see Eq.(3.121)), and hence the same conclusions follow.

3.B.1 Field theory description of canonical energy momentum and angular momentum tensor

In this appendix, we review the canonical construction of energy momentum and angular momentum tensor. Even though the total angular momentum is conserved, there is always an ambiguity in exact decomposition of it into the orbital and spin components. Let's first recall the convention as specified in Ref.[136]. For a free Dirac field whose Lagrangian density takes form,

$$\mathcal{L} = \bar{\psi}(i\hbar\gamma^{\mu}\partial_{\mu} - m)\psi \tag{3.127}$$

where including interactions can be easily generalized by $\partial_{\mu} \to D_{\mu} = \partial_{\mu} + ie\mathcal{A}_{\mu}$.

The canonical energy-momentum tensor is defined as,

$$T^{\mu\nu} = \frac{\partial \mathcal{L}}{\partial(\partial_{\mu}\psi)}\frac{\partial \psi}{\partial x_{\nu}} = \bar{\psi} i\hbar\gamma^{\mu}\partial^{\nu}\psi \tag{3.128}$$

The Lagrangian is invariant under an infinitesimal rotation, $x^{\mu} \to x'^{\mu} = x^{\mu} + \epsilon^{\mu}{}_{\nu}x^{\nu}$, where $\epsilon^{\mu}{}_{\nu}$ is an antisymmetric tensor and its magnitude is infinitesimally small. Correspondingly, under this transformation, the spinor transforms as

$$\psi(x) \to \psi'(x') = \psi(x) - \frac{i}{2}\epsilon^{\mu\nu}\Sigma_{\mu\nu}\psi(x) \tag{3.129}$$

where $\Sigma_{\mu\nu} = \frac{i}{4}[\gamma_\mu, \gamma_\nu]$. The Noether current associated with Lorentz rotation symmetry gives rise to total angular momentum tensor as,

$$J^{\mu\nu\alpha} = L^{\mu\nu\alpha} + S^{\mu\nu\alpha} \tag{3.130}$$

where $L^{\mu\nu\alpha}$ is interpreted as the orbital angular momentum and it is due to the coordinate part, and intrinsic spin $S^{\mu\nu\alpha}$ is from the spinor part. We can express $L^{\mu\nu\alpha}$ in terms of canonical energy momentum tensor,

$$L^{\mu\nu\alpha} = x^\nu T^{\mu\alpha} - x^\alpha T^{\mu\nu} = \bar{\psi} i\hbar(\gamma^\mu x^\nu \partial^\alpha - \gamma^\mu x^\alpha \partial^\nu)\psi \tag{3.131}$$

whereas spin tensor $S^{\mu\nu\alpha}$ takes form,

$$S^{\mu\nu\alpha} = \frac{\partial \mathcal{L}}{\partial(\partial_\mu \psi)}[-\frac{i}{2}\Sigma^{\nu\alpha}\psi(x)] = \frac{1}{4}\bar{\psi} i\hbar\gamma^\mu[\gamma^\nu, \gamma^\alpha]\psi. \tag{3.132}$$

One could also start from a symmetrized Dirac Lagrangian, of course this will lead to a different redefinition of spin tensor. Nevertheless, physical quantities shall be independent of the choice of Lagrangian. In our choice the total angular momentum tensor becomes

$$J^{\mu\nu\alpha} = \bar{\psi} i\hbar\gamma^\mu(x^\nu \partial^\alpha - x^\alpha \partial^\nu + \frac{1}{4}[\gamma^\nu, \gamma^\alpha])\psi \tag{3.133}$$

By using the Dirac equation one can easily check the following relation,

$$\partial_\mu L^{\mu\nu\alpha} = \bar{\psi} i\hbar(\gamma^\nu \partial^\alpha - \gamma^\alpha \partial^\nu)\psi = -\partial_\mu S^{\mu\nu\alpha} \tag{3.134}$$

Thus the conservation of total angular momentum follows manifestly $\partial_\mu J^{\mu\nu\alpha} = 0$. In nonrelativistic limit, $L^{0\nu\alpha}$ and $S^{0\nu\alpha}$ correspond to orbital and the spin part, respectively. And we are interested in S^{0ij} or $\mathbf{S}^{ij}$ which is associated with nothing but axial current.

$$S^{0ij} = \epsilon^{ijk}\frac{\hbar}{2}\bar{\psi}\gamma^k\gamma_5\psi = \epsilon^{ijk}\hbar\frac{j_5^k}{2} \tag{3.135}$$

$$S^k = \frac{1}{2}\epsilon^{ijk}S^{0ij} \tag{3.136}$$

CHAPTER 4

CONCLUSION AND OUTLOOK

4.1 Summary and outlook

I would like to summarize the dissertation in this chapter. I have applied the pQCD techniques to study the properties of hot QCD matter created in HIC with realistic hydrodynamic evolution under extreme conditions. Especially I am interested in studying the interplay between magnetic field/vorticity and QCD interactions, which lead to seven publications. Not all of them are included in this thesis due to the space limit. Nevertheless, I would like to summarize my main studies and to give some comments.

In the Chap. 2, Sec.(2.1), An effective kinetic theory of (1+1) dimensional LLL quarks interacting with (3+1) dimensional gluons is presented. We applied this framework to study the mass correction to the CME current in the presence of an extremely strong magnetic field. It would be interesting to study the longitudinal electric conductivity in the intermediate magnetic field in the future, which requires us to sum over higher Landau Level states. This shall play an important role in studying the modeling of realistic hydrodynamic evolution of QGP. And it can also help us with better understanding the backreaction from induced current to electromagnetic field, determining a more realistic lifetime of the magnetic field created in HIC, we leave this for future study.

In the Chap. 2, Sec.(2.2), we identify the emerging of low energy effective hydrodynamics in the presence of a weak magnetic field. We apply this framework to study another important transport coefficient, shear viscosity, which describes the momentum diffusion of QGP. Our framework can also be applied to study the bulk viscosity in the presence of the magnetic field. It is known that bulk viscosity may become large while approaching the QCD phase transition point[137](see [138; 139] too), this study would have important consequences for the hydrodynamic evolution with fluctuations. It would also be interesting to see how the bulk viscosity is modified in our framework and to find out its potential effect on the QCD phase transition. We delay this study to the near future.

Understanding the spin polarization of hadrons in HIC is a very challenging task. I am very happy that I can make some contributions towards understanding this topic. In the Chap. 3, Sec.(3.1), we construct the quantum kinetic description of the spin polarization of massive spin-1/2 quarks in the leading log of pQCD. This study is related to the recent observation of that spin polarization of Λ baryon[36]. It is known that the spin of Λ baryon is mostly from strange quarks. In order to have a better understanding the spin polarization of composite hadrons like Λ baryon, and so on forth, it is kind of a prerequisite for us to first study the spin polarization of massive strange quark. For simplicity, our framework is limited to spatial homogeneity, our future plan intends to extend this framework by including the spatial gradients and taking into account the vorticity and magnetic effects on the collision integral.

In Chap. 2, Sec.(3.2), using the second law of thermodynamics, we construct the non-dissipative second-order hydrodynamics upon considering a regime that is close to the uniform rotation of the fluid. We further extend the hydrodynamics to include the spin degrees of freedom. Most importantly, we demonstrate that the two hydrodynamic frameworks are equivalent to each other by the pseudo gauge transformation. A new vorticity-driven thermal hall effect is identified in the "no-drag" frame. In the future, it would be interesting to extend our framework to include the EM field too.

Last but not least, I also studied the relaxation times of anomalous transport coefficients of strongly coupled plasma by applying the holography method. They are not presented in the current thesis due to the space limit. In retrospect, those projects have provided me with invaluable academic training on the techniques of gauge/gravity correspondence. And I look forward to applying this method to studying other interesting physics in strongly correlated systems.

There are certainly other interesting and important aspects that have not been addressed in this dissertation. One challenge is to construct the collision terms for the massless chiral fermions with the EM background. The side-jump phenomena shall play an important role in this study. Other fields such as the topological insulator in condensed matter physics and topology phase transition of QCD phase diagram attract a lot of my interest. Personally, I would very much like to take them as interesting avenues for future study.

CITED LITERATURE

1. K. Hattori, S. Li, D. Satow, and H.-U. Yee, Longitudinal Conductivity in Strong Magnetic Field in Perturbative QCD: Complete Leading Order, Phys. Rev. **D95**, 076008 (2017), 1610.06839.

2. S. Li and H.-U. Yee, Shear viscosity of the quark-gluon plasma in a weak magnetic field in perturbative QCD: Leading log, Phys. Rev. **D97**, 056024 (2018), 1707.00795.

3. S. Li and H.-U. Yee, Quantum Kinetic Theory of Spin Polarization of Massive Quarks in Perturbative QCD: Leading Log, Phys. Rev. **D100**, 056022 (2019), 1905.10463.

4. S. Li, Quantum Kinetic Equation for spin polarization of massive quarks from pQCD, in *28th International Conference on Ultrarelativistic Nucleus-Nucleus Collisions (Quark Matter 2019) Wuhan, China, November 4-9, 2019* (2020), 2003.00106.

5. S. Li, M. A. Stephanov, and H.-U. Yee, Non-dissipative second-order transport, spin, and pseudo-gauge transformations in hydrodynamics (2020), 2011.12318.

6. L. Van Hove, THEORETICAL PREDICTION OF A NEW STATE OF MATTER, THE 'QUARK - GLUON PLASMA' (ALSO CALLED 'QUARK MATTER'), in *17th International Symposium on Multiparticle Dynamics* (1986), pp. 801–818.

7. T. E. O. Ericson, M. R. M. Jacob, H. Satz, and W. J. Willis, Quark matter formation and heavy ion collisions, Technical report, CERN, Geneva (1982).

8. D. E. Kharzeev, L. D. McLerran, and H. J. Warringa, The Effects of topological charge change in heavy ion collisions: 'Event by event P and CP violation', Nucl. Phys. **A803**, 227 (2008), 0711.0950.

9. A. Bzdak and V. Skokov, Event-by-event fluctuations of magnetic and electric fields in heavy ion collisions, Phys. Lett. **B710**, 171 (2012), 1111.1949.

10. W.-T. Deng and X.-G. Huang, Event-by-event generation of electromagnetic fields in heavy-ion collisions, Phys. Rev. **C85**, 044907 (2012), 1201.5108.

11. K. Fukushima, D. E. Kharzeev, and H. J. Warringa, The Chiral Magnetic Effect, Phys. Rev. **D78**, 074033 (2008), 0808.3382.

12. M. A. Metlitski and A. R. Zhitnitsky, Anomalous axion interactions and topological currents in dense matter, Phys. Rev. **D72**, 045011 (2005), hep-ph/0505072.

13. D. E. Kharzeev and H.-U. Yee, Chiral Magnetic Wave, Phys. Rev. **D83**, 085007 (2011), 1012.6026.

14. Y. Burnier, D. E. Kharzeev, J. Liao, and H.-U. Yee, Chiral magnetic wave at finite baryon density and the electric quadrupole moment of quark-gluon plasma in heavy ion collisions, Phys. Rev. Lett. **107**, 052303 (2011), 1103.1307.

15. K. Fukushima, K. Hattori, H.-U. Yee, and Y. Yin, Heavy Quark Diffusion in Strong Magnetic Fields at Weak Coupling and Implications for Elliptic Flow, Phys. Rev. **D93**, 074028 (2016), 1512.03689.

16. S. K. Das, S. Plumari, S. Chatterjee, J. Alam, F. Scardina, and V. Greco, Directed Flow of Charm Quarks as a Witness of the Initial Strong Magnetic Field in Ultra-Relativistic Heavy Ion Collisions, Phys. Lett. **B768**, 260 (2017), 1608.02231.

17. K. Tuchin, On viscous flow and azimuthal anisotropy of quark-gluon plasma in strong magnetic field, J. Phys. **G39**, 025010 (2012), 1108.4394.

18. X.-G. Huang, A. Sedrakian, and D. H. Rischke, Kubo formulae for relativistic fluids in strong magnetic fields, Annals Phys. **326**, 3075 (2011), 1108.0602.

19. S. I. Finazzo, R. Rougemont, H. Marrochio, and J. Noronha, Hydrodynamic transport coefficients for the non-conformal quark-gluon plasma from holography, JHEP **02**, 051 (2015), 1412.2968.

20. K. Hattori and X.-G. Huang, Novel quantum phenomena induced by strong magnetic fields in heavy-ion collisions, Nucl. Sci. Tech. **28**, 26 (2017), 1609.00747.

21. Z.-T. Liang and X.-N. Wang, Globally polarized quark-gluon plasma in non-central A+A collisions, Phys. Rev. Lett. **94**, 102301 (2005), [Erratum: Phys. Rev. Lett.96,039901(2006)], nucl-th/0410079.

22. J.-H. Gao, S.-W. Chen, W.-t. Deng, Z.-T. Liang, Q. Wang, and X.-N. Wang, Global quark polarization in non-central A+A collisions, Phys. Rev. **C77**, 044902 (2008), 0710.2943.

23. B. Betz, M. Gyulassy, and G. Torrieri, Polarization probes of vorticity in heavy ion collisions, Phys. Rev. **C76**, 044901 (2007), 0708.0035.

24. F. Becattini, F. Piccinini, and J. Rizzo, Angular momentum conservation in heavy ion collisions at very high energy, Phys. Rev. **C77**, 024906 (2008), 0711.1253.

25. X.-G. Huang, P. Huovinen, and X.-N. Wang, Quark Polarization in a Viscous Quark-Gluon Plasma, Phys. Rev. **C84**, 054910 (2011), 1108.5649.

26. F. Becattini, L. Csernai, and D. J. Wang, Λ polarization in peripheral heavy ion collisions, Phys. Rev. **C88**, 034905 (2013), [Erratum: Phys. Rev.C93,no.6,069901(2016)], 1304.4427.

27. L.-G. Pang, H. Petersen, Q. Wang, and X.-N. Wang, Vortical Fluid and Λ Spin Correlations in High-Energy Heavy-Ion Collisions, Phys. Rev. Lett. **117**, 192301 (2016), 1605.04024.

28. Y. Jiang, Z.-W. Lin, and J. Liao, Rotating quark-gluon plasma in relativistic heavy ion collisions, Phys. Rev. **C94**, 044910 (2016), [Erratum: Phys. Rev.C95,no.4,049904(2017)], 1602.06580.

29. Y. Sun and C. M. Ko, Λ hyperon polarization in relativistic heavy ion collisions from a chiral kinetic approach, Phys. Rev. **C96**, 024906 (2017), 1706.09467.

30. S. Shi, K. Li, and J. Liao, Searching for the Subatomic Swirls in the CuCu and CuAu Collisions, Phys. Lett. **B788**, 409 (2019), 1712.00878.

31. D.-X. Wei, W.-T. Deng, and X.-G. Huang, Thermal vorticity and spin polarization in heavy-ion collisions, Phys. Rev. **C99**, 014905 (2019), 1810.00151.

32. X.-L. Xia, H. Li, Z.-B. Tang, and Q. Wang, Probing vorticity structure in heavy-ion collisions by local Λ polarization, Phys. Rev. **C98**, 024905 (2018), 1803.00867.

33. F. Becattini and L. Ferroni, The Microcanonical ensemble of the ideal relativistic quantum gas with angular momentum conservation, Eur. Phys. J. **C52**, 597 (2007), 0707.0793.

34. W. Florkowski, A. Kumar, and R. Ryblewski, Thermodynamic versus kinetic approach to polarization-vorticity coupling, Phys. Rev. **C98**, 044906 (2018), 1806.02616.

35. J.-Y. Chen, D. T. Son, M. A. Stephanov, H.-U. Yee, and Y. Yin, Lorentz Invariance in Chiral Kinetic Theory, Phys. Rev. Lett. **113**, 182302 (2014), 1404.5963.

36. L. Adamczyk *et al.*, Global Λ hyperon polarization in nuclear collisions: evidence for the most vortical fluid, Nature **548**, 62 (2017), 1701.06657.

37. D. T. Son and P. Surowka, Hydrodynamics with Triangle Anomalies, Phys. Rev. Lett. **103**, 191601 (2009), 0906.5044.

38. N. Weickgenannt, X.-L. Sheng, E. Speranza, Q. Wang, and D. H. Rischke, Kinetic theory for massive spin-1/2 particles from the Wigner-function formalism, Phys. Rev. **D100**, 056018 (2019), 1902.06513.

39. J.-H. Gao and Z.-T. Liang, Relativistic Quantum Kinetic Theory for Massive Fermions and Spin Effects, Phys. Rev. **D100**, 056021 (2019), 1902.06510.

40. N. Mueller and R. Venugopalan, Worldline construction of a covariant chiral kinetic theory, Phys. Rev. **D96**, 016023 (2017), 1702.01233.

41. W. Florkowski, B. Friman, A. Jaiswal, and E. Speranza, Relativistic fluid dynamics with spin, Phys. Rev. **C97**, 041901 (2018), 1705.00587.

42. K. Hattori, M. Hongo, X.-G. Huang, M. Matsuo, and H. Taya, Fate of spin polarization in a relativistic fluid: An entropy-current analysis, Phys. Lett. **B795**, 100 (2019), 1901.06615.

43. X.-G. Huang, Vorticity and Spin Polarization — A Theoretical Perspective (2020), 2002.07549.

44. K. G. Wilson, Confinement of Quarks, Phys. Rev. **D10**, 2445 (1974).

45. C. T. H. Davies *et al.*, High precision lattice QCD confronts experiment, Phys. Rev. Lett. **92**, 022001 (2004), hep-lat/0304004.

46. J. M. Maldacena, The Large N limit of superconformal field theories and supergravity, Int. J. Theor. Phys. **38**, 1113 (1999), [Adv. Theor. Math. Phys.2,231(1998)], hep-th/9711200.

47. S. S. Gubser, I. R. Klebanov, and A. M. Polyakov, Gauge theory correlators from noncritical string theory, Phys. Lett. **B428**, 105 (1998), hep-th/9802109.

48. E. Witten, Anti-de Sitter space and holography, Adv. Theor. Math. Phys. **2**, 253 (1998), hep-th/9802150.

49. J. C. Collins and M. J. Perry, Superdense Matter: Neutrons Or Asymptotically Free Quarks?, Phys. Rev. Lett. **34**, 1353 (1975).

50. P. B. Arnold, G. D. Moore, and L. G. Yaffe, Effective kinetic theory for high temperature gauge theories, JHEP **01**, 030 (2003), hep-ph/0209353.

51. R. Baier, A. H. Mueller, D. Schiff, and D. T. Son, 'Bottom up' thermalization in heavy ion collisions, Phys. Lett. **B502**, 51 (2001), hep-ph/0009237.

52. P. Romatschke, New Developments in Relativistic Viscous Hydrodynamics, Int. J. Mod. Phys. **E19**, 1 (2010), 0902.3663.

53. S. Jeon and U. Heinz, Introduction to Hydrodynamics, Int. J. Mod. Phys. **E24**, 1530010 (2015), 1503.03931.

54. C. Gale, S. Jeon, and B. Schenke, Hydrodynamic Modeling of Heavy-Ion Collisions, Int. J. Mod. Phys. **A28**, 1340011 (2013), 1301.5893.

55. L. Landau and E. Lifshitz, *Fluid Mechanics*, *Course of Theoretical Physics*, volume 6 (Elsevier Science 2013).

56. D. Teaney, J. Lauret, and E. V. Shuryak, Flow at the SPS and RHIC as a quark gluon plasma signature, Phys. Rev. Lett. **86**, 4783 (2001), nucl-th/0011058.

57. B. Schenke, P. Tribedy, and R. Venugopalan, Fluctuating Glasma initial conditions and flow in heavy ion collisions, Phys. Rev. Lett. **108**, 252301 (2012), 1202.6646.

58. P. Kovtun, D. T. Son, and A. O. Starinets, Viscosity in strongly interacting quantum field theories from black hole physics, Phys. Rev. Lett. **94**, 111601 (2005), hep-th/0405231.

59. G. Baym, H. Monien, C. J. Pethick, and D. G. Ravenhall, Transverse Interactions and Transport in Relativistic Quark - Gluon and Electromagnetic Plasmas, Phys. Rev. Lett. **64**, 1867 (1990).

60. H. Heiselberg, Color, spin and flavor diffusion in quark - gluon plasmas, Phys. Rev. Lett. **72**, 3013 (1994), hep-ph/9401317.

61. P. B. Arnold, G. D. Moore, and L. G. Yaffe, Transport coefficients in high temperature gauge theories. 1. Leading log results, JHEP **11**, 001 (2000), hep-ph/0010177.

62. P. B. Arnold, G. D. Moore, and L. G. Yaffe, Transport coefficients in high temperature gauge theories. 2. Beyond leading log, JHEP **05**, 051 (2003), hep-ph/0302165.

63. V. Skokov, A. Yu. Illarionov, and V. Toneev, Estimate of the magnetic field strength in heavy-ion collisions, Int. J. Mod. Phys. **A24**, 5925 (2009), 0907.1396.

64. D. Lai, Matter in strong magnetic fields, Rev. Mod. Phys. **73**, 629 (2001), astro-ph/0009333.

65. G. S. Bali, F. Bruckmann, G. Endrodi, Z. Fodor, S. D. Katz, S. Krieg, A. Schafer, and K. K. Szabo, The QCD phase diagram for external magnetic fields, JHEP **02**, 044 (2012), 1111.4956.

66. G. S. Bali, F. Bruckmann, G. Endrodi, F. Gruber, and A. Schaefer, Magnetic field-induced gluonic (inverse) catalysis and pressure (an)isotropy in QCD, JHEP **04**, 130 (2013), 1303.1328.

67. K. Fukushima and Y. Hidaka, Magnetic Catalysis Versus Magnetic Inhibition, Phys. Rev. Lett. **110**, 031601 (2013), 1209.1319.

68. J. Braun, W. A. Mian, and S. Rechenberger, Delayed Magnetic Catalysis, Phys. Lett. **B755**, 265 (2016), 1412.6025.

69. K. Hattori, T. Kojo, and N. Su, Mesons in strong magnetic fields: (I) General analyses, Nucl. Phys. **A951**, 1 (2016), 1512.07361.

70. D. T. Son and B. Z. Spivak, Chiral Anomaly and Classical Negative Magnetoresistance of Weyl Metals, Phys. Rev. **B88**, 104412 (2013), 1206.1627.

71. D. Grabowska, D. B. Kaplan, and S. Reddy, Role of the electron mass in damping chiral plasma instability in Supernovae and neutron stars, Phys. Rev. **D91**, 085035 (2015), 1409.3602.

72. G. F. Giudice and M. E. Shaposhnikov, Strong sphalerons and electroweak baryogenesis, Phys. Lett. **B326**, 118 (1994), hep-ph/9311367.

73. D. Bodeker, On the effective dynamics of soft nonAbelian gauge fields at finite temperature, Phys. Lett. **B426**, 351 (1998), hep-ph/9801430.

74. P. B. Arnold, D. T. Son, and L. G. Yaffe, Effective dynamics of hot, soft nonAbelian gauge fields. Color conductivity and log(1/alpha) effects, Phys. Rev. **D59**, 105020 (1999), hep-ph/9810216.

75. G. D. Moore and M. Tassler, The Sphaleron Rate in SU(N) Gauge Theory, JHEP **02**, 105 (2011), 1011.1167.

76. G. Basar and D. E. Kharzeev, The Chern-Simons diffusion rate in strongly coupled N=4 SYM plasma in an external magnetic field, Phys. Rev. **D85**, 086012 (2012), 1202.2161.

77. K. Tuchin, Photon decay in strong magnetic field in heavy-ion collisions, Phys. Rev. **C83**, 017901 (2011), 1008.1604.

78. K. Fukushima, Magnetic-field Induced Screening Effect and Collective Excitations, Phys. Rev. **D83**, 111501 (2011), 1103.4430.

79. K. Hattori and D. Satow, Electrical Conductivity of Quark-Gluon Plasma in Strong Magnetic Fields, Phys. Rev. **D94**, 114032 (2016), 1610.06818.

80. M. Stephanov and H.-U. Yee, (Unpublished). .

81. A. Selikhov and M. Gyulassy, Color diffusion and conductivity in a quark - gluon plasma, Phys. Lett. **B316**, 373 (1993), nucl-th/9307007.

82. J. Bloczynski, X.-G. Huang, X. Zhang, and J. Liao, Azimuthally fluctuating magnetic field and its impacts on observables in heavy-ion collisions, Phys. Lett. **B718**, 1529 (2013), 1209.6594.

83. K. Tuchin, Electromagnetic field and the chiral magnetic effect in the quark-gluon plasma, Phys. Rev. **C91**, 064902 (2015), 1411.1363.

84. L. McLerran and V. Skokov, Comments About the Electromagnetic Field in Heavy-Ion Collisions, Nucl. Phys. **A929**, 184 (2014), 1305.0774.

85. K. Hattori, X.-G. Huang, D. H. Rischke, and D. Satow, Bulk Viscosity of Quark-Gluon Plasma in Strong Magnetic Fields, Phys. Rev. **D96**, 094009 (2017), 1708.00515.

86. S. I. Finazzo, R. Critelli, R. Rougemont, and J. Noronha, Momentum transport in strongly coupled anisotropic plasmas in the presence of strong magnetic fields, Phys. Rev. **D94**, 054020 (2016), [Erratum: Phys. Rev.D96,no.1,019903(2017)], 1605.06061.

87. X.-G. Huang, M. Huang, D. H. Rischke, and A. Sedrakian, Anisotropic Hydrodynamics, Bulk Viscosities and R-Modes of Strange Quark Stars with Strong Magnetic Fields, Phys. Rev. **D81**, 045015 (2010), 0910.3633.

88. J. Hernandez and P. Kovtun, Relativistic magnetohydrodynamics, JHEP **05**, 001 (2017), 1703.08757.

89. S. Grozdanov, D. M. Hofman, and N. Iqbal, Generalized global symmetries and dissipative magnetohydrodynamics, Phys. Rev. **D95**, 096003 (2017), 1610.07392.

90. K. Hattori, Y. Hirono, H.-U. Yee, and Y. Yin, MagnetoHydrodynamics with chiral anomaly: phases of collective excitations and instabilities, Phys. Rev. **D100**, 065023 (2019), 1711.08450.

91. G. Inghirami, L. Del Zanna, A. Beraudo, M. H. Moghaddam, F. Becattini, and M. Bleicher, Numerical magneto-hydrodynamics for relativistic nuclear collisions, Eur. Phys. J. **C76**, 659 (2016), 1609.03042.

92. V. Roy, S. Pu, L. Rezzolla, and D. H. Rischke, Effect of intense magnetic fields on reduced-MHD evolution in $\sqrt{s_{\mathrm{NN}}} = 200$ GeV Au+Au collisions, Phys. Rev. **C96**, 054909 (2017), 1706.05326.

93. X.-G. Huang, Y. Yin, and J. Liao, In search of chiral magnetic effect: separating flow-driven background effects and quantifying anomaly-induced charge separations, Nucl. Phys. **A956**, 661 (2016), 1512.06602.

94. E. V. Gorbar, V. A. Miransky, and I. A. Shovkovy, Normal ground state of dense relativistic matter in a magnetic field, Phys. Rev. **D83**, 085003 (2011), 1101.4954.

95. U. Gursoy, D. Kharzeev, and K. Rajagopal, Magnetohydrodynamics, charged currents and directed flow in heavy ion collisions, Phys. Rev. **C89**, 054905 (2014), 1401.3805.

96. K. Fukushima and Y. Hidaka, Electric conductivity of hot and dense quark matter in a magnetic field with Landau level resummation via kinetic equations, Phys. Rev. Lett. **120**, 162301 (2018), 1711.01472.

97. J. Hong and D. Teaney, Spectral densities for hot QCD plasmas in a leading log approximation, Phys. Rev. **C82**, 044908 (2010), 1003.0699.

98. X.-L. Xia, H. Li, X.-G. Huang, and H. Z. Huang, Feed-down effect on spin polarization, Phys. Rev. **C100**, 014913 (2019), 1905.03120.

99. F. Becattini, G. Cao, and E. Speranza, Polarization transfer in hyperon decays and its effect in relativistic nuclear collisions, Eur. Phys. J. **C79**, 741 (2019), 1905.03123.

100. S. Li and H.-U. Yee, Relaxation times for chiral transport phenomena and spin polarization in a strongly coupled plasma, Phys. Rev. **D98**, 056018 (2018), 1805.04057.

101. N. Mueller and R. Venugopalan, Constructing phase space distributions with internal symmetries, Phys. Rev. **D99**, 056003 (2019), 1901.10492.

102. K. Hattori, Y. Hidaka, and D.-L. Yang, Axial Kinetic Theory and Spin Transport for Fermions with Arbitrary Mass, Phys. Rev. **D100**, 096011 (2019), 1903.01653.

103. C. Manuel and J. M. Torres-Rincon, Dynamical evolution of the chiral magnetic effect: Applications to the quark-gluon plasma, Phys. Rev. **D92**, 074018 (2015), 1501.07608.

104. A. Jimenez-Alba and H.-U. Yee, Second order transport coefficient from the chiral anomaly at weak coupling: Diagrammatic resummation, Phys. Rev. **D92**, 014023 (2015), 1504.05866.

105. G. D. Moore and D. Teaney, How much do heavy quarks thermalize in a heavy ion collision?, Phys. Rev. **C71**, 064904 (2005), hep-ph/0412346.

106. M. A. Valle Basagoiti, Transport coefficients and ladder summation in hot gauge theories, Phys. Rev. **D66**, 045005 (2002), hep-ph/0204334.

107. G. Aarts and J. M. Martinez Resco, Ward identity and electrical conductivity in hot QED, JHEP **11**, 022 (2002), hep-ph/0209048.

108. P. B. Arnold, D. Son, and L. G. Yaffe, The Hot baryon violation rate is O (alpha-w**5 T**4), Phys. Rev. **D55**, 6264 (1997), hep-ph/9609481.

109. J. M. Martinez Resco and M. A. Valle Basagoiti, Color conductivity and ladder summation in hot QCD, Phys. Rev. **D63**, 056008 (2001), hep-ph/0009331.

110. D. T. Son and N. Yamamoto, Berry Curvature, Triangle Anomalies, and the Chiral Magnetic Effect in Fermi Liquids, Phys. Rev. Lett. **109**, 181602 (2012), 1203.2697.

111. M. A. Stephanov and Y. Yin, Chiral Kinetic Theory, Phys. Rev. Lett. **109**, 162001 (2012), 1207.0747.

112. J.-W. Chen, S. Pu, Q. Wang, and X.-N. Wang, Berry Curvature and Four-Dimensional Monopoles in the Relativistic Chiral Kinetic Equation, Phys. Rev. Lett. **110**, 262301 (2013), 1210.8312.

113. C. Duval and P. A. Horvathy, Chiral fermions as classical massless spinning particles, Phys. Rev. **D91**, 045013 (2015), 1406.0718.

114. J.-h. Gao, S. Pu, and Q. Wang, Covariant chiral kinetic equation in the Wigner function approach, Phys. Rev. **D96**, 016002 (2017), 1704.00244.

115. S. Carignano, C. Manuel, and J. M. Torres-Rincon, Consistent relativistic chiral kinetic theory: A derivation from on-shell effective field theory, Phys. Rev. **D98**, 076005 (2018), 1806.01684.

116. J.-Y. Chen, D. T. Son, and M. A. Stephanov, Collisions in Chiral Kinetic Theory, Phys. Rev. Lett. **115**, 021601 (2015), 1502.06966.

117. Y. Hidaka, S. Pu, and D.-L. Yang, Relativistic Chiral Kinetic Theory from Quantum Field Theories, Phys. Rev. **D95**, 091901 (2017), 1612.04630.

118. D.-L. Yang, Side-Jump Induced Spin-Orbit Interaction of Chiral Fluids from Kinetic Theory, Phys. Rev. **D98**, 076019 (2018), 1807.02395.

119. W. Florkowski, A. Kumar, and R. Ryblewski, Relativistic hydrodynamics for spin-polarized fluids, Prog. Part. Nucl. Phys. **108**, 103709 (2019), 1811.04409.

120. A. Gallegos and U. Gürsoy, Holographic spin liquids and Lovelock Chern-Simons gravity (2020), 2004.05148.

121. M. Stephanov and Y. Yin, Hydrodynamics with parametric slowing down and fluctuations near the critical point, Phys. Rev. D **98**, 036006 (2018), 1712.10305.

122. F. Becattini and L. Tinti, Nonequilibrium Thermodynamical Inequivalence of Quantum Stress-energy and Spin Tensors, Phys. Rev. D **87**, 025029 (2013), 1209.6212.

123. E. Speranza and N. Weickgenannt, Spin tensor and pseudo-gauges: from nuclear collisions to gravitational physics (2020), 2007.00138.

124. S. Bhattacharyya, Constraints on the second order transport coefficients of an uncharged fluid, JHEP **07**, 104 (2012), 1201.4654.

125. K. Jensen, M. Kaminski, P. Kovtun, R. Meyer, A. Ritz, and A. Yarom, Towards hydrodynamics without an entropy current, Phys. Rev. Lett. **109**, 101601 (2012), 1203.3556.

126. N. Banerjee, J. Bhattacharya, S. Bhattacharyya, S. Jain, S. Minwalla, and T. Sharma, Constraints on Fluid Dynamics from Equilibrium Partition Functions, JHEP **09**, 046 (2012), 1203.3544.

127. S. Bhattacharyya, Entropy Current from Partition Function: One Example, JHEP **07**, 139 (2014), 1403.7639.

128. J. Erdmenger, M. Haack, M. Kaminski, and A. Yarom, Fluid dynamics of R-charged black holes, JHEP **01**, 055 (2009), 0809.2488.

129. R. Baier, P. Romatschke, D. T. Son, A. O. Starinets, and M. A. Stephanov, Relativistic viscous hydrodynamics, conformal invariance, and holography, JHEP **04**, 100 (2008), 0712.2451.

130. F. Becattini and L. Tinti, The Ideal relativistic rotating gas as a perfect fluid with spin, Annals Phys. **325**, 1566 (2010), 0911.0864.

131. A. Aristova, D. Frenklakh, A. Gorsky, and D. Kharzeev, Vortical susceptibility of finite-density QCD matter, JHEP **10**, 029 (2016), 1606.05882.

132. M. A. Stephanov and H.-U. Yee, No-Drag Frame for Anomalous Chiral Fluid, Phys. Rev. Lett. **116**, 122302 (2016), 1508.02396.

133. J.-H. Gao, Z.-T. Liang, Q. Wang, and X.-N. Wang, Disentangling covariant Wigner functions for chiral fermions, Phys. Rev. D **98**, 036019 (2018), 1802.06216.

134. K. Fukushima and S. Pu, Spin Hydrodynamics and Symmetric Energy-Momentum Tensors – A current induced by the spin vorticity – (2020), 2010.01608.

135. N. Weickgenannt, E. Speranza, X.-l. Sheng, Q. Wang, and D. H. Rischke, Generating spin polarization from vorticity through nonlocal collisions (2020), 2005.01506.

136. K. Fukushima, S. Pu, and Z. Qiu, Eddy magnetization from the chiral Barnett effect, Phys. Rev. **A99**, 032105 (2019), 1808.08016.

137. F. Karsch, D. Kharzeev, and K. Tuchin, Universal properties of bulk viscosity near the QCD phase transition, Phys. Lett. **B663**, 217 (2008), 0711.0914.

138. P. Romatschke and D. T. Son, Spectral sum rules for the quark-gluon plasma, Phys. Rev. **D80**, 065021 (2009), 0903.3946.

139. G. D. Moore and O. Saremi, Bulk viscosity and spectral functions in QCD, JHEP **09**, 015 (2008), 0805.4201.

APPENDICES

Appendix I: Reuse License for Sec.(2.1)

American Physical Society Reuse and Permissions License

09-Feb-2021

This license agreement between the American Physical Society ("APS") and Shiyong Li ("You") consists of your license details and the terms and conditions provided by the American Physical Society and SciPris.

Licensed Content Information

License Number:	**RNP/21/FEB/036266**
License date:	09-Feb-2021
DOI:	10.1103/PhysRevD.95.076008
Title:	Longitudinal conductivity in strong magnetic field in perturbative QCD: Complete leading order
Author:	Koichi Hattori et al.
Publication:	Physical Review D
Publisher:	American Physical Society
Cost:	USD $ 0.00

Request Details

Does your reuse require significant modifications: No

Specify intended distribution locations:	United States
Reuse Category:	Reuse in a thesis/dissertation
Requestor Type:	Author of requested content
Items for Reuse:	Whole Article
Format for Reuse:	Electronic

Information about New Publication:

University/Publisher:	University of Illinois at Chicago
Title of dissertation/thesis:	Transport Dynamics of Quark-Gluon Plasma in Perturbative QCD with Magnetic fields/Vorticity
Author(s):	Shiyong Li
Expected completion date:	Mar. 2021

License Requestor Information

Name:	Shiyong Li
Affiliation:	Individual
Email Id:	sli72@uic.edu
Country:	United States

American Physical Society
Reuse and Permissions License

TERMS AND CONDITIONS

The American Physical Society (APS) is pleased to grant the Requestor of this license a non-exclusive, non-transferable permission, limited to Electronic format, provided all criteria outlined below are followed.

1. You must also obtain permission from at least one of the lead authors for each separate work, if you haven't done so already. The author's name and affiliation can be found on the first page of the published Article.
2. For electronic format permissions, Requestor agrees to provide a hyperlink from the reprinted APS material using the source material's DOI on the web page where the work appears. The hyperlink should use the standard DOI resolution URL, http://dx.doi.org/{DOI}. The hyperlink may be embedded in the copyright credit line.
3. For print format permissions, Requestor agrees to print the required copyright credit line on the first page where the material appears: "Reprinted (abstract/excerpt/figure) with permission from [(FULL REFERENCE CITATION) as follows: Author's Names, APS Journal Title, Volume Number, Page Number and Year of Publication.] Copyright (YEAR) by the American Physical Society."
4. Permission granted in this license is for a one-time use and does not include permission for any future editions, updates, databases, formats or other matters. Permission must be sought for any additional use.
5. Use of the material does not and must not imply any endorsement by APS.
6. APS does not imply, purport or intend to grant permission to reuse materials to which it does not hold copyright. It is the requestor's sole responsibility to ensure the licensed material is original to APS and does not contain the copyright of another entity, and that the copyright notice of the figure, photograph, cover or table does not indicate it was reprinted by APS with permission from another source.
7. The permission granted herein is personal to the Requestor for the use specified and is not transferable or assignable without express written permission of APS. This license may not be amended except in writing by APS.
8. You may not alter, edit or modify the material in any manner.
9. You may translate the materials only when translation rights have been granted.
10. APS is not responsible for any errors or omissions due to translation.
11. You may not use the material for promotional, sales, advertising or marketing purposes.
12. The foregoing license shall not take effect unless and until APS or its agent, Aptara, receives payment in full in accordance with Aptara Billing and Payment Terms and Conditions, which are incorporated herein by reference.
13. Should the terms of this license be violated at any time, APS or Aptara may revoke the license with no refund to you and seek relief to the fullest extent of the laws of the USA. Official written notice will be made using the contact information provided with the permission request. Failure to receive such notice will not nullify revocation of the permission.
14. APS reserves all rights not specifically granted herein.
15. This document, including the Aptara Billing and Payment Terms and Conditions, shall be the entire agreement between the parties relating to the subject matter hereof.

VITA

Shiyong Li
Department of Physics
University of Illinois at Chicago
845 W Taylor St, Chicago, IL 60607

Curriculum Vitae
Email: sli72@uic.edu
Phone:+1-312-804-0529

EDUCATION

- **University of Illinois at Chicago** — Chicago, IL, USA
  Ph.D. Nuclear Theory — *Aug. 2012 - Apr. 2021*
  - Advisor: Prof. Ho-Ung Yee
- **Central South University** — Changsha, Hunan, China
  B.S. Applied Physics — *Sep. 2008 - June. 2012*

RESEARCH INTERESTS

• *Transport coefficients of Quark-Gluon Plasma(QGP) and chiral transport phenomena and its possible applications in the Heavy-Ion Collisions, Astrophysics and Condensed matter systems.*
• *Relativistic Hydrodynamics (and/or with spin degrees of freedom).*
• *Quantum Chromodynamics(QCD) phase diagram and QCD critical point.*
• *The application of Anti-de Sitter space/Conformal Field Theory(AdS/CFT) correspondence to Heavy-Ion Collisions and Condensed matter systems.*

PUBLICATIONS

7. S. Li, M. Stephanov, and H. U. Yee, "Non-dissipative second order transport, spin and pseudo gauge transformations in hydrodynamics",arXiv:2011.12318[hep-th]

6. S. Li, "Quantum Kinetic Equation for spin polarization of massive quarks from pQCD",Quark Matter 2019 proceeding, arXiv:2003.00106[hep-ph]

5. S. Li and H. U. Yee, "Quantum Kinetic Theory of Spin Polarization of Massive Quarks in Perturbative QCD: Leading Log," Phys.Rev. D100 (2019) no.5, 056022

4. S. Li and H. U. Yee, "Relaxation times for chiral transport phenomena and spin polarization in a strongly coupled plasma,"Phys.Rev. D98 (2018) no.5, 056018.

3. S. Li and H. U. Yee, "Shear viscosity of the quark-gluon plasma in a weak magnetic field in perturbative QCD: Leading log," Phys.Rev. D97 (2018) no.5, 056024.

2. K. Hattori, S. Li, D. Satow and H. U. Yee,"Longitudinal Conductivity in Strong Magnetic Field in Perturbative QCD: Complete Leading Order," Phys.Rev. D95 (2017) no.7, 076008.

1. S. Li, K. A. Mamo and H. U. Yee,"Jet quenching parameter of the quark-gluon plasma in a strong magnetic field: Perturbative QCD and AdS/CFT correspondence," Phys.Rev. D94 (2016) no.8, 085016.

PRESENTATIONS

6. **S. Li**, "Quantum Kinetic Theory of Spin Polarization of Massive Quarks in Perturbative QCD:

Leading Log", Oral presentation in the parallel session, "Quark Matter 2019: the 28th International Conference on Ultra-relativistic Nucleus-Nucleus Collisions" Conference, Wuhan, China, 4-9 Nov.

5. **S. Li**, "Quantum Kinetic Theory of Spin Polarization of Massive Quarks in Perturbative QCD: Leading Log", Contributed talk, "Initial Stage 2019:The fifth installment on the physics of the initial stages of high energy nuclear collisions" Conference, Columbia University, NY, June 24-28.

4. **S. Li**, "Relaxation times for chiral transport phenomena and spin polarization in a strongly coupled plasma", Contributed talk, "BEST Collaboration Meeting 2018", LBNL, San Francisco, CA, Aug 20-21st.

3. **S. Li**, "Relaxation times for chiral transport phenomena and spin polarization in a strongly coupled plasma",Poster presentation, "Quark matter 2018", Venice, Italy, May 13-19th.

2. **S. Li**, "Transport Properties of Quark-Gluon Plasma in Magnetic Fields", Oral presentation in the parallel session, "CPOD2017: Critical Point and Onset of Deconfinement" Conference, Stony Brook University, Stony Brook, NY, Aug, 9th.

1. **S. Li**, "Longitudinal Conductivity in Strong Magnetic Field in Perturbative QCD: Complete Leading Order", Invited talk, "The Workshop on Chirality, Vorticity and Magnetic Field in Heavy Ion Collisions", University of California, Los Angeles, CA, Mar. 27-30th.